Dissertation

In utero programming of human feto-placental cells: The link to fetal developmental programming and disease susceptibility in adulthood

Dipl.-Ing. Silvija Cvitic

For the academic degree of
Doctor of Philosophy
(PhD)

at the
Medical University of Graz
Department of Obstetrics and Gynecology

under supervision of
Assoc. Prof. Dr. Gernot Desoye

2013

Declaration

I hereby declare that this thesis is my own original work and that I have fully acknowledged by name all of those individuals and organizations that have contributed to the research for this thesis. Due acknowledgment has been made in the text to all other material used. Throughout this thesis and in all related publications I followed the guidelines of “Good Scientific Practice”.

Please note that parts of this thesis are already accepted for publication in Cvitic S, Longtine MS, Hackl H, Wagner W, Nelson MD, Desoye G, Hiden U. The human placental sexome differs between trophoblast epithelium and villous vessel endothelium. PLoS ONE, 2013

_____

Silvija Cvitic

Graz, September 2013

Acknowledgements

Foremost, I would like to express my sincere gratitude to my supervisor Prof. Gernot Desoye for the continuous support of my research, his motivation and guidance, great enthusiasm, and fruitful discussions.

Special thanks to Dr. Ursula Hiden and to all colleagues from Forschungslabor-team that have helped me with their advice and support whenever needed.

Furthermore, I thank Dr. Richard Saffery and Dr. Veronica White for hosting me in their laboratories and to all colleagues in Melbourne and Buenos Aires for the warm welcome and new lab skills acquired during my visits.

My warmest thanks go to my family and friends for being there for me at any hour, and to my boyfriend for his eternal support.

Last but not least, I thank God for giving me prudence and strength to make decisions that have guided me to where I am today.

Abstract

The 'Developmental Origin of Health and Disease' (DOHaD) hypothesis holds that an adverse maternal environment during the intrauterine development of an individual has great influence on adult phenotype and disease development in adulthood. As a multifunctional organ that synthesizes, metabolizes, and transports nutrients to the fetus, the placenta influences maternal, placental and fetal metabolism. Hence, it determines the course of fetal development and plays a key role in fetal programming. Epigenetic mechanisms bear the potential for gene regulation upon environmental stimuli and are, thus, a crucial factor in the pathogenesis of complex disorders characterized by sexual dimorphism in their prevalence and severity.

The current thesis investigated the intrauterine programming of the feto-placental cells by gestational diabetes mellitus (GDM), whereby endothelial cells from two distinct vascular beds, arterial (AEC) and venous endothelial cells (VEC) were used. The cellular batch was further extended by adding cytotrophoblasts (CT) and syncytiotrophoblast (SCT) when investigating fetal sex influence on placental gene expression.

Primary AEC isolated from human term placentas after GDM pregnancies (diabetic AEC) under identical culture conditions differ in their functional characteristics, i.e. proliferation and network formation, from cells isolated after healthy pregnancies (normal AEC). Genome-wide DNA methylation and transcription profile of normal and diabetic AEC and VEC clearly show individual diabetic signatures accentuating and potentially explaining the observed functional differences. All four cell types analyzed *in vitro* varied in the extent of sex-biased gene expression, despite the fact that these cells originate from the same organ.

Overall, the data reveal that GDM-derived feto-placental endothelial cells persistently differ from cells isolated from uncomplicated pregnancies. This demonstrates that the placental endothelial cells *in vitro* remember their diabetic *in vivo* phenotype. Furthermore, the observed differences in gene expression and functional differences between male and female feto-placental cells argue for an intrinsic program that enables cells to remember fetal sex. Hence, this thesis introduces new evidence of cellular memory and intrinsic cellular changes depending on the *in utero* exposure to the adverse maternal environment i.e. GDM,

affected placental vascular bed i.e arterial vs. venous, and fetal sex. It is plausible that these intrinsic changes *in utero* contribute to altered disease susceptibility in adulthood.

Zusammenfassung

Die “Developmental Origin of Health and Disease“ (DOHaD)-Hypothese besagt, dass eine nachteilige mütterliche Umgebung während der intrauterinen Entwicklung eines Individuums großen Einfluss auf den Phänotyp des Erwachsenen und die Entwicklung von Krankheiten im Erwachsenenalter hat. Als multifunktionales Organ, welches Nährstoffe metabolisiert, synthetisiert und an den Fetus transportiert, beeinflusst die Plazenta den mütterlichen, plazentaren und fetalen Stoffwechsel. Daher bestimmt die Plazenta den Verlauf der fetalen Entwicklung und spielt eine wichtige Rolle in der fetalen Programmierung. Epigenetische Mechanismen beinhalten das Potential der Genregulation als Reaktion auf Reize aus der Umwelt und sind somit ein entscheidender Faktor in der Pathogenese von komplexen Erkrankungen, die durch sexuellen Dimorphismus in ihrer Häufigkeit und Schwere gekennzeichnet sind.

Die vorliegende Arbeit untersucht die intrauterine Programmierung der feto-plazentaren Zellen durch Gestationsdiabetes (gestational diabetes mellitus=GDM), wofür Endothelzellen aus zwei verschiedenen Gefäßbetten, arterielle (AEC) und venöse Endothelzellen (VEC) verwendet wurden. Der zelluläre Ansatz wurde durch Zugabe von Cytotrophoblasten (CT) und Syncytiotrophoblasten (SCT) erweitert, um den Einfluss von fetalem Geschlecht auf plazentare Genexpression zu untersuchen.

Primäre AEC isoliert aus humanen Plazenten am Gestationsende nach GDM (diabetische AEC) unterscheiden sich unter identischen Kulturbedingungen in ihren funktionellen Eigenschaften, z.B. Proliferation und Netzwerkbildung, von Zellen, die nach gesunden Schwangerschaften isoliert wurden (normale AEC). Genomweite DNA-Methylierungs- und Transkriptionsprofile von normalen und diabetischen AEC und VEC zeigen deutliche individuelle diabetische Charakteristika, welche die beobachteten funktionellen Unterschiede akzentuieren und möglicherweise erklären. Alle vier *in vitro* analysierten Zelltypen variierten im Maße der geschlechtsbeeinflussten Genexpression, trotz der Tatsache, dass diese Zellen aus demselben Organ stammen.

Insgesamt zeigen die Daten, dass sich die feto-plazentaren Endothelzellen von GDM Schwangerschaften anhaltend von Zellen von unkomplizierten Schwangerschaften unterscheiden. Dies zeigt, dass die plazentaren Endothelzellen

in vitro ihren diabetischen in vivo Phänotyp beibehalten. Ferner argumentieren die beobachteten Unterschiede in der Genexpression und die funktionellen Unterschiede zwischen männlichen und weiblichen feto-plazentaren Zellen für eine intrinsische Programmierung, die den Zellen die Erinnerung an ihr fetales Geschlecht ermöglicht. Daher erbringt diese These neue Beweise für ein zelluläres Gedächtnis und intrinsische zelluläre Veränderungen in Abhängigkeit von 1) der *in utero* Exposition gegenüber unerwünschten intrauterinen Bedingungen wie z.B. GDM, 2) des betroffenen plazentaren Gefäßbettes d.h. arteriell vs. venös und 3) des fetalen Geschlechts. Es ist plausibel, dass diese intrinsischen Veränderungen während der intrauterine Entwicklung zu einer veränderten Krankheitsanfälligkeit im Erwachsenenalter beitragen.

Contents

1. INTRODUCTION 1

1.1. THE PLACENTA 1
1.1.1. PLACENTAL DEVELOPMENT 1
1.1.2. PLACENTAL STRUCTURE AT TERM 2
1.1.3. PLACENTAL CELL TYPES FORMING PLACENTAL VILLI 3
1.1.3.1. TROPHOBLAST EPITHELIUM 4
1.1.3.2. VILLOUS VESSEL ENDOTHELIUM 4
1.2. GESTATIONAL DIABETES MELLITUS 6
1.3. DEVELOPMENTAL ORIGINS OF HEALTH AND DISEASE – THE INTRAUTERINE PROGRAMMING 7
1.3.1. EPIGENETIC MECHANISMS IN FETAL PROGRAMMING 8
1.3.2. PROGRAMMING BY GDM 10
1.3.3. PROGRAMMING OF CELL TYPE 11
1.3.4. PROGRAMMING BY FETAL SEX 13

2. HYPOTHESIS AND OBJECTIVES 15

3. MATERIALS AND METHODS 17

3.1. ETHICS STATEMENT 17
3.2. ISOLATION, CULTURE AND CHARACTERIZATION OF THIRD TRIMESTER HUMAN PLACENTAL AEC AND VEC 17
3.3. ISOLATION, CULTURE AND CHARACTERIZATION OF THIRD TRIMESTER HUMAN PLACENTAL TROPHOBLAST CELLS 17
3.4. DETERMINATION OF CELL NUMBER 18
3.5. DETERMINATION OF PROLIFERATION BY DIRECT COUNTING OF VIABLE AND DEAD CELLS 18
3.6. DETERMINATION OF PROLIFERATION BY MEASURING BROMODEOXYURIDINE (BRDU) INCORPORATION INTO DNA USING ENZYME-LINKED IMMUNOSORBENT ASSAY (ELISA) 18
3.7. FLOW CYTOMETRIC ANALYSIS OF CELL CYCLE AND CELL SURVIVAL 19
3.8. EXPRESSION OF CELL ADHESION MOLECULES IN AEC 20
3.9. DETERMINATION OF THE RELATIVE LEVELS OF CYTOKINES AND CHEMOKINES IN THE CONDITION MEDIA OF AEC 20
3.10. QUANTITATIVE DETERMINATION OF CYTOKINES AND CHEMOKINES IN THE CONDITION MEDIA 21
3.11. CELL CYCLE PROTEIN ARRAY 22
3.12. *IN VITRO* 2D-NETWORK FORMATION ASSAY ON MATRIGEL 23
3.13. RNA ISOLATION AND VALIDATION 24
3.14. SEX CONFIRMATION 24
3.15. RNA MICROARRAY HYBRIDIZATION AND SCANNING 24
3.16. BIOSTATISTICAL ANALYSIS OF MICROARRAY DATA 25
3.17. SEMI QUANTITATIVE RT-PCR 26
3.18. GENOME-SCALE DNA METHYLATION ANALYSIS (ILLUMINA HUMANMETHYLATION450) 26
3.19. LOCUS-SPECIFIC DNA METHYLATION 27

4. RESULTS 29

4.1. *IN UTERO* PROGRAMMING BY GDM 29
4.1.1. PROLIFERATIVE CAPACITY OF HUMAN PLACENTAL AEC IS REDUCED BY GDM 29

4.1.2. Different proliferation rate of diabetic AEC is a consequence of changes in the cell cycle and not in cellular apoptosis 31
4.1.3. Expression of cell cycle related proteins is altered in GDM 33
4.1.4. 2D-network formation of human placental AEC is increased by GDM 33
4.1.5. Hyperglycemia alters 2D-network formation of normal AEC 35
4.1.6. Correlation of proliferation and 2D-network formation with maternal, newborn and placental clinical parameters 36
4.1.7. Markers of low-grade inflammation 37
4.1.8. Cell adhesion molecules 40
4.2. *In utero* programming of cell phenotype 41
4.2.1. Influence of GDM on global DNA methylation profile of human placental AEC vs. VEC 41
4.2.2. Distinct and shared GDM signatures in DNA methylation profile of placental AEC vs. VEC 46
4.2.3. Influence of GDM on transcriptome of human placental AEC vs. VEC 48
4.2.4. Concordant methylation and expression changes 53
4.2.5. GDM programming by DNA methylation might influence cellular function of AEC 56
4.3. *In utero* programming by fetal sex 58
4.3.1. Sex dependent gene expression in four distinct feto-placental cell types 58
4.3.2. Sex dependent gene expression profile differences in trophoblast epithelium vs. villous vessel endothelium 62
4.3.3. Sex regulated genes in villous vessel endothelium and trophoblast epithelium and implications for biological relevance 63
4.3.4. Fetal sex influences proliferation and 2D-network formation of AEC 72

5. DISCUSSION 74

5.1. Feto-placental endothelial cells remember their *in utero* diabetic environment 75
5.2. Feto-placental endothelial cells display cell type specific metabolic memory 78
5.3. Feto-placental cells remember fetal sex 80

6. REFERENCES 84

1. Introduction

1.1. The placenta

The placenta is a highly specialized, transient fetal organ that supports the normal growth and development of the fetus throughout the course of pregnancy. During pregnancy growth and function of the placenta are precisely regulated and coordinated to ensure adequate exchange of nutrients and waste products between the maternal and fetal circulations. The placenta acts to provide oxygen and nutrients to the fetus, mediated by feto-placental arteries, whilst removing carbon dioxide and other waste products, by feto-placental veins. The placenta helps to protect the fetus against certain xenobiotic molecules, infections and maternal diseases. It metabolizes a number of substances and releases metabolic products and hormones into both, maternal and fetal circulations to affect pregnancy, parturition, metabolism, fetal growth, and other functions. Many placental functional changes occur that accommodate the increasing metabolic demands of the developing fetus throughout gestation (1).

1.1.1. Placental development

During the first days of pregnancy the fertilized egg undergoes a series of mitotic divisions forming a cluster of cells called morula. With further divisions and polarization of morula a peripheral layer, trophoectoderm, and an inner cell mass layer, embryoblast, are formed. During the course of pregnancy trophoectoderm will differentiate into the placenta and embryoblast will develop into the fetus (2).

Differentiation of trophoectoderm begins with the formation of distinct trophoblast cell types required for the complex biological processes of implantation, immunological adaption and vascular connection to the maternal circulation that will ultimately provide blood flow to the placenta (3). Attachment of the blastocyst and implantation into the maternal endometrium (decidua), is preceded by secretion of multiple mediators i.e. prostaglandins, proteolitic enzymes, chemokines and cytokines (4). As the blastocyst invasion proceeds, the mononucleated trophoblast cells, cytotrophoblasts (CT), proliferate and fuse to form an outer syncytium of terminally differentiated syncytiotrophoblast (SCT). Within SCT vacuolae are formed

that fuse to form lacunae. Lacunae are the primitive intervillous space that will be filled with maternal blood with erosion of maternal capillaries.

To enable nutrient and waste exchange between the mother and the fetus the human placenta is highly vascularized, and the main exchange unit is called placental villus. In the placenta there is no sprouting of embryonic vessels through the umbilical cord that connects the fetus to the placenta, and placental blood vessels are formed by vasculogenesis within the connective tissues of the placenta. The vessel connection and further growth of the villous tree are achieved by angiogenesis. Early villus development begins by the invasion of CT into SCT layer forming a primary villous with the central core of CT. Fetal mesenchyme invades primary villi transforming them into secondary villi. Fetal capillaries formed in the mesenchyme, convert the secondary villi to tertiary villi that undergo progressive branching and thinning (2).

1.1.2. Placental structure at term

Placenta at term weighs an average of 500 g (5) and its weight is directly proportional to fetal weight. It connects to the fetus by an umbilical cord which contains two umbilical arteries and one umbilical vein (6). The umbilical cord inserts into the chorionic plate and the vessels branch out over the surface of the placenta. This results in the formation of villous tree structures that are, on the maternal side, grouped into cotyledons (Figure 1).

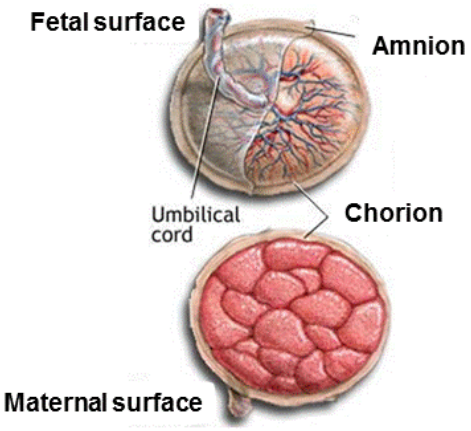

Figure 1. Illustration of the human placenta at term. The illustration depicts the chorionic or fetal side of the placenta. The umbilical cord inserts within the chorionic plate and the chorionic vessels are shown supplying each cotyledon. The veins carry oxygenated blood, red, while arteries carry deoxygenated blood, blue. The surface seen in the lower illustration is in contact with the maternal endometrium, decidua, and is divided into cotyledons. Downloaded and modified from http://www.healthtip.info/week-after-week-development-of-the-fetus-during-pregnancy.

1.1.3. Placental cell types forming placental villi

As already noted, placental chorionic villi are the main units for exchange of nutrients and waste products between the mother and the fetus. Placental villi are finger-like structures that form a tree-like structure composed of intermediate villi that branch and form terminal villi (Figure 2). Cross section of a terminal mesenchymal villus reveals distinct cell types each bearing a specific function (Figure 3).

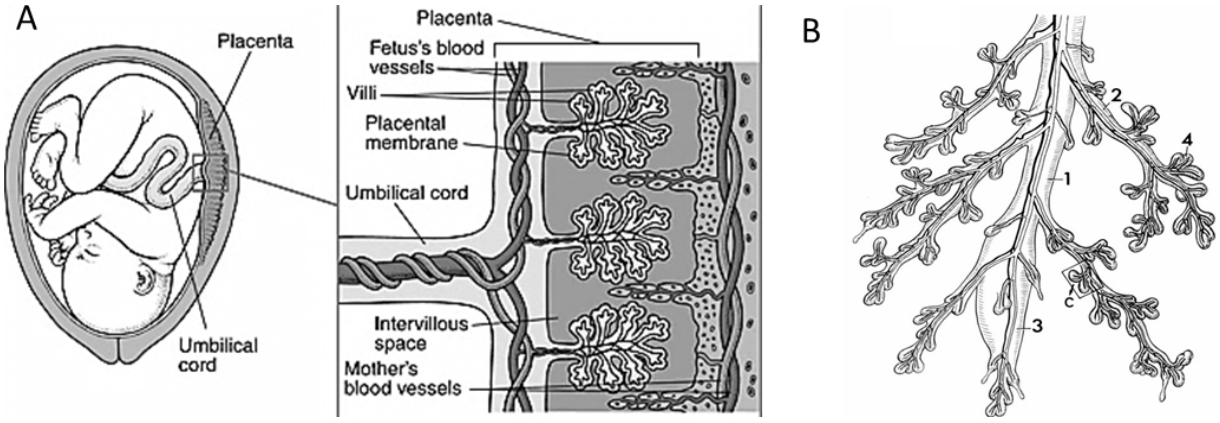

Figure 2. Simplified illustration of the human placental cross section and placental villus tree. Placental cross section reveals complex villous trees that function as main exchange units between the mother and the fetus. The chorionic villous trees project from the chorionic plate into the intervillous space and bathe in maternal blood coming from maternal arteries (A). Peripheral ramifications of the mature villous tree (B), consisting of a stem villus (1), which continues in a bulbous immature intermediate villus (3); the slender side branches (2) are the mature intermediate villi, the surface of which is densely covered with grape-like terminal villi (4). Parts of the illustration are taken and modified from http://www.merckmanuals.com/ home/womens_health_issues.html and from (7).

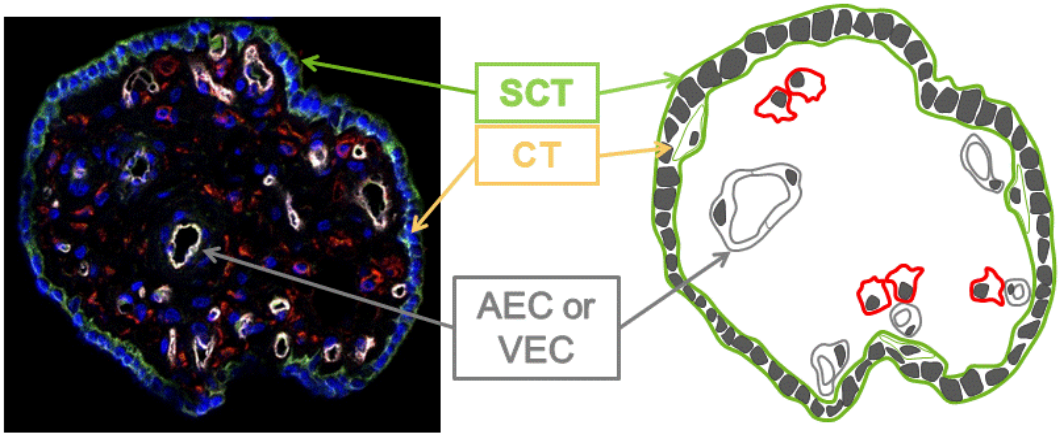

Figure 3. Constituents of a terminal villus. On the right is an immunohistological staining of a human placental terminal villus cross section and on the left its simplified illustration. The outermost layer, trophoblast epithelium i.e., syncytiotrophoblast (SCT) and cytotrophoblasts (CT) (syncytial progenitors) is bathed by the maternal blood while the fetal circulation is in direct contact with villous vessel endothelium, composed of arterial (AEC) and venous endothelial cells (AEC).

1.1.3.1. Trophoblast epithelium

The outermost layer of the placental villi is comprised of a surface layer of multinucleated SCT that is in direct contact with maternal blood and that shares a basement membrane with a subjacent stem-cell population of mononucleated CT that differentiate and fuse with the syncytium (Figure 3). In terms of fetal-maternal communication, it is mainly the syncytialized trophoblast that orchestrates the complex biomolecular interactions between the fetus and the mother. Not only do placental trophoblasts provide structural and biochemical barriers between the maternal and the fetal compartments during pregnancy, they also serve as an important endocrine organ that synthesizes and secretes many proteins and steroid hormones and growth factors, including placental lactogen and chorionic gonadotropin that support and regulate placental and fetal development (7,8).

A myriad of studies have shown that mononucleated CT isolated by enzymatic digestion of term placental tissue and cultured in medium containing fetal calf serum or bovine serum aggregate and fuse to form a multinucleated syncytium that synthesizes and secretes placental lactogen, chorionic gonadotropin, progesterone and many other proteins and steroids that are secreted by SCT *in vivo* (9,10).

The in vitro differentiation of primary human CT to a SCT phenotype has been arbitrarily divided into two stages (Figure 3). During the initial stage, referred to as morphological differentiation, the villous CT proliferate, aggregate and fuse to form a syncytium. During the second stage, referred to as biochemical differentiation, the cells begin to express genes involved in substrate transport, hormone synthesis and secretion, metabolism, and other functions of terminally differentiated SCT. Several studies have demonstrated that the two phases of differentiation are linked and that morphological differentiation is required before the cells undergo biochemical differentiation (9,10).

1.1.3.2. Villous vessel endothelium

The villous vessel endothelium is derived from the mesoderm and its inner surface is lined by a monolayer of endothelial cells. Arterial endothelial cells (AEC) line the feto-placental arteries and venous endothelial cells (VEC) line the feto-placental veins (Figure 3). In general, endothelium participates in several processes including control of vascular tone, developing and remodeling of the vasculature and blood

flow and trafficking of nutrients and gases. Arteries and veins differ in their morphology and function. Veins are usually larger in diameter than arteries with thinner walls. The walls are mainly composed of collagens and elastic fibers enabling the vessels to stretch, and smooth muscle cells that provide support. Endothelial cells are heterogeneous concerning their morphology and function and differ according to their origin. AEC are usually thicker than VEC and are long and narrow, probably as a consequence of their alignment in the direction of the undisturbed blood flow. VEC are short and wide, due to the lower blood flow in the venous as compared to the arterial circulation. In general in the body, arteries transport oxygenated blood to the tissues, whereas veins transport low oxygenated blood. The exceptions are the pulmonary and the placental vascular system (11).

Importantly, when isolated feto-placental AEC and VEC maintain their different phenotype *in vitro* (Figure 4). AEC have a polygonal cell shape with a smooth surface and grow in a characteristic endothelial cobblestone-like pattern whereas the VEC have a spindle-shaped appearance growing closely apposed to each other, reaching in confluence a fibroblastoid form. Furthermore, these cells express different sets of genes and have distinct functions, as they respond to distinct growth factors (11,12).

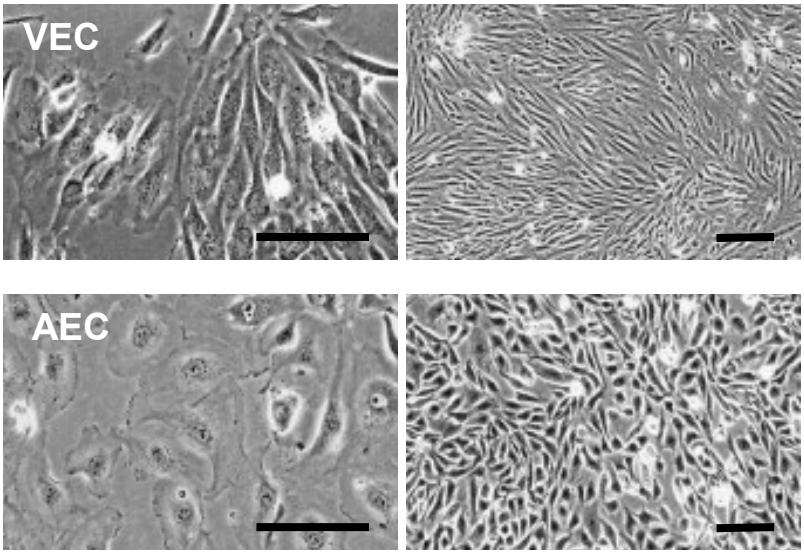

Figure 4. **Phase-contrast micrographs of arterial (AEC) and venous (VEC) placental endothelial cells.** AEC have polygonal-shape, grow in loose arrangements and exhibit the classical cobblestone-like appearance, whereas spindle-shaped VEC, grow closely apposed to each other and form swirling monolayers. Scale bar = 100µm.

Although endothelial cells originate from the same embryonic precursor cells (hemangioblasts), they exhibit different morphology, behavior and function depending on their vascular bed (13,14).

The placental villous vessel endothelium is continuous with the fetal vasculature and transports fetal blood. As such it is subject to influence of any change occurring in the fetal circulation. Moreover, because of its high degree of vascularisation and easy assessment, the placenta is an excellent source of feto-placental endothelial cells, AEC and VEC (12).

Aside from the vascular endothelium, villus stroma comprises several other cell types i.e. pericytes, fibroblasts, macrophages ("Hofbauer cells"), mesenchymal, smooth muscle, reticulum, mast, natural killer and plasma cells (7,15,16).

1.2. Gestational diabetes mellitus

Maternal gestational diabetes mellitus (GDM) is a glucose intolerance state due to a transient insulin resistance and is characterized first by maternal and subsequently by fetal hyperglycemia (17). GDM clinically manifests in the 2nd gestational trimester and usually resolves after birth. Despite the short duration GDM has been shown to affect perinatal outcome and it is known to exhibit long term consequences for both, the mother and the offspring. Long term implications of GDM include increased risk of later diabetes in the mother and metabolic disorders including Type II diabetes, obesity or hypertension in the offspring. As other types of diabetes and resulting from the obesity epidemic, GDM is a growing problem worldwide. Only in Europe, on average 2-6% of all pregnancies are affected by GDM, bearing in mind the high prevalence populations such as Finland, the West of Ireland and Sardinia reaching 22% (18). Besides obesity, high maternal age, parity, and previous delivery of a macrosomic infant are well established predictors of GDM (19).

The most prominent long term consequences of diabetes and hyperglycemia are endothelial and vascular dysfunction that associate with macro- and microangiopathies and hence, significantly contribute to the mortality and morbidity of diabetes (20,21). Hyperglycemia is the leading cause of endothelial dysfunction however, other factors and conditions altered in diabetes i.e. insulin sensitivity, hyperinsulinemia and altered leptin levels may also contribute (22,23).

1.3. Developmental origins of health and disease – the intrauterine programming

The 'Developmental Origin of Health and Disease' (DOHaD) hypothesis holds that the adverse maternal environment i.e. diet (24), smoking (25) and diabetes (26-29) has great influence on adult phenotype and disease development in adulthood by affecting the events occurring during the intrauterine life of an individual (Figure 5). As a multifunctional organ that synthesizes, metabolizes, and transports nutrients to the fetus and as a vital source of hormones, the placenta influences maternal, placental and fetal metabolism. Hence, it determines the course of fetal development and plays a key role in fetal programming. Importantly, disease development in adulthood has been linked to altered placental function in pregnancy complications (30).

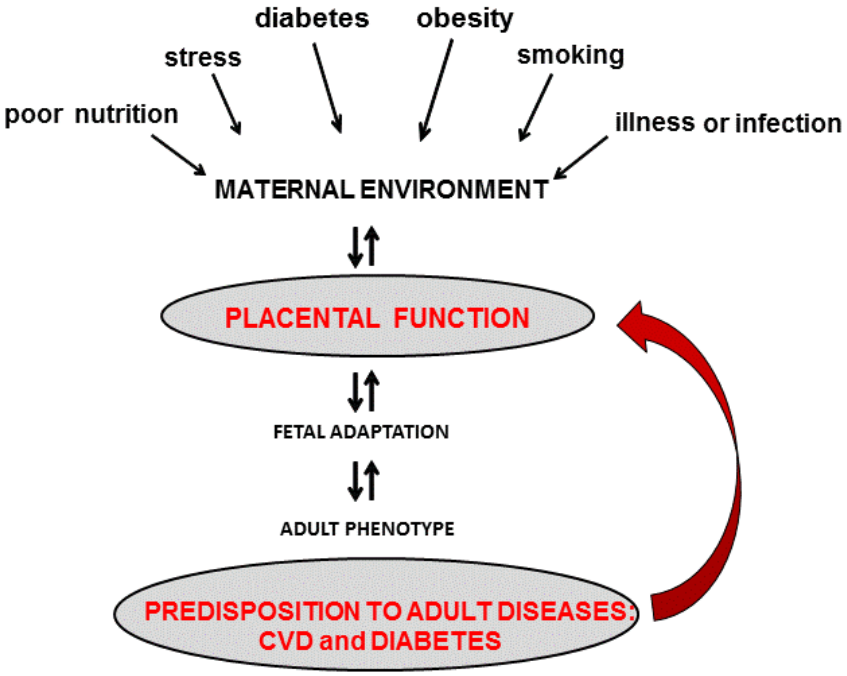

Figure 5. Illustration showing influence of the maternal environment on disease development in adults and the role of the placenta. Altered maternal environment has been shown to have a great impact on adult phenotype and disease development in adulthood. Due to its role as the interface between the mother and the fetus placenta plays a crucial role in fetal programming.

Adverse intrauterine environment can cause permanent changes that influence disease development in adults. The genotype of an individual has been shown to account for a small portion of heritability of complex diseases and cannot be shaped by the environment unlike epigenetic mechanisms. Epigenetic gene regulation is a key factor in the pathogenesis of complex disorders (31).

1.3.1. Epigenetic mechanisms in fetal programming

Due to their complexity and environmental plasticity epigenetic mechanisms have been mostly proposed to drive fetal programming and disease susceptibility in adults. They are chromatin based mechanisms important in the regulation of gene expression that do not involve changes in the DNA sequence. Epigenetic mechanisms include DNA methylation, histone packing, posttranslational modifications of histones and RNA-based mechanisms (32) (Figure 6).

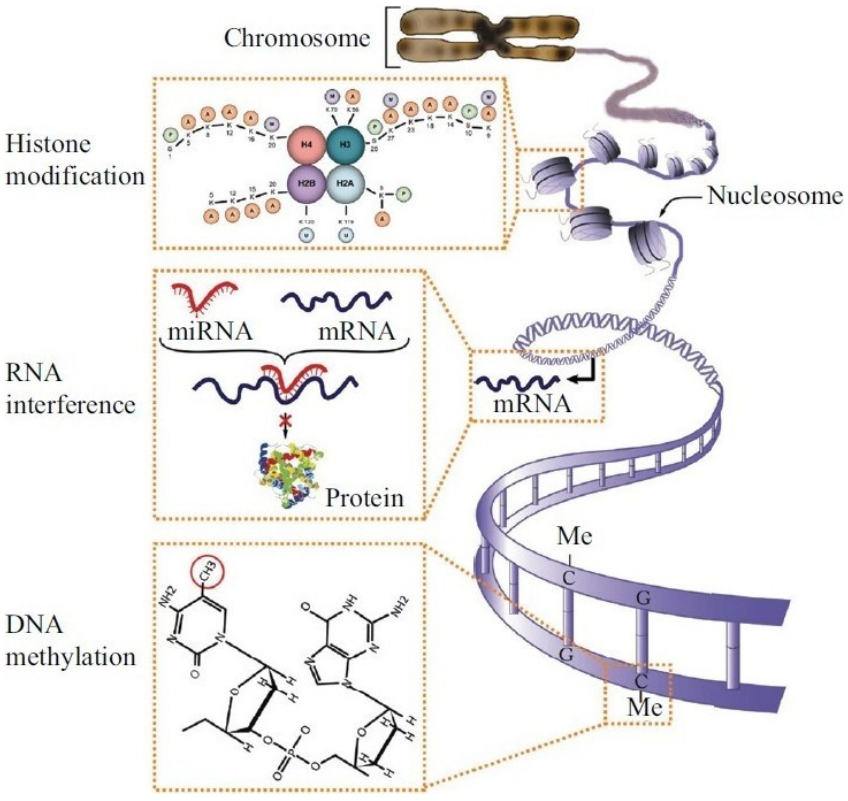

Figure 6. Illustration of the epigenetic mechanisms implicated in the regulation of gene expression. DNA methylation, histone modifications, and RNA-mediated gene silencing constitute three distinct mechanisms of epigenetic regulation. DNA methylation is a covalent modification of the cytosine (C) that is located 5' to a guanine (G) in a CpG dinucleotide. Histone (chromatin) modifications refer to covalent post-translational modifications of N-terminal tails of four core histones (H3, H4, H2A, and H2B). The most recent mechanism of epigenetic inheritance involves RNAs. Reproduced from (33).

DNA methylation describes the process of adding a methyl group to the 5'-position of cytosine to form 5-methyl-cytosine (34). It is catalyzed by four distinct enzymes, DNA methyltransferases (DNMTs). DNMT1, the "maintenance" methyltransferase, transmits DNA methylation patterns during mitotic cell division. In contrast, DNMT2, DNMT3a and DNMT3b function act as *de novo* methyltransferases that establish DNA methylation patterns during embryonic development (34). On the basis of its potential to silence promoters, DNA methylation has been hypothesized to play an important role in cell-type-specific gene expression. Rare examples of tissue-specific promoter DNA methylation exist (35,36), while other studies on individual genes failed to establish a strong connection between changes in expression and dynamic methylation (37). Indeed, ~60% of genes in mammalian genomes contain promoter-proximal CpG islands, which are believed to be always unmethylated (38). Recent comprehensive datasets confirmed that most CpG island promoters are unmethylated in different types of human primary cells, but revealed that a subset (2–5%) of CpG island promoters show high DNA methylation in primary tissues (35,39-41). Moreover, CpG island methylation has also been reported to regulate lineage-specific expression in the Rhox gene cluster (42). Thus, protection of CpG islands from *de novo* methylation can be overcome in primary cells on specific target genes. Furthermore, comparison of methylation profiles between tissues suggests that a large proportion of differentially methylated regions is located outside promoters (39,40), suggesting that DNA methylation could also modulate the activity of distal enhancers. Moreover, non-CpG methylation has been observed in early development, endogenous LINE-1 retroelements, and integrated plasmid DNA. Several studies indicate that DNA methylation is involved in the maintenance rather than the initiation of gene silencing (43).

In the nucleus, DNA is packaged into chromatin as repeating units of nucleosomes, which form a "beads-on-a-string" structure that can compact into higher order structures to affect gene expression. Nucleosomes are composed of 146-bp DNA wrapped in histone octamers (composed of two H2A, H2B, H3, and H4) and are connected by a linker DNA, which can associate with histone H1 to form heterochromatin. Histone proteins contain a globular domain and an amino-terminal tail, with the latter being posttranslationally modified. Currently, more than 60 modifications have been described, including the posttranslational modification

of lysine (acetylation, methylation, ubiquitination, sumoylation), arginine (methylation), and serine and threonine (phosphorylation). Many of these modifications are known to play functional roles in transcription (Table 1). The histone code hypothesis proposes that the combination of histone posttranslational modifications encode regulatory information interpretable by the cell (43).

RNA-based mechanisms of epigenetic gene regulation involve the coordinated activities of noncoding RNAs (ncRNA) with other epigenetic activities, such as DNA methylation and histone posttranslational modifications. Studies suggest that long and short ncRNAs, which are distinguished by an arbitrary size cutoff of 200 nucleotides, can regulate the chromatin state of genomic loci (65). A large number of large intervening non-coding RNAs (lincRNAs) have just been described in the genomes of humans and mice. A total of ~3,300 lincRNAs have been identified with computationally predicted roles in various cellular processes, including cell-cycle regulation (44). lincRNAs can recruit chromatin modifying activity and regulate gene expression at target loci (44).

Importantly, epigenetic marks like DNA methylation can permanently modify the phenotype and be propagated during cell division and even transmitted to the next generation. Epigenetic modifications are dynamic (reversible) and subject to both internal and external influences. Hence, they bare the potential to explain the mechanisms involved in the gene-environment interactions, sexual dimorphism, and metabolic programming during fetal development (31).

1.3.2. Programming by GDM

There is mounting evidence that the diabetic intrauterine environment can program the fetus and determine the long term development of the offspring into adulthood. This is supported by a variety of long term consequences of GDM for the fetus in adulthood. These include a higher risk for developing metabolic disorders and vascular dysfunction (26-29) highlighting the role of the intrauterine environment on later life. By 7-14 years, offspring of diabetic pregnancies have significantly higher systolic and mean arterial blood pressure than offspring of non-diabetic pregnancies (45) and this was independent of adiposity of the offspring (46). Also children born to GDM pregnancies have increased cardiovascular risk biomarkers (47).

In a pregnancy complicated by GDM, maternal hyperglycemia leads to fetal hyperglycemia, and consequently to fetal hyperinsulinemia. Hence, it is not only the

mother possessing metabolic and hormonal derangements, but also the placenta and other fetal tissues are compromised. Endothelial dysfunction has been demonstrated in women with GDM (48), and there is evidence for endothelial dysfunction in the placenta and the umbilical cord, both fetal tissues (49,50). Feto-placental endothelial dysfunction in GDM was shown by an altered response to vaso-relaxing agents (51,52). Furthermore, the expression of junction molecules in the placental vasculature is affected by GDM (53) as well as the growth of new blood vessels (54).

In the placenta, the growth of blood vessels from preexisting ones is achieved by angiogenesis and it is crucial for placental growth and development. It serves to maintain demanding placental functions throughout the pregnancy by enabling adequate exchange between the mother and the fetus. Placentas of diabetic pregnancies are characterized by increased weight and size (55,56) and demonstrate increased capillary proliferation (57) that may affect the feto-maternal exchange rates. Notably, alterations in placental transport and metabolism i.e. the expression of the glucose transporter GLUT1 have been reported (58). Hence, the fetuses are exposed to distinct metabolic abnormalities in GDM pregnancies. As a consequence of an increased metabolic demand to increased glucose levels fetal hypoxia arises and lower oxygen levels are reported for both, umbilical artery and vein (59). Furthermore, high glucose concentrations in diabetes can lead to increased ROS production in the feto-placental circulation. Diabetic patients generally have impaired antioxidant defense mechanism and thus an imbalance between ROS production and the antioxidant defense mechanisms and oxidative stress (2). Excessive ROS production can further lead to massive cellular damage of proteins, lipids and DNA (60).

Several studies have reported that oxidative stress appears to be a key event in diabetic complication (61). This notion is supported by the findings of reduced antioxidant capacity of superoxide dismutase in diabetic women (62). Also mitochondrial superoxide production is increased under hyperglycemic conditions as compared to cells cultured at low glucose levels (63).

1.3.3. Programming of cell type

Increasing evidence linking environmental exposures in early life to later risk of cardiovascular disease has led to rising interest in the process of vascular

development *in utero* (64,65). In general, there are two vascular beds, arterial and venous, defined by physiologic factors such as the direction and pressure of blood flow and by functional and anatomical differences such as the arrangement of smooth muscle cells around the vessels. Not surprisingly, given their different physiologic functions, the identity of arterial and venous endothelial cells is established before the onset of circulation (66,67) in association with distinct gene expression signatures that define endothelial cell identity (12,68). This includes endothelial nitric oxide synthase (eNOS, *NOS3*), von Willebrand factor (*VWF*), vascular endothelial cadherin (VE-cadherin, *CDH5*), intracellular adhesion molecular-2 (*ICAM2*), vascular endothelial growth factor receptor tyrosine kinases VEGF-R1 (*FLT1*) and VEGFR2 (*FLK1*, *KDR*), angiopoietin receptors *TIE1* and *TIE2* (TEK) and *NOTCH4* [Reviewed in (32,69)]. Notably, the feto-placental AEC and VEC show distinct patterns of gene expression potentially explaining their different phenotype. Importantly, different phenotype characteristic of AEC and VEC are maintained after isolation and during *in vitro* culture (for more detail see 1.1.3.2.).

Numerous lines of evidence suggest that the endothelial compartment represents a potential target tissue for transmission of environmentally mediated risk of complex disease via a process of epigenetic disruption in early development (70,71). Epigenetic mechanisms, including DNA methylation, are now widely accepted to underpin developmentally regulated changes in cell morphology and function (72), however little is known about the role of such modifications, and their relative plasticity, during endothelial cell development. It is clear that one of the key regulators of vascular function, *NOS3* is under epigenetic control by several mechanisms, including DNA methylation (73). Importantly, NOS3 and other genes implicated in specific endothelial function i.e. *NOS2, vWF*, *NOTCH4*, *KDR*, *SELE* showed distinct DNA methylation patterns between feto-placental AEC and VEC. Furthermore, *NOS3* and *VWF* showed reciprocal directions of DNA methylation and gene expression change (Joo JE et al, 2013) confirming cell type specific regulation. These and other concordantly regulated genes were linked to specific cellular pathways such as “cardiovascular pathway genes” by gene ontology software (Joo JE et al, 2013).

1.3.4. Programming by fetal sex

Males and females express multiple phenotypic differences, but recent attention has focused on molecular mechanisms underlying sexual dimorphism in mammals and the sex-biased susceptibility for selected diseases in adulthood. Moreover, predisposition to many adult diseases originates *in utero*, secondary to placental dysfunction, a hypothesis commonly referred to as the Developmental Origins of Health and Disease (DOHaD). Importantly, fetal sex influences *in utero* development in both uncomplicated pregnancies and pregnancies with sub-optimal outcomes. For example, male fetuses have a higher risk for peri- and postnatal mortality and are generally larger than female (74-77). In addition, male fetuses in pregnancy maladies have poorer outcomes than female fetuses (78,79) and are more likely to develop hypertension, diabetes mellitus, or metabolic syndrome (80,81).

Sex influences on fetal programming are supported by a plethora of animal studies. For example, dietary interventions in experimental animals results in sex-specific changes in the placental methylome and transcriptome (82-84).

Differences in the expression of genes that are dependent upon fetal sex have recently been identified to influence several key signaling pathways in the placenta, including insulin-like growth factors, responses to cortisol, and placental cytokine cascades (85). Murphy and colleagues (86) speculate that male fetuses adapt placental functions to allow for maximal fetal growth in a potentially hostile maternal allograft environment, while female fetuses reduce growth to survive such maternal influences *in vivo*. *In utero* adjustments of male and female fetuses precede observed differences in survival in the first 48 hours of preterm neonates during postnatal life: female neonates adapt better than male neonates to *ex utero* life, especially when delivered at very early gestational ages compatible with survival (87).

The above observations raise the theory that functional differences in gestations from male and female fetuses may be influenced by sex-biased gene expression in placental villi. Support for this theory of sex-bias in gene expression is derived from initial observations of single (85), and global (88) gene expression in biopsies of whole villi. The term ‘placental sexome’ reflects the sum of sex-biased effects on gene networks and cell systems (89). Identification of cell types and

dissection of the mechanisms involved in sex-specific regulation will likely reveal novel pathways of physiological regulation and targets for therapeutic interventions.

2. Hypothesis and Objectives

Developmental origins of health and disease paradigm suggest nutritional and endocrine cues during intrauterine life for setting long-term functional, biological and behavioral strategies for the postnatal life. Epigenetic mechanisms have the capacity to respond to distinct environments and they are important regulators of development, cell-and tissue-specific gene expression and can be inherited by the next generation.

Complex diseases in adulthood that associate with endothelial dysfunction i.e. cardiovascular disease and diabetes have now been proposed to originate *in utero* and their susceptibility is known to differ between males and females. Of utmost importance is the maternal metabolic state that influences placental and consequently fetal development. Maternal diabetes is known to cause changes in the fetal environment and may thus affect the endothelial cells lining the feto-placental vasculature.

Against this background it was hypothesized that fetal programming relies on the capacity of distinct feto-placental cell types to memorize the intrauterine environment they were exposed to. Hence, distinct *in vivo* metabolic milieu will cause permanent changes in the feto-placental cells influencing their gene expression and function and giving rise to an intrinsic biological program that will persist during *in vitro* culture. The intrinsic cellular program will depend on the presence of a pregnancy disorder i.e. GDM, affected placental vascular bed i.e arterial vs. venous (cell type) and fetal sex.

In this context metabolic memory of feto-placental endothelial cells was investigated *in vitro* after *in utero* exposure to maternal diabetic environment. Firstly, the focus was placed on assessing endothelial function in AEC by investigating proliferation and 2D-network formation as a proxy measure of angiogenesis. To distinguish intrinsic from environmental factors AEC isolated from gestational diabetes mellitus (GDM) affected placentas (diabetic AEC) were cultured under identical culture conditions as their healthy counterparts (normal AEC). Subsequently both, normal and diabetic cells were exposed to normal and diabetic cord blood serum (CBS) to test for environmental effect. Secondly, to understand the nature of revealed differences global DNA methylation profile and global gene expression analysis were performed in cultured normal and diabetic AEC. Here,

also venous endothelial cells (VEC) were included, both normal and diabetic, to reveal common and cell type specific diabetic signatures. Lastly, the influence of fetal sex on cellular memory of four distinct feto-placental cell types, isolated after a health pregnancy, was investigated in terms of global gene expression analysis. Furthermore, the sex specific functional differences were investigated in feto-placental AEC by measuring proliferation and 2D-network formation.

3. Materials and Methods

3.1. Ethics statement

Informed written consent was obtained from the women and ethical approval was obtained from the Medical University of Graz, Graz, Austria for placentas used for the isolation of endothelial cells. Placentas for trophoblast isolation were obtained by a protocol approved by the IRB at Washington University School of Medicine, St. Louis, MO, USA. In both cases, the sex of the infant was recorded.

3.2. Isolation, culture and characterization of third trimester human placental AEC and VEC

Primary arterial (AEC) and venous endothelial cells (VEC) were isolated from third trimester human placentas after uncomplicated vaginal delivery or a caesarean section following a standard protocol (12). Endothelial cells were characterized by a rigorous immuno-cytochemical analysis and internalization of acetylated low-density-lipoprotein (Biomedical Technologies, Stoughton MA)(90). Unless stated otherwise, isolated AEC and VEC were cultured on 1% (v/v) gelatin-coated flasks (75 cm²) using Endothelial Basal Medium (EBM, Cambrex, Clonetics, USA) supplemented with the EGM-MV BulletKit (Clonetics). To mimic the oxygen variation in placental vascular beds AEC were expanded at 12% O_2 and 37^{o}C and VEC at 21% O_2 and 37^{o}C, respectively.

3.3. Isolation, culture and characterization of third trimester human placental trophoblast cells

Primary human villous CT were isolated following digestion of placental tissue from term, uncomplicated pregnancies with trypsin-dispase-DNAse and Percoll-gradient centrifugation, as described (91). The isolated CT were cultured at 21% O_2 and 37˚C in DMEM with 10% FBS, 20 mM HEPES pH7.4, and penicillin/streptomycin on 3.5 cm diameter tissue-culture-treated plastic plates with daily media changes. To obtain CT, cells were cultured for 24 h in the above medium, except using charcoal-stripped FBS, and samples were then collected. From 24-48 h of culture in this system, CT spontaneously and efficiently differentiate and fuse, as indicated by greatly increased hCG secretion and hPL secretion, and fuse, with over 80% of the

nuclei present in syncytium from 48-72 h of culture with the remaining present as mononucleated cells(91). After 48 h, culture medium was changed to media with charcoal-stripped FBS and SCT samples were isolated after 72 h of culture.

3.4. Determination of cell number

Prior to each experiment the number of AEC and/or VEC was determined by the cell counter and analyser system CASY 1® (Schärfe System GmbH, Reutlingen, Germany) using a 150 µm capillary. Measurements with this system are based on detection of conductivity changes along an aperture during the flow of a cell containing liquid. The result is a size distribution curve of the cells in which cell debris, dead cells and viable cells can be identified by their distinct diameters. Dead cells are characterized by the volume of their cell nucleus which solely contributes to the conductivity.

3.5. Determination of proliferation by direct counting of viable and dead cells

AEC were cultured as described previously in supplemented EBM with 5% FCS at 12%O_2. The cells were then harvested with trypsin/EDTA (Clonetics TM, Lonza Walkersville, Inc.) and resuspended in EBM with 5% FCS and without supplements. 6-well plates pre-coated with 1% gelatin were used for seeding. 75,000 viable cells were seeded per well in triplicates and cultured at 12% and 21% O_2 at 37^{o}C with daily media change. After 24, 48 and 96 h the cells were harvested and counted by automatic counting system CASY 1 (Schärfe System, Reutlingen, Germany) using a 150 µm capillary.

3.6. Determination of proliferation by measuring bromodeoxyuridine (BrdU) incorporation into DNA using Enzyme-linked Immunosorbent Assay (ELISA)

BrdU incorporation into the DNA of growing cells was used as a method to investigate cellular growth (92). The assay was performed according to manufacturer's instructions (CycLex BrdU ELISA Kit, CycLex Co., Ltd). After optimization for the appropriate cell density, 5,000 AEC were seeded per well in a 96-well micro-plate in a final volume of 100 µL of un-supplemented EBM with 5% FCS. After culture for 48 h at 21% O_2 and 37°C BrdU was added to a final

concentration of 10 µM and incubated for two hours at 37°C. Media was removed and cells were fixed and denaturized within 30 min incubation at room temperature. Fixing was followed by 1 h incubation with primary anti-BrdU monoclonal antibody and then 1 h incubation with HRP conjugated anti-mouse IgG secondary antibody and with washing steps in between. 50 µL of substrate reagent was added and after 15 min incubation the stop solution in the same order. Absorbance was measured immediately at 450/540 nm on FluoSTAR Optima 413 spectrofluorimeter (BMG Labtechnologies, Offenburg, Germany).

3.7. Flow cytometric analysis of cell cycle and cell survival

Cell cycle of AEC was assessed after 48 h by parallel analysis of total DNA content (7-AAD staining) and S-phase activity (BrdU staining for only newly synthesized DNA) by flow cytometry. The cells were prepared according to manufacturer's instructions (BD Pharmingen, San Jose, US). 8.000 cells/cm^2 were cultured for 48 h at 21% O_2 and 37°C. BrdU was added to a final concentration of 10 µM and incubated for two hours at 37°C. The cell pellet was collected and the cells were fixed and permeabilized with Cytofix/Cytoperm Buffer and after incubation on ice for 15 min washed with BD Perm/Wash Buffer. Cells were then pelleted (10,000 x g) and the pellet was resuspended in 100 µl BD Cytoperm Plus Buffer and incubated for additional 10 min on ice. Pellet was washed (BD Perm/Wash Buffer), re-fixed (Cytofix/Cytoperm Buffer) and incubated 5 min at room temperature. After washing the cells were treated with 60 µL DNase (300 µg/mL) for 1 h at 37°C to expose BrdU epitopes. The cells were then washed and stained for 20 min with flourochrome conjugated anti-BrdU. After the last washing step the cells were stained with 7-AAD and resuspended in 200 µL of staining buffer (PBS with 3% FCS and 0.09% sodium azide).

For the analysis of the cell survival the cells were cultured as described above and the assay was performed according to manufacturer's instructions (BD Pharmingen, San Jose, US). After pelleting, the cells were washed twice with cold 1X PBS, then resuspend cells in BD Cytofix/Cytoperm™ solution at a concentration of 10^6 cells/0.5 mL. The cells were incubated for 20 min on ice, pelleted and washed twice with BD Perm/Wash™ buffer (1X) at a volume of 0.5 ml buffer/10^6 cells at room temperature. After washing (BD Perm/Wash™ buffer) the cells were stained for 30 min at room temperature an anti-active caspase 3 antibody (rabbit,

PE). The cells were washed and then resuspended in 0.5 ml BD Perm/Wash™ buffer (1X) for measurement.

Both, cell cycle and cell survival was analyzed by flow cytometry at the Flow Cytometry Core Facility at the Center for Medical Research (ZMF) of the Medical University of Graz. Measurements were made using a BD FACSCaliburTM system (BD Biosciences) with BD CellQuest Pro software (BD Biosciences) for data analysis.

3.8. Expression of cell adhesion molecules in AEC

ICAM1, VCAM1, VE-cadherin and E-selectin expressions at the cell surface were measured by means of flow cytometry (FACSCalibur, BD Biosciences). AEC were gently detached by detachment buffer (25 mM HEPES (Boehringer Mannheim GmbH, Germany), 10 mM EDTA (Pierce, Rockford, IL) in Dulbecco's PBS without calcium and magnesium (PAA, Pasching, Austria)). Endothelial cells were incubated for 30 min at 4°C in dark with primary antibodies against ICAM1 (FITC mouse anti-human CD54; Beckman Coulter, Brea, CA, USA), VCAM1 (PE-CyTM5 mouse anti-human CD106; BD Pharmingen, San Jose, CA, USA), VE-cadherin (PE mouse anti-human CD144; BD Pharmingen, Vienna, Austria), and E-selectin (PE mouse anti-human CD62E; BD Pharmingen) which were diluted 1:40 or with respective isotype-matched control antibodies in antibody diluents solution (DAKO North America, Inc., CA, USA; catalogue number S3022). After the cells were washed once with PBS and were resuspended in fixative solution (FACS flow solution, distilled water, BD CellFixTM), flow cytometric analysis was performed by FACS Diva software (Becton Dickinson). Flow cytometric analyses were done in collaboration with Viktoria Konya and Akos Heinemann, from the Institute of Experimental and Clinical Pharmacology, Medical University of Graz.

3.9. Determination of the relative levels of cytokines and chemokines in the condition media of AEC

AEC condition media was collected after 48 h of culture and the array procedure was performed using ProteomeProfiler^{TM} kit for the parallel determination of the relative levels of selected human cytokines and chemokines according to the protocol provided by the manufacturer (R&D Systems Europe Ltd., Abingdon, UK). 4-Well Multi-dish was covered with 2.0 mL of Array Buffer 4 and membranes pre-

coated with the antibodies were placed on top and incubated for one hour on a rocking platform shaker. 500 µL of each sample was diluted in 1.5 mL of Array Buffer 4. 15 µL of reconstituted Human Cytokine Array Panel A Detection Antibody Cocktail was added to each prepared sample and the mix was incubated at room temperature for 1 h. Array Buffer 4 was then removed from the wells of the 4-Well Multi-dish and sample-antibody mix was added and incubated overnight at 2-8 °C on a rocking platform. Next day membranes were washed with 20 mL of 1X Wash Buffer 3 x for 10 minutes on a rocking platform shaker. 2 mL of the streptavidin-HRP, diluted in Array Buffer 5, was placed on the membranes and incubated for 30 min at room temperature on a rocking platform shaker. Membranes were finally washed and placed on the bottom sheet of the plastic sheet protector. 1 mL of the prepared Chemi Reagent Mix was evenly placed onto each membrane and incubated for 1 min. Membranes were then covered with a plastic wrap, placed in an autoradiography film cassette and exposed to X-ray film for 1 min.

3.10. Quantitative determination of cytokines and chemokines in the condition media

Concentrations of adiponectin and serpin E1 were determined by Human Obesity Base Kit and of IL6, IL8 and MCP1 by Human Base Kit A following manufacturer´s instructions (R&D Systems Europe Ltd., Abingdon, UK). The filter-bottomed microplate was pre-wet by adding 100 µL of Wash Buffer and dried by a vacuum manifold. Microparticle concentrate was mixed with microparticle diluent and homogenized by vortexing. 50 µL of the microparticle mixture was added to each well of the microplate. Addition of the same volume of sample followed. The plate was sealed with a foil and incubated for 3 h at room temperature on a horizontal orbital microplate shaker set at 500 ± 50 rpm. Using a vacuum manifold device the liquid was removed and each well was washed with Wash Buffer (100 µL) and removing the liquid again. Then 50 µL of diluted Biotin Antibody Cocktail was added to each well, covered with a foil plate sealer and incubate for 1 h at room temperature on the shaker set at 500 ± 50 rpm. After washing each well was incubated with 50 µL Streptavidin-PE for 30 minutes at room temperature on the shaker set at 500 ± 50 rpm. Wells were washed and the microparticles were resuspended by adding 100 µL of Wash Buffer to each well. After 2 min incubation

Bio-Rad Analyzer was used to read the plate. Standard curves were constructed following manufacturer´s instructions.

3.11. Cell cycle protein array

The level of cell cycle related proteins of AEC isolated from diabetic placentas vs. healthy controls was determined using an Antibody Microarray (Full Moon BioSystems, Inc, Sunnyvale, USA). The cells were seeded at a density of 8.000 cells/cm^2 and cultured for 48 h at 21% O_2 and 37°C. All preparation steps were carried out according to the manufacturer's instruction. Briefly, cells were washed once with ice-cold 1X PBS and around 2x10^6 cells were collected by scraping from the flaks. Cell suspension was washed again three times with ice-cold PBS and centrifuged at 4°C and 350 x g for 5 min. Cell pellet was dissolved in 200 µL Extraction Buffer, cell lysate was mixed rigorously by vortexing for 30 sec and immediately incubated for 10 min on ice and centrifuged at 4°C and 10.000 x g for 15 min. The clear supernatant was transferred to a new 1.5 mL Eppendorf tube and kept on ice. Meanwhile, preparation of gel columns was performed. Therefore columns were reconstituted by adding 650 µL of Labeling Buffer and vortexed vigorously for about 5 sec. Air bubbles were removed by sharply tapping the bottom of the column. The columns were kept at RT for 30 min to allow hydration. To remove excess fluid the columns were spun at 750 x g for 2 min and subsequently the protein extracts (100 µL) were carefully transferred to the centre the columns without disturbing the gel surface. Each column was placed in a collection tube and centrifuged at 750 x g for 2 min. The purified protein was collected and used for further steps. The protein concentration was determined using BCA protein assay according to the manufacturer's instruction. 2-10 µg/µL protein was filled up to a volume of 75 µL and 3 µL of Biotin/DMF solution was added to each protein sample. The mixture was incubated at RT for 1 h. 35 µL of Stop Reagent was added and incubated for another 30 min at RT with mixing. The samples were stored at -80°C until the following day. On the next day the Antibody Microarray slides were warmed up to RT for 45 min. In a 100 x 150 mm Petri dish each slide was blocked with 30 mL Blocking Solution on an orbital shaker rotating at 55 rpm for 30 min at RT. The slides were washed 6 x 10 min with 1X Washing Buffer at 55 rpm and twice with Milli-Q grade H_2O. The next step was to couple the protein sample. 50 µg biotin labeled protein was mixed with 100 µL Coupling Solution and

vortexed briefly. In the meantime, antibody spots on the slides were marked with a PapPen (DakoPen; Dako). All 100 µL Protein Coupling Mix was slowly pipetted on the slide and incubated in a Coupling Chamber for 1 h at RT in the dark covered with aluminum foil. After coupling, the slides were again washed 6 x 10 min with Washing Buffer and twice with Milli-Q grade H_2O. For detection, 60 µL of Cy3-Streptavidin (0.5 mg/mL) was added to 60 mL of Detection Buffer. Coupled slides were put in Petri dish and incubated with 30 mL of Cy-3 Streptavidin Solution on an orbital shaker at 55 rpm for 20 min at RT in the dark and subsequently washed 6 x 10 min with Washing Buffer and twice with Milli-Q grad H_2O. Excess water was shaken off and slides were dried with compressed nitrogen. The Microarray slides were scanned using DNA Microarray Scanner (Agilent Technologies, Santa Clara, USA) and relative protein expression was calculated using Gene pix pro 6.0 Software (Molecular Devises, Sunnyvale, USA).

3.12. *In vitro* 2D-network formation assay on Matrigel

Induction of *in vitro* tube formation was performed using a growth factor reduced Matrigel basement membrane matrix (BD Biosciences). AEC were cultured in supplemented EBM, harvested and re-suspended in EBM without FCS and supplements. 8,000 cells per well were then added onto a gel of the polymerized matrices in 96-well plates in triplicates and incubated with FCS (5%) or gender matched 2% cord blood serum (normal or diabetic) at 21% O_2. Network formation was monitored at 21% O_2 for 24 h and images were taken using a digital camera attached to an inverted phase-contrast microscope (Zeiss). Images showing tube-like structures from 3, 6, 12 and 24 h were quantified by measuring the total tube length, the number of branching points and the number of meshes of the network using AngioJ-Matrigel assay plugin for the ImageJ software (NIH). As all parameters showed the same trend in the results the total tube length is shown as a representative parameter. The plugin was developed and kindly provided by Diego Guidolin, Department of Human Anatomy and Physiology, Section of Anatomy, University of Padova, Padova, Italy.

For the high glucose experiment 75.000 viable cells were seed in a 75 cm^2 flask and cultured in EBM with and without the addition of 20 mM D-glucose to mimic the diabetic and normal conditions, respectively. After 48 h the cells were harvested and the 2D-network formation assay was performed as described above.

3.13. RNA isolation and validation

Total RNA from the pelleted cells was isolated and purified with RNeasy mini Kit (Qiagen, Hilden, Germany). RNA was tested for quality using a BioAnalyzer BA2100 (Agilent, Foster City, CA, USA) with the RNA 6000 Nano LabChip Kit (Agilent, Foster City, CA, USA). Only samples with a RIN (RNA Integrity Number) ≥ 8.5 were used for further analyses.

3.14. Sex confirmation

Because SCT samples derived by fusion from CT, fetal sex was confirmed only in CT. Sex of endothelial cells was confirmed by testing the presence or absence of the *SRY* gene (sex-determining region Y) (93) on the Y chromosome using GeneAmp PCR Kit from Invitrogen. Genomic DNA from each sample was isolated with the QIAamp DNA Mini Kit (Qiagen, Hilden, Germany). PCR was performed using Mastercycler (Eppendorf, USA) for 27 cycles at 94°C for 30 s (denature), 58°C for 30 s (anneal) and for 72°C for 1 min (extension) with an initial denaturation step for 15 min at 95°C.

Sex of the CT was confirmed by assaying expression of the *DDX3Y* gene (DEAD (Asp-Glu-Ala-Asp) box polypeptide 3, Y-linked) on the Y chromosome (94) by RT-PCR using One-step Kit (Qiagen).

Specific primers for *SRY* (forward 5'-CTCCGGAGAAGCTCTTCCTT-3' and reverse 5'-CAGCTGCTTGCTGATCTCTG-3') and *DDX3Y* gene (forward 5'-ATTGGCAATCGTGAAAGACC-3' and reverse 5'- TACTGCCGGTTGCCTCTACT-3') were purchased from Ingenetix (Austria). PCR products were separated by electrophoresis through 2% (wt/vol) agarose gel, stained with ethidium bromide and visualized under UV light.

3.15. RNA microarray hybridization and scanning

Total RNA was labeled using Ambion WT Expression Kit for Affymetrix GeneChip Whole transcript (WT) Expression Arrays (Life Technologies; Carlsbad, CA, USA). Hybridization of all samples to GeneChip Human 1.0 ST arrays was performed according to the manufacturer's instructions (Affymetrix, Santa Clara, CA, USA). For each sample, 200 ng of total RNA were reverse transcribed to double stranded cDNA. During the second cycle of the cDNA synthesis, single-stranded cDNA was

generated. Washing and staining (GeneChip® HT hybridization, Wash and Stain Kit, Affymetrix, Santa Clara, CA, USA) was done with the Affymetrix Genechip® fluidics station 450. Arrays were scanned with the Affymetrix GeneChip scanner GCS3000. Labeling controls and hybridization controls were evaluated with Expression Console EC 1.1.

Hybridization and first analysis were carried out at the Division Core Facility for Molecular Biology at the Centre of Medical Research at the Medical University of Graz, Graz, Austria with the help from Karin Wagner. Microarray data were analyzed with RMA (robust multi-chip average) - including background correction, quantile normalization across all arrays, log2 transformation, and median polish summarization using Genomic Suite v6.5 (Partek Inc, St Louis, MO, USA) (95). Hierarchical clustering analysis and Principal Component Analysis were performed to compare the global expression profile for each sample and to check for outliers.

3.16. Biostatistical analysis of microarray data

In order to reveal significantly differentially expressed genes influenced by sex in seven different conditions (SCT, CT, AEC and VEC, villous vessel endothelium, trophoblast epithelium and placental villi, Figure 22) we performed one-way ANOVA for each of these conditions comparing male vs. female. P-values were adjusted for multiple hypothesis testing based on the false discovery rate (FDR) by the Benjamini-Hochberg method (R/Bioconductor package 'multtest'). Probes showing p-value <0.05 (or where indicated FDR <5%), fold-change >1.3, and annotated as RefSeq transcript/gene (NM_) were considered differentially expressed and further analyzed. Biostatistical analysis and construction of graphs was done with the help from Huber Hackl, Division of Bioinformatics, Biocenter, Innsbruck Medical University, Innsbruck, Austria.

To reveal the importance and function of the sex-biased genes in trophoblast epithelium and villous vessel endothelium, we visualized gene expression levels (log2 fold changes) as heatmaps using Genesis (96) and investigated affected biological pathways and networks with Ingenuity Pathway Analysis (IPA) (Ingenuity® Systems, Ink, Redwood City, CA, USA), Pathway Studio® (Ariadne Genomics, Ink, Rockville, MD, USA) (97). Gene Ontology analysis was performed using the Database for Annotation, Visualization and Integrated Discovery (DAVID)

(98), Pathway Studio® and Panther (99). Distribution of gene expression (log2(M/F)) were generated using (Gaussian) kernel density estimation within R.

3.17. Semi quantitative RT-PCR

The cDNA was synthesized from 50 ng total RNA according to the manufacturer's instructions (SuperScript II Reverse Transcriptase protocol from Invitrogen, USA). Real-time was performed with TaqMan gene expression assays from Applied Biosystems (CA, USA) for the respective genes and the ABI Prism 5,700 Sequence Detection System. The expression of hypoxanthine-guanine phosphoribosyltransferase (*HPRT1*) gene was used as an internal control as its expression was not influenced by fetal sex or gestational diabetes. Data were analyzed according to the $2^{-\Delta\Delta Ct}$ method (100). For statistical analysis a student t-test was performed using SigmaPlot software package. RT-qPCR validation experiments were performed with the help from a PhD student Fancisca Isidora Diaz Pérez, Department of Obstetrics and Gynecology, Medical University of Graz, Austria.

3.18. Genome-scale DNA methylation analysis (Illumina HumanMethylation450)

Infinium HumanMethylation450 (HM450) BeadChip interrogates the methylation status of 485,577 CpGs in the human genome. The Infinium assay detects methylation status with single base resolution. The 50 bp Infinium methylation probes query a [C/T] polymorphism created by bisulfite conversion of unmethylated cytosines in the genome. However, the HM450 methylation platform is unique in that it uses a combination of two distinct probe types, Infinium I and II that differ in their design. Due to reported technical differences between the two probe types the Subset-quantile Within Array Normalization (SWAN) is recommended as one of steps in pre-processing data. Using the SWAN method substantially reduces the technical variability between the assay designs whilst maintaining the important biological differences. The SWAN method makes the assumption that the number of CpGs within the 50 bp probe sequence reflects the underlying biology of the region being interrogated. Hence, the overall distribution of intensities of probes with the same number of CpGs in the probe body should be the same regardless of design type. The method then uses a subset quantile normalization approach to

adjust the intensities of each array the overall distribution of intensities of probes with the same number of CpGs in the probe body should be the same regardless of design type (101).

1 µg of DNA isolated from 9 normal AEC and 9 normal VEC, 5 diabetic AEC and 9 diabetic VEC cell populations was bisulphite converted using the MethylEasyTM bisulphite modification kit (Human Genetic Signatures, Sydney, Australia), according to the manufacturer's instructions. Conversion efficiency was assessed by bisulphite-specific PCR. Hybridization of bisulfite-treated samples to Illumina Infinium Human Methylation450 (HM450) Beadchips was performed at the Australian Genome Research Facility (AGRF).

Raw data (IDAT files) were exported from GenomeStudio (Illumina, San Diego, CA). The Bioconductor package minfi was used to read the data into R, carry out quality control, preprocessing and normalization using the subset-quantile within array normalization (SWAN) method (101). Additional quality control was carried out using the Bioconductor packages arrayQualityMetrics and limma. One sample was removed to due concerns about possible mis-labelling. The limma package was used to fit a linear model to compare the control samples to diabetic samples, for both the arterial and the venous cell types, with patient treated as a random effect and allowing for batch effects.

M-values were calculated after removing probes on the sex chromosomes to eliminate any potential gender bias and any poor performing probes, defined as those with a detection p-value cut-off >0.05 for all samples. β-values were derived from intensities as defined by the ratio of methylated to unmethylated probes given by β =M / (U+M+100) and were used as a measure of effect 149 size.

The global methylation profile of normal and diabetic AEC and VEC was performed and analyzed in collaboration with Richard Saffery and Lavinia Gordon, Murdoch Children´s Research Institute and Department of Pediatrics, University of Melbourne, Melbourne, Australia.

3.19. Locus-specific DNA methylation

DNA methylation levels at the chosen gene regions of *NOSTRIN*, *CAV2*, *DDX60L* and *NPPC* that showed methylation changes with the Infinium methylation analysis was quantified using the Sequenom MassARRAY EpiTYPER platform as previously described (102). Primer pairs for amplification were designed using EpiDesigner

Web tool (http://www. epidesigner.com/). The regions of the respective genes were targeted using the following primers: forward 5′ aggaagagagTTGTAATTAAGGTTGGGTGTGTTTT 3′ and reverse 5′ cagtaatacgactcactatagggagaaggctATTCAAAACTCAAAATCCTACCCTC 3′ for NOSTRIN, forward 5′ aggaagagagAGGAGGGTTTTTTGGTTATTTTTTT 3′ and reverse 5′ cagtaatacgactcactatagggagaaggctAAATACCACAACCCCCATTTTAC 3′ for CAV2, 5′ aggaagagagTTTATTTGGATGTTGAAGGAATTTT 3′ and reverse 5′ cagtaatacgactcactatagggagaaggctTTCTCAAAATAAACCAATACAAACC 3′ for DDX60L, forward 5′ aggaagagagGTGAATTTTTTTTGTGGGAATAATG 3′ and reverse 5′ cagtaatacgactcactatagggagaaggctACTAAAAAACTCTCTCCCCAACCTA 3′ for NPPC. Amplification was performed after bisulfite conversion of genomic DNA with the MethylEasyXceed bisulphite conversion kit (Human Genetic Signatures, North Ryde, Australia). Amplification conditions were 40 cycles of 95°C for 5 min, 56°C for 1 min 30 s and 72°C for 1 min 30 s, and then 72°C for 7 min. Locus-specific DNA methylation was performed with the help from Boris Novakovic, Murdoch Children´s Research Institute and Department of Pediatrics, University of Melbourne, Melbourne, Australia

4. Results

4.1. *In utero* programming by GDM

Diabetic intrauterine environment can programme the fetus and determine the long term development of the offspring into adulthood (45). To investigate the influence of GDM on the feto-placental endothelial function proliferation and 2D-network formation were studied in normal and diabetic AEC. Furthermore, cell adhesion molecules and makers of low grade inflammation were investigated.

4.1.1. Proliferative capacity of human placental AEC is reduced by GDM

To get an insight into endothelial cell proliferation the number of viable and dead cells was determined by direct counting of normal and diabetic AEC after 24, 48 and 96 h in culture at 12% and 21% O_2. Diabetic AEC had a significantly lower number of viable cells than normal AEC after 96 h in culture at both oxygen concentrations, (ANOVA $p<0.001$ for 12% and $p=0.003$ for 21% O_2) (Figure 7A and Figure 8A). The proportion of dead cells did not vary between normal and diabetic AEC at any of the measured time points neither at 12% (Figure 7B) nor at 21% O_2 (Figure 8B). These data suggested that the difference in proliferation between diabetic vs. normal AEC is oxygen-independent, so the influence of oxygen was directly compared. Oxygen did not influence the number of viable cells neither in normal nor in diabetic AEC (Figure 9A and B). Therefore, all sequent experiments were performed only at 21% O_2.

The differences in the viable and the dead cell number between normal and diabetic AEC were not affected when the sex of the fetus was taken into consideration neither at 12% nor at 21% O_2 (Figure 10).

Reduced proliferation potential of diabetic AEC was confirmed with ELISA by adding BrdU after 48 h culture of normal and diabetic cells and measuring its integration into the newly synthesized DNA during DNA replication. Diabetic AEC had significantly less incorporated BrdU than normal cells indicating lower amount of cells in the S-phase of the cells cycle (Figure 11).

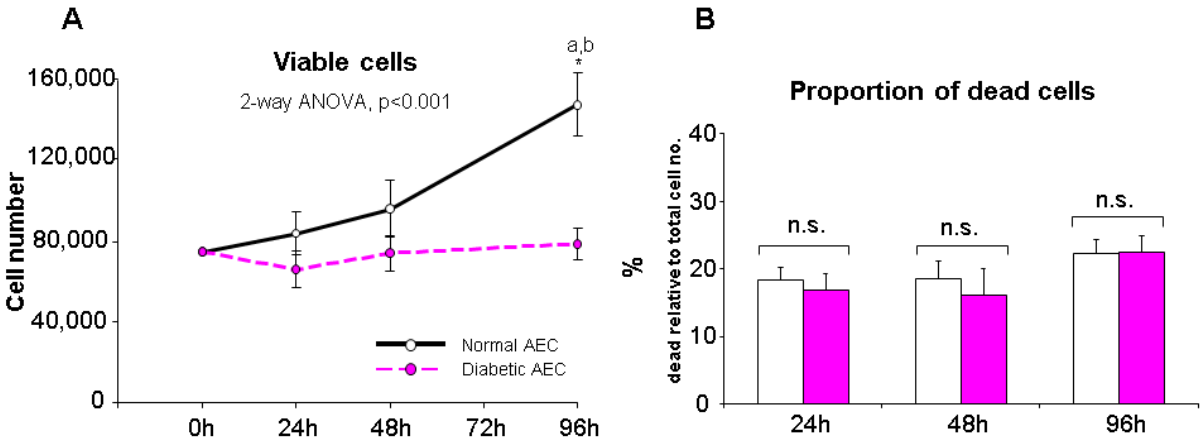

Figure 7. **Proliferation of normal and diabetic AEC at 12% O_2 determined by direct cell counting.** Number of viable cells (A) and percentage of dead cells (B) after 24, 48 and 96 h in culture. Data are indicated as mean ± SD of 8 normal vs. 7 diabetic endothelial cell isolations each in triplicates.

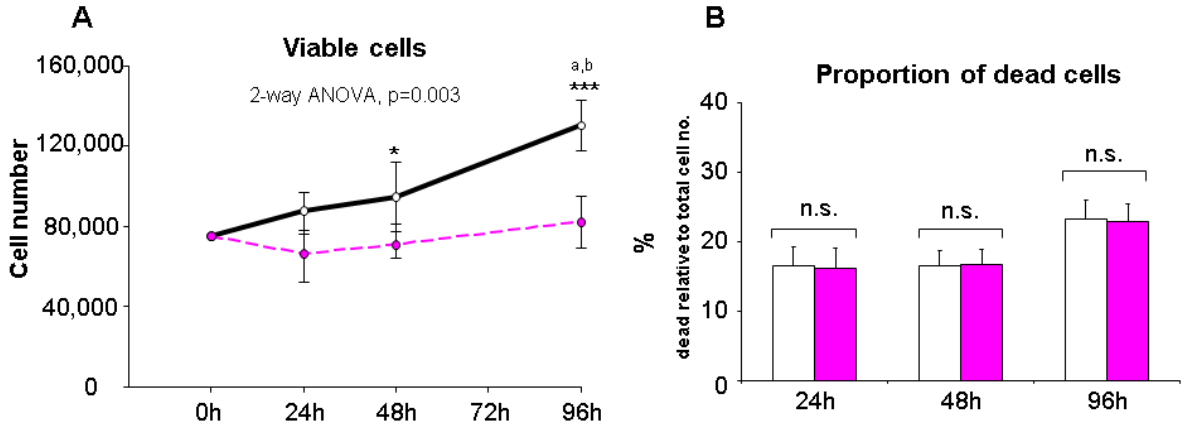

Figure 8. **Proliferation of normal and diabetic AEC at 21% O_2 determined by direct cell counting.** Number of viable cells (A) and percentage of dead cells after 24, 48 and 96 h in culture (B). Data are indicated as mean ± SD of 8 normal vs. 7 diabetic endothelial cell isolations each in triplicates.

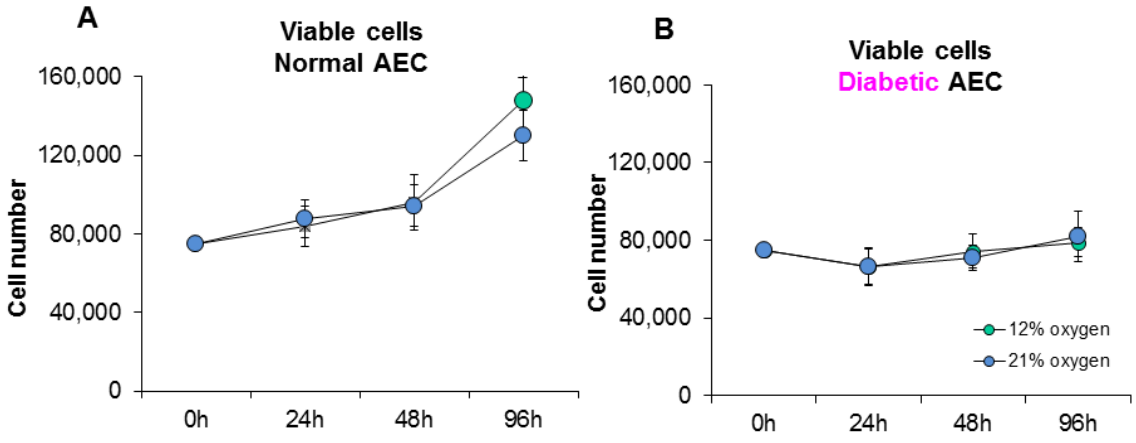

Figure 9. **Influence of oxygen on proliferation of normal and diabetic AEC determined by direct cell counting.** Number of viable cells in normal (A) and diabetic AEC (B) after 24, 48 and 96 h in culture. Data are indicated as mean ± SD of 8 normal vs. 7 diabetic endothelial cell isolations at 12% and 21% O_2 each in triplicates.

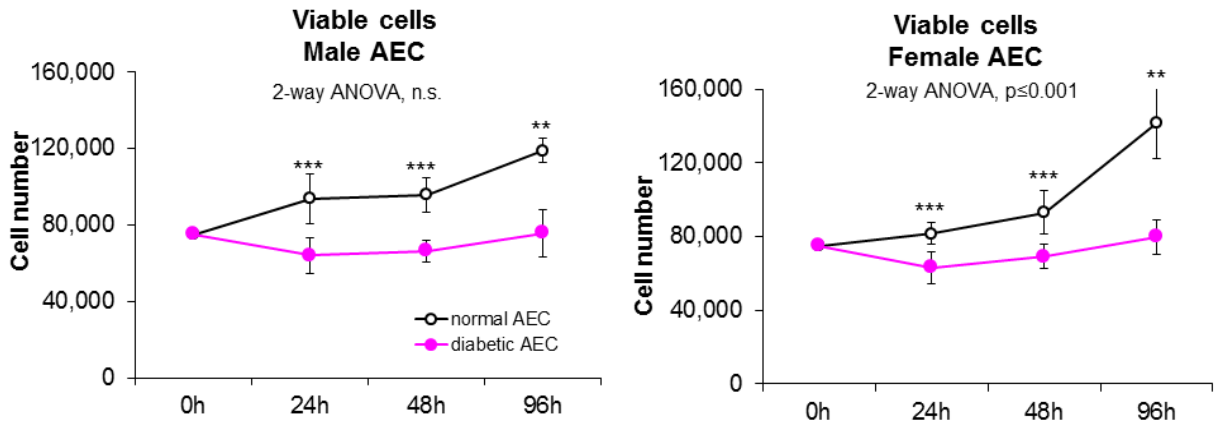

Figure 10. **Influence of fetal sex on differences in proliferation of normal and diabetic AEC determined by direct cell counting.** Number of viable cells in normal and diabetic male (A) and female AEC (B) after 24, 48 and 96 h in culture. Representative results measured at 21% O_2 are shown. Data are shown are indicated as mean ± SD of 3 normal male vs. 4 diabetic male and 4 normal female vs. 4 diabetic female endothelial cell isolations each in triplicates.

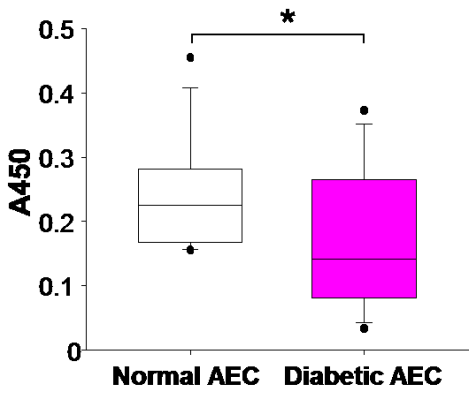

Figure 11. **Proliferation of normal and diabetic AEC at 21% O_2 determined by ELISA measuring BrdU incorporation into the DNA.** The amount of the incorporated BrdU was determined in cells cultured for 48 h. Data are indicated as mean ± SD of 8 normal vs. 9 diabetic endothelial cell isolations each in duplicates.

4.1.2. Different proliferation rate of diabetic AEC is a consequence of changes in the cell cycle and not in cellular apoptosis

Cell cycle analysis was assessed by a bivariate analysis by 7-AAD staining of total DNA content and BrdU staining of newly synthesized DNA by flow cytometer. Diabetic AEC showed a significant decrease in S-phase and a significant increase in G1-phase vs. normal AEC after 48 h in culture. Compared to normal cells the G2/M-phase was unchanged in diabetic AEC (Figure 12).

As a measure of cellular death the presence of an active caspase-3 fragment was investigated by flow cytometry in normal and diabetic AEC after 48 h in culture.

At the measured time point no significant difference in the amount of apoptotic cells was observed between the two groups (Figure 13).

These results corroborate the finding of the reduced proliferation potential of diabetic AEC as compared to normal AEC and indicate that the observed difference is due to changes in the cell cycle of diabetic AEC and not to their distinct apoptosis rate.

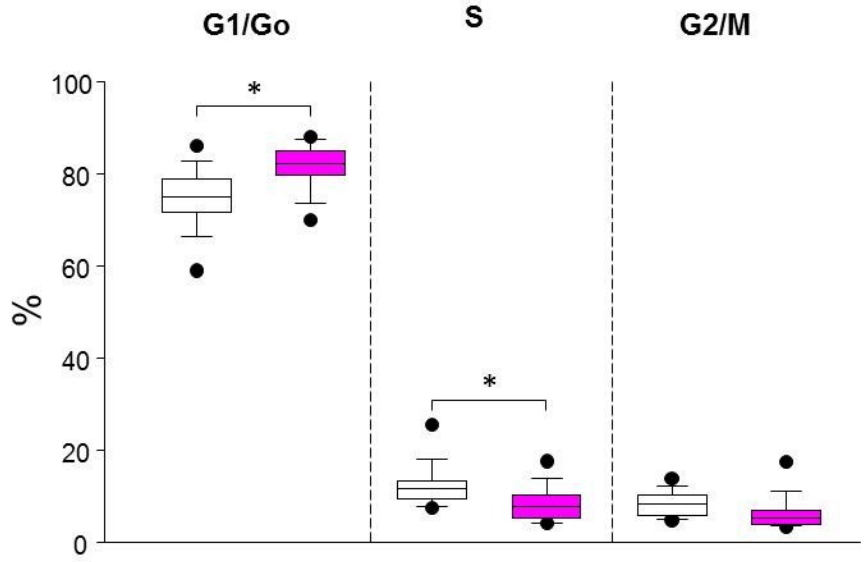

Figure 12. **Proliferation and cell cycle analysis of normal and diabetic AEC at 21% O_2 determined by FACS measuring BrdU incorporation into the DNA.** The amount of the incorporated BrdU was determined in cells cultured for 48 h. Data are indicated as mean ± SD of 12 normal (white whiskers) vs. 12 diabetic (pink whiskers) endothelial cell isolations each in duplicates.

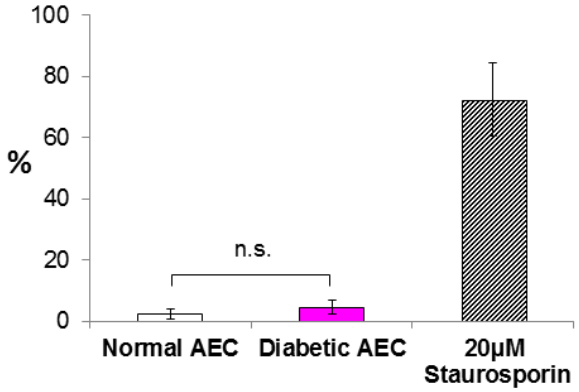

Figure 13. **Survival of normal and diabetic AEC at 21% O_2.** The amount of active caspase 3 positive cells was determined by FACS in the cells cultured for 48 h. Data are indicated as mean ± SD of 5 normal vs. 4 diabetic endothelial cell isolations each in duplicates.

4.1.3. Expression of cell cycle related proteins is altered in GDM

To investigate protein content in diabetic AEC vs. normal AEC a protein array containing a panel of cell cycle antibodies was used. From 14 proteins that were detected in all normal and diabetic cell isolations 9 showed altered expression in diabetic AEC (Figure 14). The expression of all proteins was upregulated in cells from GDM pregnancies with significance as follows: 14.3.3, Pan ($p<0.01$), Cdc14A ($p<0.001$), Cdc47 or Mcm7 ($p<0.001$), cyclin- dependent kinase 5 (Cdk5; $p<0.05$), cyclin- dependent kinase 8 (Cdk8; $p<0.05$), Cullin-1 (Cul-1; $p<0.05$), Cullin-3 (Cul-3; $p<0.01$), cyclin C (CcnC; $p<0.05$) and Cdkn1B (p27Kip1; $p<0.05$).

Based on these results we can conclude that GDM alters the protein profile of feto-placental endothelial cells.

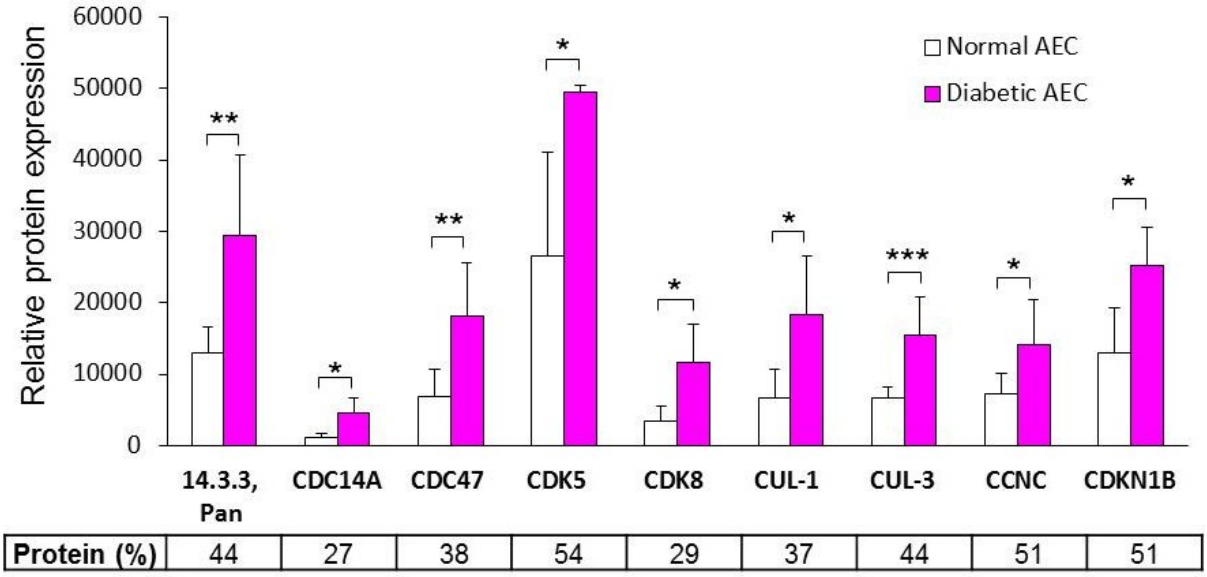

Protein (%)	44	27	38	54	29	37	44	51	51

Figure 14. Cell cycle protein expression in normal and diabetic AEC at 21% O_2. Protein content was measured in cells after 48 h in culture. Relative protein amount is shown as mean ± SD of 5 normal vs. 4 diabetic endothelial cell isolations.

4.1.4. 2D-network formation of human placental AEC is increased by GDM

It has been shown that as a consequence of the diabetic environment in GDM placental vascular surface is increased (103). In order to reveal whether diabetic AEC maintain this increased angiogenic potential an *in vitro* 2D-network formation assay was performed and total tube length, number of branching points and number of meshes were monitored as proxy measures of angiogenesis.

In the presence of 5% FCS diabetic AEC had increased total tube length, more branching points and more meshes as compared to normal AEC at all hours ($p < 0.001$) (Figure 15A).

To mimic the physiological conditions in the vascular bed the 2D-network formation was performed with human 2% normal and diabetic CBS. In the presence of normal and diabetic CBS total tube length was increased by 45±10% and 60±14%, respectively (Figure 15A and B) in diabetic vs. normal AEC (ANOVA $p < 0.001$). Diabetic CBS did not influence network formation potential neither of normal nor of diabetic AEC (Figure 16).

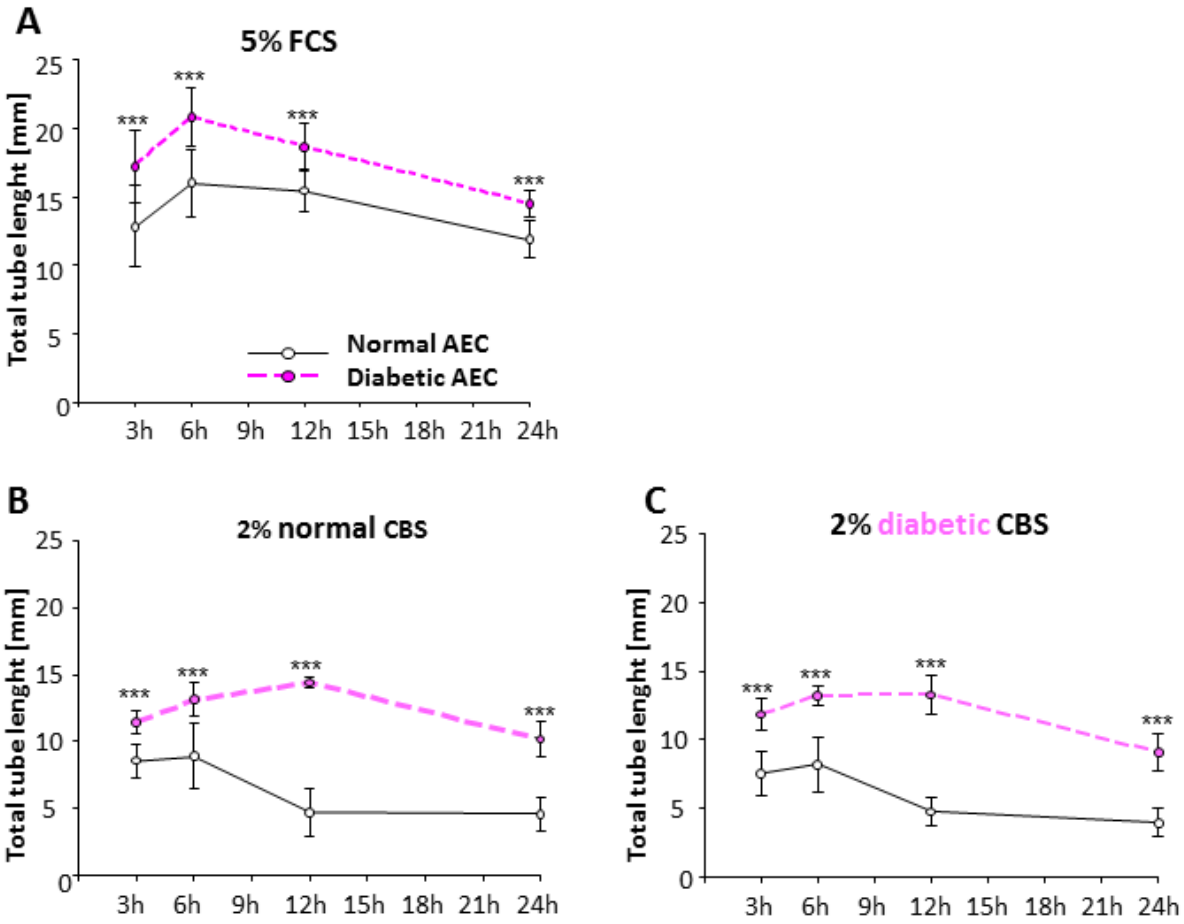

Figure 15. 2D-network formation of normal and diabetic AEC. The total tube length (mm) was evaluated after 3, 6, 12 and 24 h on a growth reduced Matrigel in the presence of 5% FCS (A) and 2% normal (B) and diabetic CBS (C) at 21% O_2. Data are indicated as mean ± SD of 6 normal vs. 9 diabetic endothelial cell isolations each in quadruplicates.

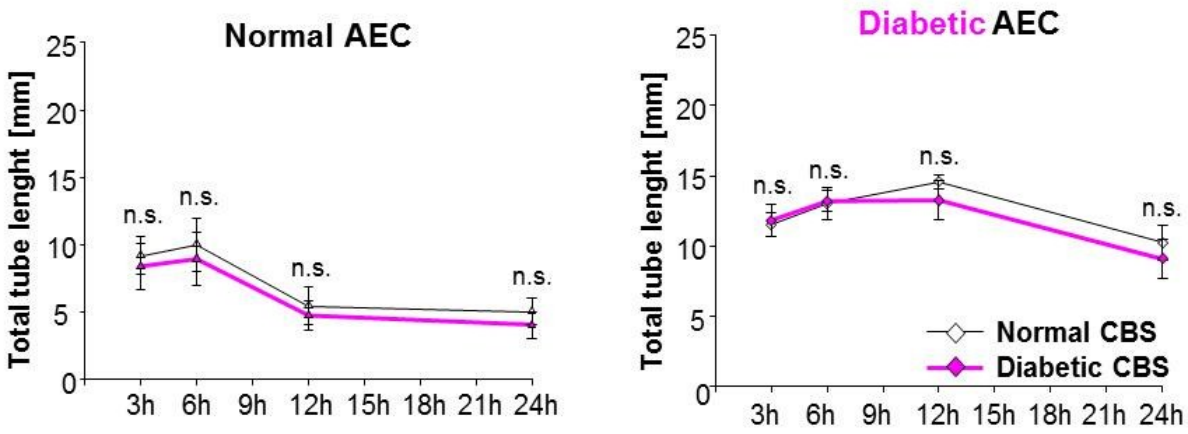

Figure 16. Influence of 2% normal and diabetic CBS on 2D-network formation of normal and diabetic AEC at 21% O_2. The total tube length (mm) was evaluated after 3, 6, 12 and 24 h on a growth reduced Matrigel in the presence 2% normal and diabetic CBS at 21% O_2. Data are indicated as mean ± SD of 6 normal vs. 9 diabetic endothelial cell isolations each in quadruplicates.

As the diabetic environment in culture (diabetic CBS) did not influence network formation of diabetic AEC these results indicate that the altered proliferation and tube formation are a result of an intrinsic program of the cells.

As all measured parameters showed the same trend, total tube length is shown as a representative parameter in Figures 15 and 16.

4.1.5. Hyperglycemia alters 2D-network formation of normal AEC

Main characteristic of the diabetic environment is increased glucose level. Therefore, the effect of transient exposure of normal AEC to hyperglycemic culture conditions was investigated by monitoring their ability to form networks.

Normal cells that were exposed to high glucose for 48 h prior to the assay showed increased total tube length at all-time points measured (Figure 17): at 3h by 40±29%, at 6 h by 24±32%, at 12 h by 23±32% and at 24 h by 25±47% ($p<0.001$ for all hours).

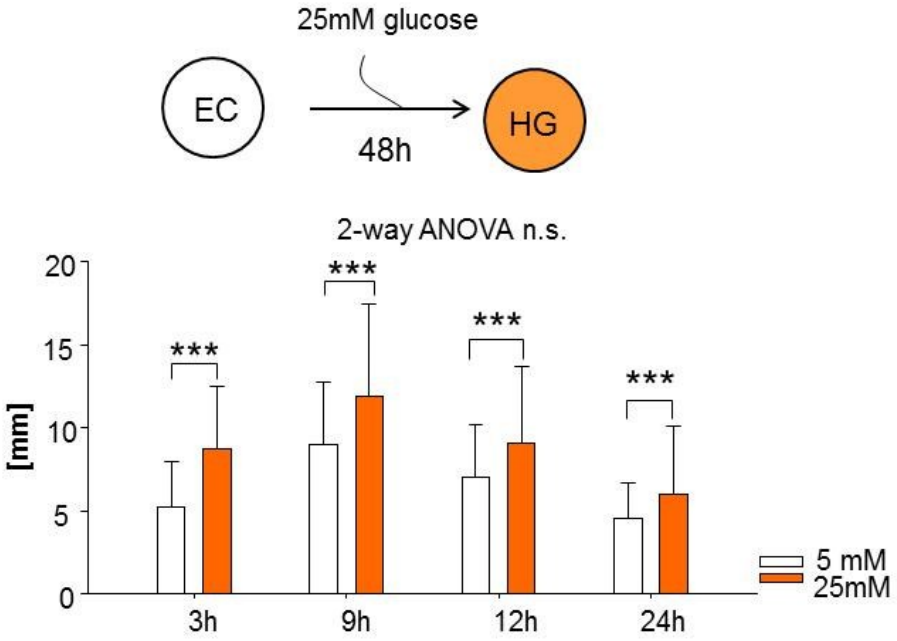

Figure 17. 2D-network formation of normal AEC after transient exposure to hyperglycemic conditions at 21% O_2. Normal AEC were cultured for 48 h in the presence of 5 mM D-glucose (normoglycemic conditions) or 25 mM D-glucose (hyperglycemic conditions). The total tube length (mm) was evaluated after 3, 6, 12 and 24 h on a growth reduced Matrigel in the presence 5% FCS at 21% O_2. Data are indicated as mean ± SD of 8 endothelial cell isolations cultured at normoglycemic vs. 8 cultured at hyperglycemic conditions each in triplicates.

4.1.6. Correlation of proliferation and 2D-network formation with maternal, newborn and placental clinical parameters

To investigate if the observed endothelial dysfunction in GDM, reduced proliferation and increased network formation, associate with available maternal, fetal or placental parameters, clinical data were correlated with proliferation and network formation data.

Feto-placental weight ratio correlated with cumulative population doubling (CPD, a proliferation index) after 96 h ($p=0.05$), while maternal weight gain ($p<0.05$), maternal height ($p<0.01$) and fetal ponderal index ($p=0.01$) correlated with total tube length at 6h (Figure 18). Cord blood insulin, glucose, C-peptide and C-reactive protein levels, offspring's weight and length, placental weight, maternal weight and BMI before and at the end of pregnancy did not show any correlation with proliferation or network formation.

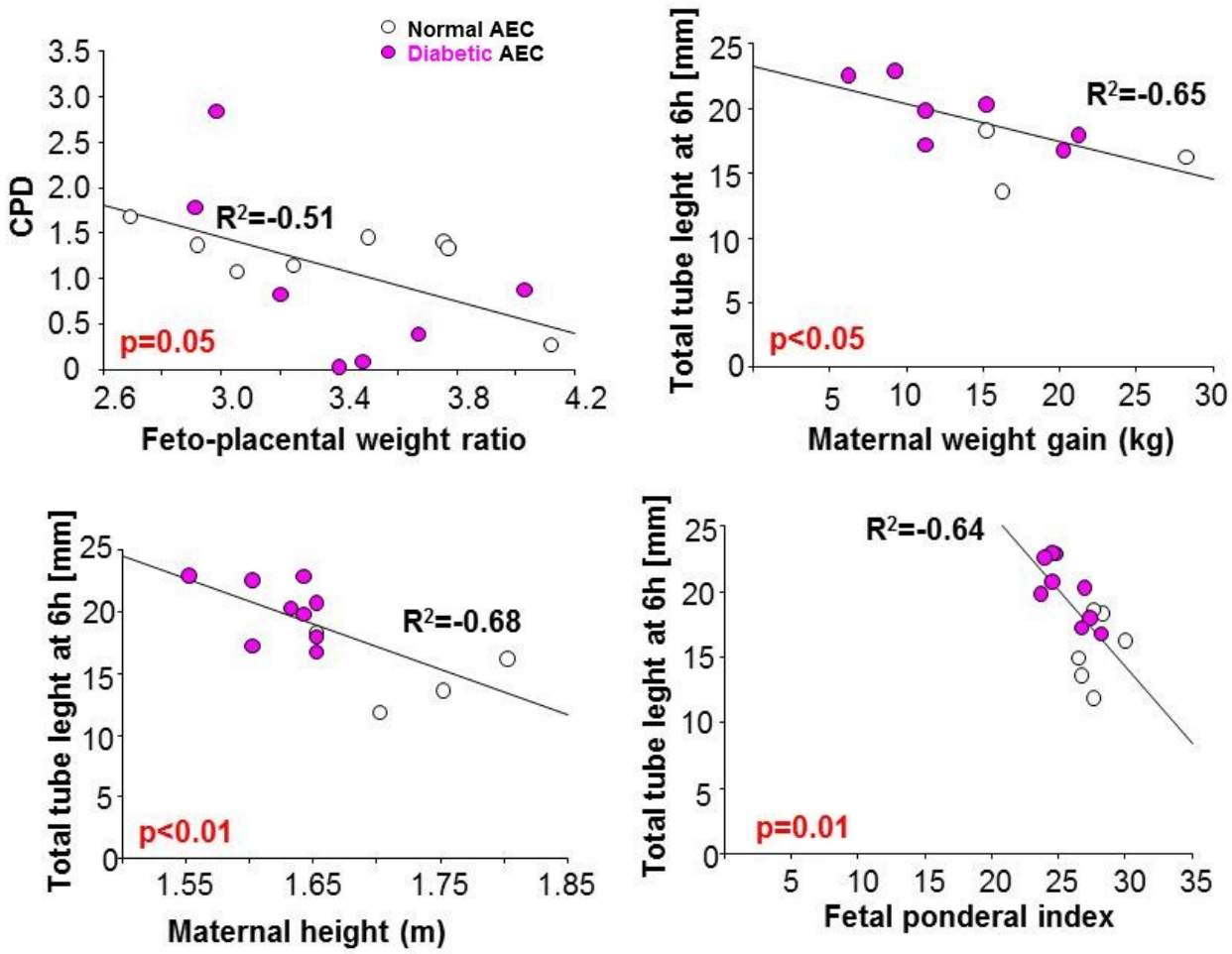

Figure 18. Correlation of clinical parameters with proliferation and 2D network formation measurements. Pearson correlation test was performed to investigate correlation of cumulative population doubling (CPD, proliferation index) after 96h of culture and the total tube length at 6h with clinical data.

4.1.7. Markers of low-grade inflammation

Diabetes associated altered expression of low-grade inflammation markers by vascular endothelium has been reported (47,104). Therefore, the level of different cytokines and chemokines has been investigated in the conditioned media of normal vs. diabetic AEC after 48 h of culture firstly by a human cytokine array panel and subsequently by quantitative multiplex ELISA.

From 36 assessed analytes (Table 1) only GROα, IL6, IL8, MCP1, MIF and Serpin E1 were detected in the conditioned media with IL6, IL8, MCP1 and Serpin E1 showing slight differences in the intensity of the spots between normal and diabetic cells indicating different concentrations (Figure 19).

Table 1. Cytokines, chemokines, and acute phase proteins investigated in culture supernatant of AEC

1	C5a	13	IL4	25	IL32 alpha
2	CD40 ligand	14	IL5	26	CXCL10/IP10
3	G-CSF	15	IL6	27	CXCL11/I-TAC
4	GM-CSF	16	IL8	28	CCL2/MCP1
5	CXCL1/GRO alpha	17	IL10	29	MIF
6	CCL1/I309	18	IL12 p70	30	CCL3/MIP1 alpha
7	ICAM1	19	IL13	31	CCL4/MIP1 beta
8	IFN-gamma	20	IL16	32	CCL5/RANTES
9	IL1 alpha	21	IL17	33	CXCL12/SDF1
10	IL1 beta	22	IL17E	34	Serpin E1/PAI1
11	IL1ra	23	IL23	35	TNF-alpha
12	IL2	24	IL27	36	TREM1

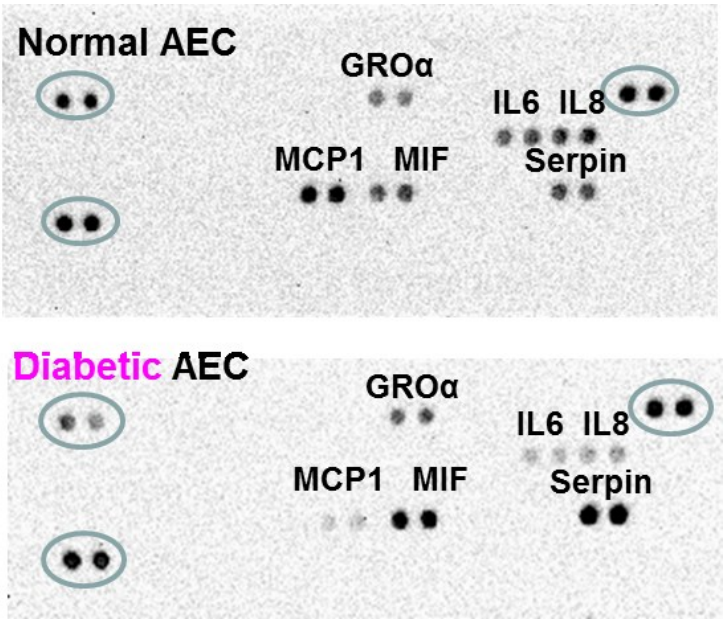

Figure 19. Cytokines in the conditioned media from normal and diabetic AEC. Cytokines are detected using Proteome profiler in the conditioned media from normal and diabetic AEC after 48 h. Dots in light blue circles represent reference samples.

Quantitative ELISA revealed that there are no differences in the concentrations of interleukins (IL6 and IL8), chemokines (MCP1 or CCL2) or plasminogen activator inhibitor (PAI1 or SERPIN E1) in the conditioned media of normal vs. diabetic AEC (Figure 20A). Additionally, due to its important anti-inflammatory properties, concentration of adiponectin (ADIPOQ1) in the conditioned media was investigated. There was no difference in adiponectin concentration

between normal and diabetic AEC (Figure 20A). Maternal cord blood insulin levels may be a potential indicator of IL6 concentrations since there was a significant (p=0.001) and strong (R^2=0.97) correlation (Figure 20B).

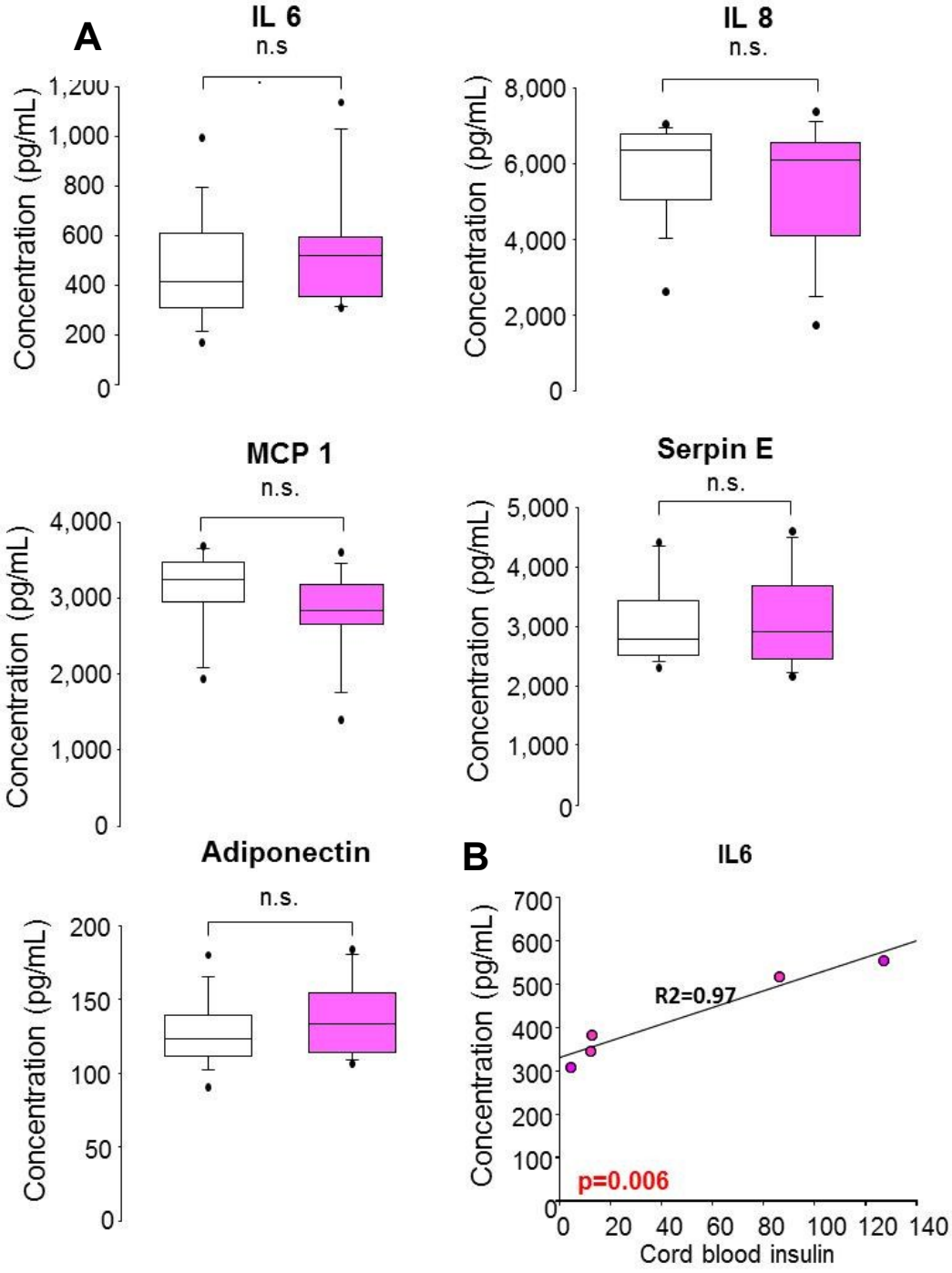

Figure 20. Concentration of inflammation markers in the conditioned media of normal and diabetic AEC after 48h in culture at 21% O_2. Concentrations of IL6, IL8, MCP1, Serpin E1 and adiponectin determined by multiplex ELISA (A). Correlation of IL6 concentration measured in conditioned media with insulin levels measured in cord blood (B). Data are indicated as mean ± SD of 11 normal vs. 9 diabetic endothelial cell isolations each in duplicates.

4.1.8. Cell adhesion molecules

An overexpression of cell adhesion molecules on the surface of endothelial cells is one of the first steps in a high glucose-mediated endothelial dysfunction in diabetes (104,118). Therefore, the expression of intracellular adhesion molecule 1 (ICAM1), vascular cell adhesion molecule 1 (VCAM1), VE-cadherin and E-selectin was investigated by flow cytometry.

ICAM1 expression was reduced by 41±15% in diabetic AEC as compared to normal cells ($p<0.05$). No difference in VE-cadherin expression was observed between normal and diabetic AEC. VCAM1 and E-selectin could not be detected using this method (Figure 21).

VE-cadherin levels correlated with cord blood insulin ($p=0.02$, $R^2= -0.98$), feto-placental weight ratio ($p=0.049$, $R^2= 0.75$), maternal weight before and at the end of pregnancy ($p=0.03$, $R^2= -0.92$ and $p=0.02$, $R^2= -0.78$, respectively) and maternal BMI before and at the end of pregnancy ($p=0.02$, $R^2= -0.93$ and $p=0.02$, $R^2= -0.89$, respectively). In contrast, no significant correlation was observed for ICAM1 although fetal ponder index was close to significance ($p=0.07$, $R^2= -0.5$).

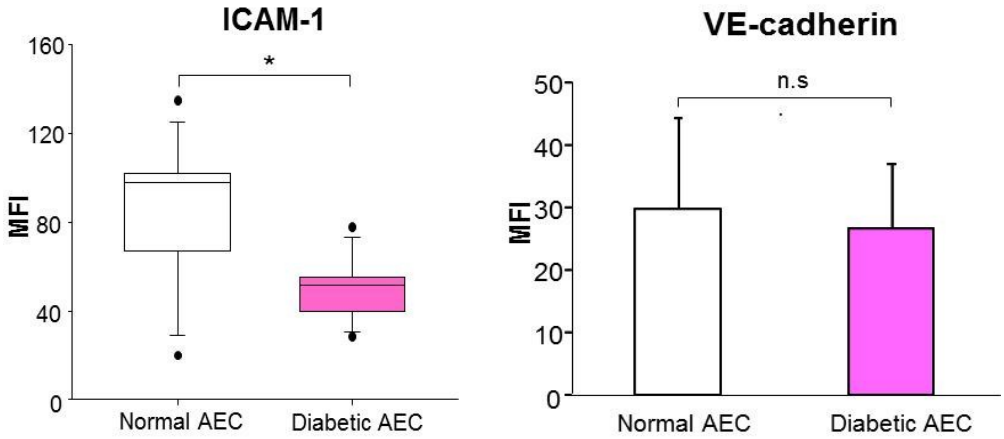

Figure 21. Expression of cell adhesion molecules in normal and diabetic AEC after 48 h in culture at 21% O_2. Concentration of analytes was determined by flow cytometry. Data are indicated as mean ± SD of 8 normal vs. 7 diabetic for ICAM1 and 4 normal vs. 4 diabetic endothelial cell isolations for VE-cadherin each in triplicates.

4.2. *In utero* programming of cell phenotype

Epigenetic modifications are the leading mechanisms proposed to drive fetal programming *in utero* (105). In order to reveal whether the diabetic *in utero* environment affects placental endothelial cells by altering their DNA methylation pattern global DNA methylation analysis of AEC and VEC from healthy (normal AEC and normal VEC) and GDM complicated pregnancies (diabetic AEC and diabetic VEC) was investigated. If changes in methylation also lead to concordant gene expression changes was assessed by a transcriptome analysis.

4.2.1. Influence of GDM on global DNA methylation profile of human placental AEC vs. VEC

Cluster dendrogram of the methylation arrays showed that cell type had the greatest influence on sample separation - venous samples clearly separated from the arterial samples. Within these two main branches clustering of the diabetic samples was better within the venous group (Figure 22A). Global methylation pattern was further depicted with the Principal Component Analysis that also showed clear sample separation based on cell type, but here samples also separated based on GDM. Influence of GDM was more pronounced in VEC (Figure 22B).

Based on quality control and clustering analysis sample AEC14d (red arrow in Figure 22A) was identified as an outlier and was excluded from further analysis. In the cluster dendrogram two venous samples, VEC2d and VEC112, clustered separately forming an individual group, but as they passed all quality control tests they were included in sequent analyses. To control for inter-array variability technical replicates of sample VEC10d were used and compared pairwise. Technical replicates grouped appropriately in the clustering analysis (black circle in Figure 22A) and showed very good correlations in pairwise comparison scatter plots (Figure 23). For further analysis one randomly selected replicate was used.

As a first quantitative measure of global methylation change in diabetes in the two cell types, an average ß-value (methylation index) was calculated across all samples in a respective group. Methylation index showed significant global loss of methylation in diabetic cells, 5% in diabetic AEC ($p \leq 0.001$) vs. 3% in diabetic VEC ($p \leq 0.001$) (Figure 24).

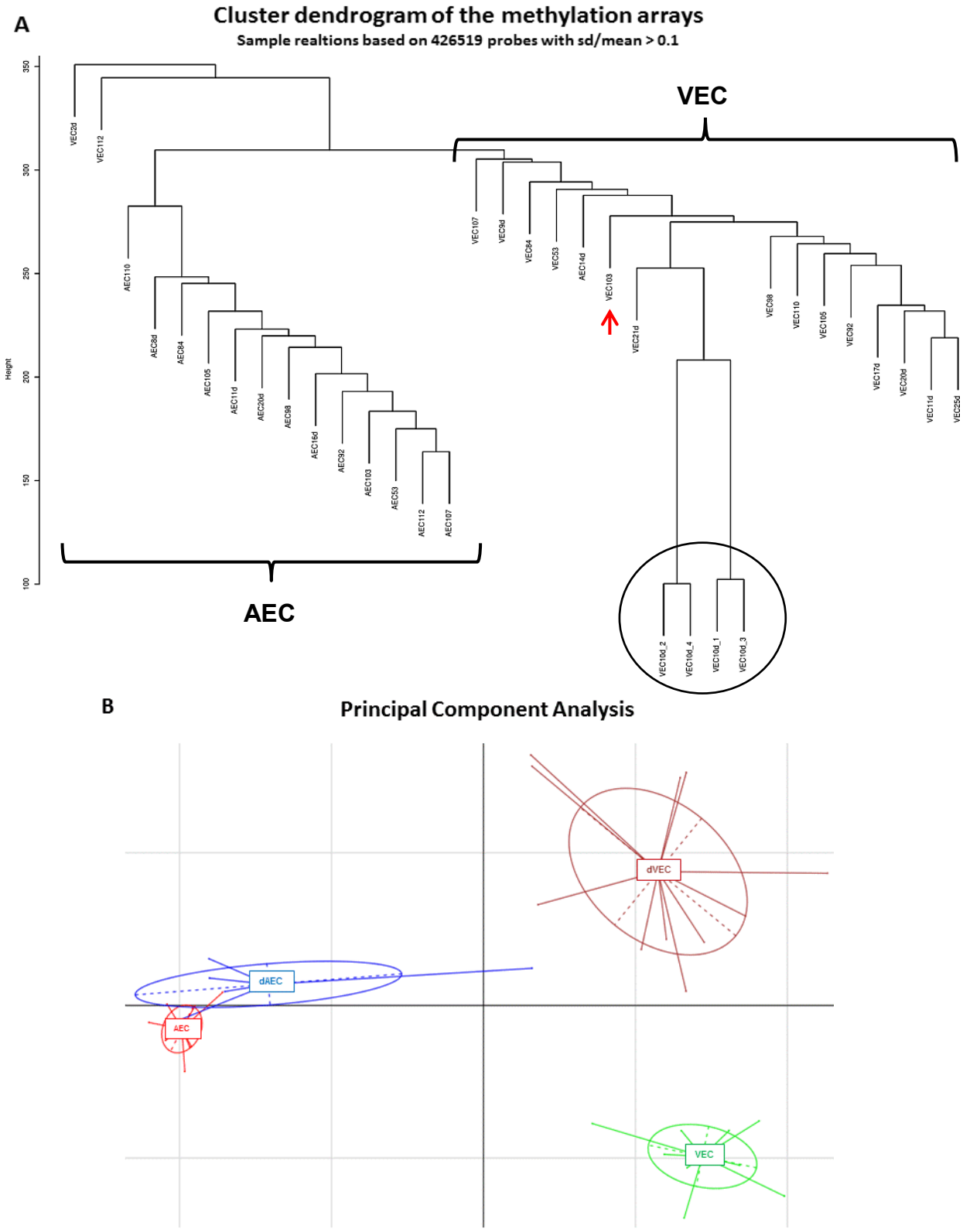

Figure 22. Global DNA methylation profile of normal and diabetic AEC and normal and diabetic VEC. Cluster dendrogram showing influence of cell type and GDM on sample clustering (A). Red arrow marks the outlier sample in the arterial group of cells AEC14d that clusters with venous samples. Black circle indicates four technical replicated of sample VEC10d used to control for inter-array variability. Principal Component Analysis plot showing global methylation differences between normal and diabetic AEC (dAEC) and normal and diabetic VEC (dVEC), respectively. The distance between the circled areas serves as a proxy measure of the variation between the samples (B).

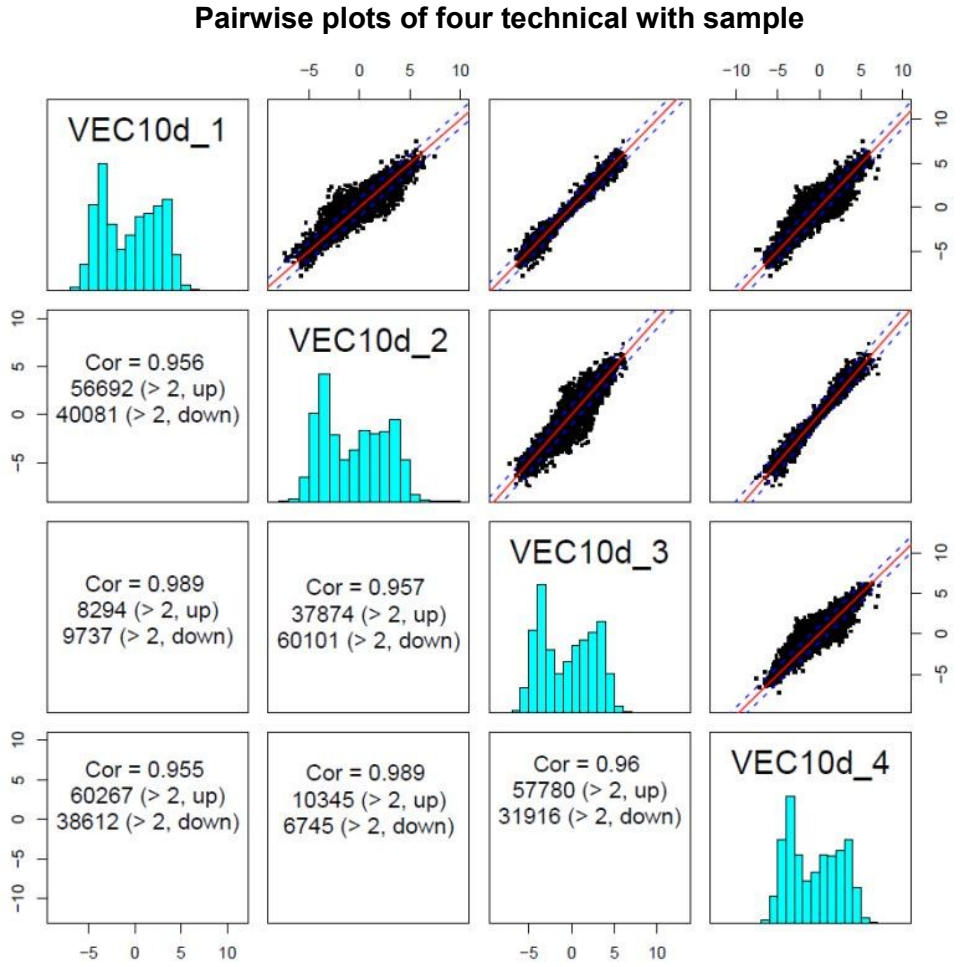

Figure 23. Scatterplots of the four technical replicates. Four technical replicates of sample VEC10d were used to control for inter-array variability (Figure 17A). Pairwise comparison was performed on all investigated CpG probes.

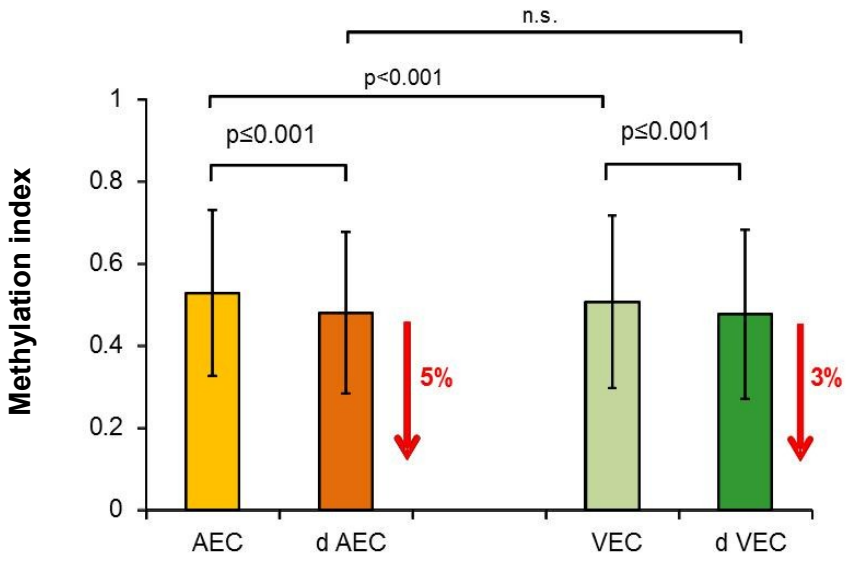

Figure 24. Average methylation of all samples for normal and diabetic AEC and VEC. Methylation Index (MI) was calculated for each group by calculating the mean of all Infinium β-values for that sample. The MIs were then grouped by cell type and disease and significance was tested with a student t-test.

To identify sets of differentially methylated CpG probes between normal and diabetic cells, average ß-values were calculated for each probe in diabetic cells and subtracted from average ß-values for the respective probe in normal cells. Linear regression analysis revealed that GDM influenced methylation level ($p<0.05$ and $\Delta\beta \geq 0.2$) of 2699 CpGs that annotate to 2120 genes in diabetic AEC, whereas diabetic VEC had 1384 differentially methylated genes and 11595 CpGs vs. normal VEC (Figure 25). Opposite to diabetic VEC where there was an equal distribution of hyper- and hypomethylated CpGs in GDM vs. control, diabetic AEC had 33% of the CpGs hypermethylated and 67% hypomethylated (Figure 25) when compared to normal cells.

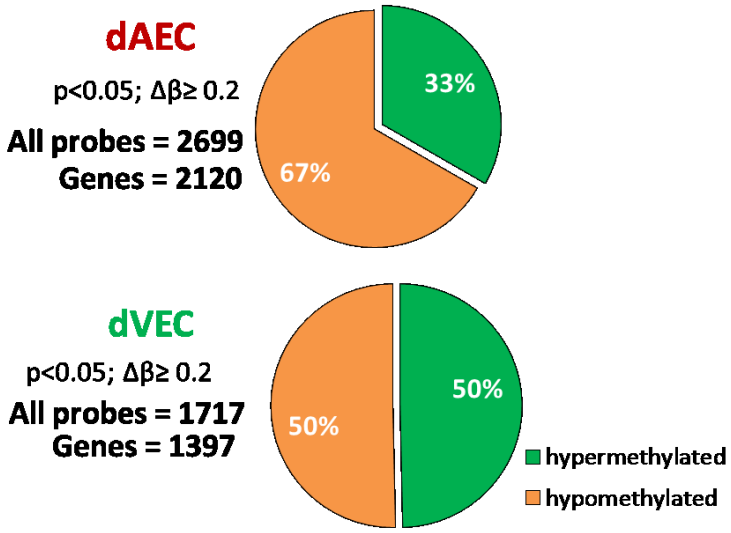

Figure 25. Differentially methylated CpG probes in diabetic AEC and diabteic VEC. The number of differentially methylated CpGs and the associated genes is shown for both, dAEC and dVEC ($p<0.05$, $\Delta\beta \geq 0.2$) vs. control cells. Pie charts represent the percentage of hypo- and hypermethylated CpG in relative to the total number of all CpG probes showing changes in methylation.

Importantly, HM450 DNA methylation platform was validated using locus-specific SEQUENOM MassARRAY EpiTYPER platform. Genes for validation were chosen based on the methylation change between normal and diabetic cells (Δβ) and the size of the differentially methylated region (number of differentially methylated adjacent CpGs). Significant difference in methylation of one CpG within caveolin 2 (*CAV2*) and one within natriuretic peptide C (*NPPC*) gene investigated with HM450 was confirmed with MassARRAY system (Figure 26A). Although nitric oxide synthase trafficker (*NOSTRIN*) and DEAD (Asp-Glu-Ala-Asp) box polypeptide 60-like (*DDX60L*) did not show a significant methylation change with MassARRAY

system in the CpGs that are in common with the HM450, the average methylation change in the respective gene region was significantly altered in diabetic cells. Furthermore, methylation status of *NOSTRIN* and *CAV2* genes for AEC and *DDX60L* and *NPPC* genes for VEC obtained with HM450 significantly correlated with the methylation data from MassARRAY system thereby validating the HM450 platform (Figure 26B).

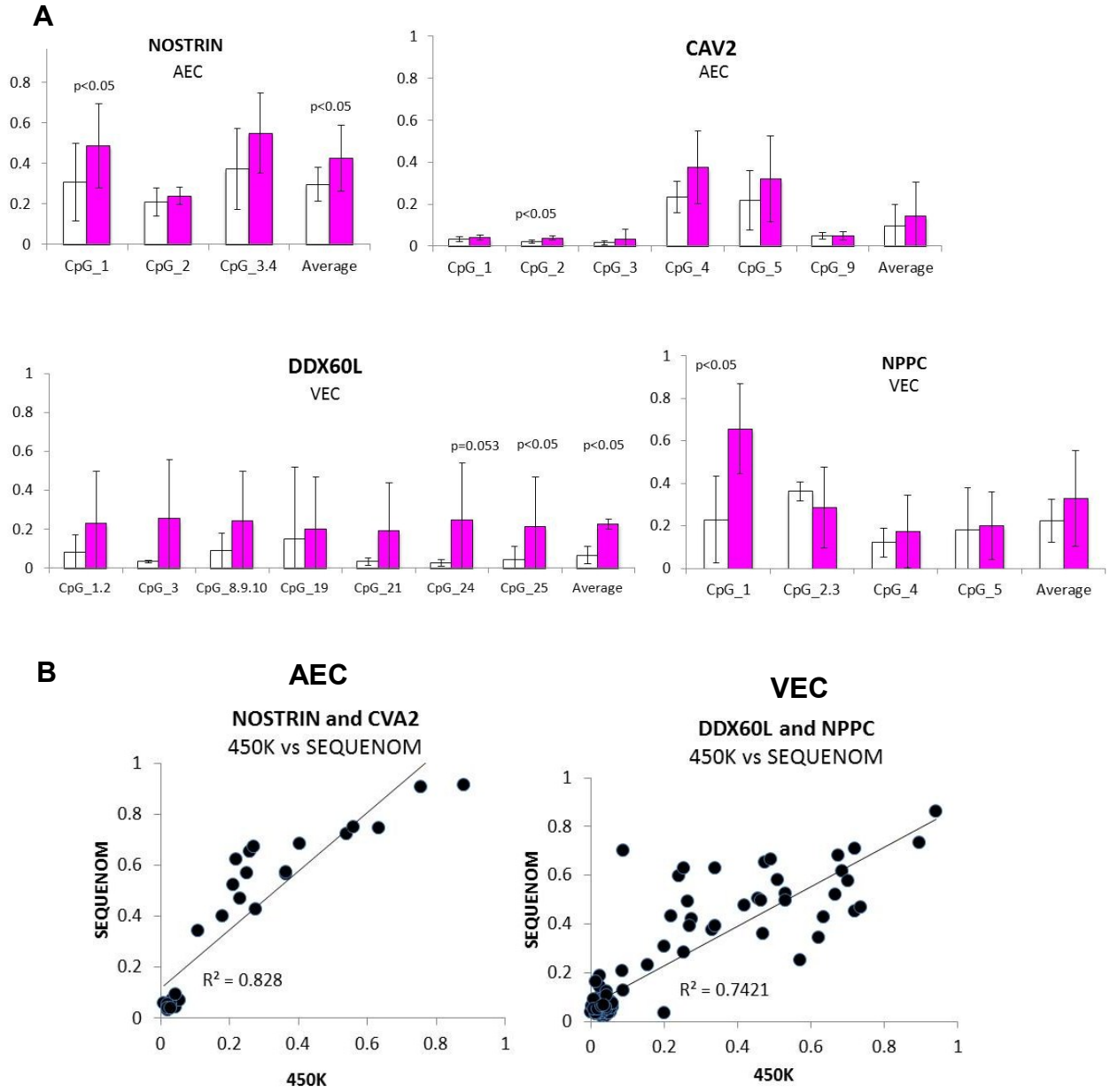

Figure 26. Validation of Infinium HumanMethylation450 BeadChip arrays via MassARRAY system. *NOSTRIN* and *CAV2* were chosen for validation of methylation differences of diabetic AEC and *DDX60L* and *NPPC* of diabetic VEC. Methylation status of individual CpGs from the MassaARRAY measurement is shown. CpG2 and CpG3.4 for *NOSTRIN*, CpG2, CpG4, CpG5 and CpG9 for *CAV2*, CpG3, CpG21 and CpG25 *DDX60L* and all shown CpGs for *NPPC* are in common with the HM450 (A). Methylation status of the chosen probes obtained with HM450 array significantly correlated with the methylation data from Sequenom (B).

4.2.2. Distinct and shared GDM signatures in DNA methylation profile of placental AEC vs. VEC

Gene ontology revealed that differentially methylated genes in diabetic AEC and diabetic VEC vs. control cells were distributed across all cellular compartments with cytoplasm being the most and extracellular space the least prominent. Similar results were obtained when analyzing only genes that show a methylation change within a promoter sequence i.e. probes located at TSS and/or 5'UTR sites (Table 2).

Table 2. Cellular localization of genes with differentially methylated probes in diabetic AEC and VEC.

dAEC: all probes

Cellular localization	No of molecules	Proportion (%)
Nucleus	326	15
Cytoplasm	446	21
Plasma Membrane	334	16
Extracellular Space	152	7
Unknown	862	41
	2120	100

dAEC: TSS and 5'UTR

Cellular localization	No of molecules	Proportion (%)
Nucleus	36	12
Cytoplasm	69	23
Plasma Membrane	36	12
Extracellular Space	14	5
Unknown	150	49
	629	100

dVEC: all probes

Cellular localization	No of molecules	Proportion (%)
Nucleus	189	14
Cytoplasm	260	19
Plasma Membrane	235	17
Extracellular Space	93	7
Unknown	607	44
	1384	100

dVEC: TSS and 5'UTR

Cellular localization	No of molecules	Proportion (%)
Nucleus	22	12
Cytoplasm	38	20
Plasma Membrane	35	19
Extracellular Space	7	4
Unknown	86	46
	188	100

Cellular localization was investigated using Ingenuity Pathway Analysis (www.ingenuity.com) with differentially methylated genes in diabetic AEC and diabetic VEC vs. control cells ($p<0.05$, $\Delta\beta \geq 0.2$). Analysis was performed with genes displaying a methylation change regardless of the genomic position and separately with genes caring a methylation change within the promoter.

Importantly, gene ontology defined that differentially methylated genes in both, diabetic AEC and diabetic VEC were linked with the highest significance to diabetes mellitus and glucose metabolism disorder functions that were further categorized to the endocrine system disorder and gastrointestinal and metabolic disease (Figure 27). Distinct influence of GDM on arterial and venous vascular beds was observed when investigating molecular functions where only genes involved in cellular function and maintenance were shared in the two cell types. Otherwise, i.e. cell cycle in diabetic AEC and carbohydrate metabolism in diabetic VEC were identified as unique diabetic signatures and were enriched with genes with a methylation change within a promoter (Figure 27).

Furthermore, differentially methylated genes were linked to distinct pathways in diabetic AEC and diabetic VEC as compared to control cells (Table 3). Different influence of GDM on two cell types was even more pronounced when affected networks were studied (Table 4). Endocrine system disorder, cellular growth and proliferation and inflammatory response network were significantly enriched in diabetic AEC, while cell and tissue morphology and cellular assembly and organization were linked to the differentially methylated genes in diabetic VEC.

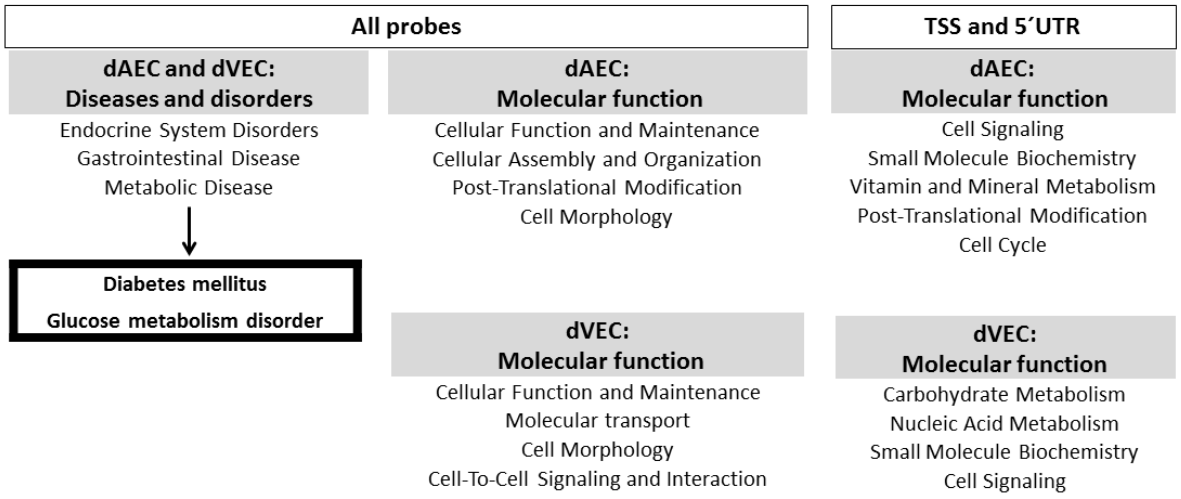

Figure 27. Diseases, disorders and molecular functions in arterial and venous cells types affected by GDM. Analysis was performed using Ingenuity Pathway Analysis (www.ingenuity.com) with differentially methylated genes in diabetic AEC and diabetic VEC vs. control cells ($p<0.05$, $\Delta\beta \geq 0.2$). Analysis was performed with genes displaying a methylation change regardless of the genomic position and separately with genes caring a methylation change within the gene promoter.

Table 3. Pathways in AEC and VEC affected by GDM.

Pathway	dAEC	p-value	Ratio
Transcriptional Regulatory Network in Embryonic Stem Cells		2,21E-05	15/40
Antigen Presentation Pathway		1,69E-04	13/40
OX40 Signaling Pathway		9,82E-04	15/61
Wnt/ß-catenin Signaling		1,61E-03	33/170
Cytotoxic T Lymphocyte-mediated Apoptosis of Target Cells		3,27E-03	13/52

Pathway	dVEC	p-value	Ratio
Axonal Guidance Signaling		1,31E-04	52/457
Cardiac ß-adrenergic Signaling		5,04E-04	21/139
Transcriptional Regulatory Network in Embryonic Stem Cells		1,96E-03	9/40
p70S6K Signaling		2,19E-03	18/122
Epithelial Adherens Junction Signaling		3,96E-03	20/144

Pathway analysis was investigated using Ingenuity Pathway Analysis (www.ingenuity.com) with differentially methylated genes in diabetic AEC and diabetic VEC vs. control cells ($p<0.05$, $\Delta\beta \geq 0.2$).

Table 4. Top networks in AEC and VEC affected by GDM.

Top Networks	dAEC	Score	Focus molecules
Cancer, Endocrine System Disorders, Reproductive System Disease		27	32
Cell-To-Cell Signaling and Interaction, Molecular Transport, Small Molecule Biochemistry		25	31
Cancer, Gastrointestinal Disease, Cellular Growth and Proliferation		23	30
Inflammatory Response, Cell-To-Cell Signaling and Interaction, Cellular Function and Maintenance		22	29
Cardiovascular Disease, Organismal Injury and Abnormalities, Tissue Morphology		22	29

Top Networks	dVEC	Score	Focus molecules
Cell Morphology, Nervous System Development and Function, Tissue Morphology		40	32
Cell Signaling, Molecular Transport, Vitamin and Mineral Metabolism		36	30
Cancer, Hematological Disease, Immunological Disease		34	29
Cardiovascular System Development and Function, Connective Tissue Disorders, Dermatological Diseases and Conditions		32	28
Skeletal and Muscular System Development and Function, Tissue Development, Embryonic Development		32	28
Cellular Assembly and Organization, Hereditary Disorder, Skeletal and Muscular Disorders		31	28

Influenced networks were investigated using Ingenuity Pathway Analysis (www.ingenuity.com) with differentially methylated genes in diabetic AEC and diabetic VEC vs. control cells ($p<0.05$, $\Delta\beta \geq 0.2$).

4.2.3. Influence of GDM on transcriptome of human placental AEC vs. VEC

Unsupervised hierarchical clustering clearly discriminated arterial form venous samples again highlighting the greatest influence of cell type (Figure 28A). Further, the average global transcriptome differences were depicted with a Principal Component Analysis that showed clear separation between normal and diabetic AEC and VEC, respectively (Figure 28B). Focusing the analysis on significantly regulated genes ($p<0.05$) showing expression changes >1.5 fold, diabetic AEC had 812 differentially expressed genes with 36% being up- and 64% downregulated. Diabetic VEC had 211 genes in total with changed expression, 57% up- and 43% downregulated vs. normal cells (Figure 29).

Genes whose expression was substantially regulated by GDM in diabetic AEC, based on fold-change, were selected for validation by RT-qPCR (Table 5). All selected genes, except GADD45B reached statistical significance and were confirmed to be differentially expressed between normal and diabetic AEC, thus validating the microarray platform.

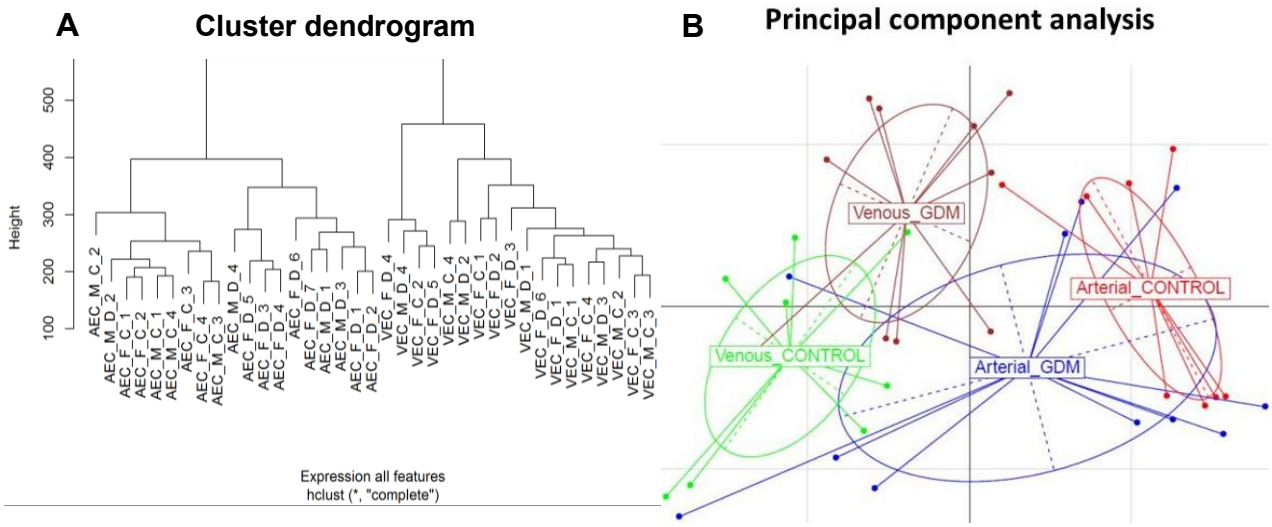

Figure 28. Global transcriptome differences of normal and diabetic AEC and VEC. Alternative PCA plot showing global transcriptome differences between normal and diabetic AEC and VEC, respectively. The distance between the circled areas serves as a proxy measure of the variation between the samples.

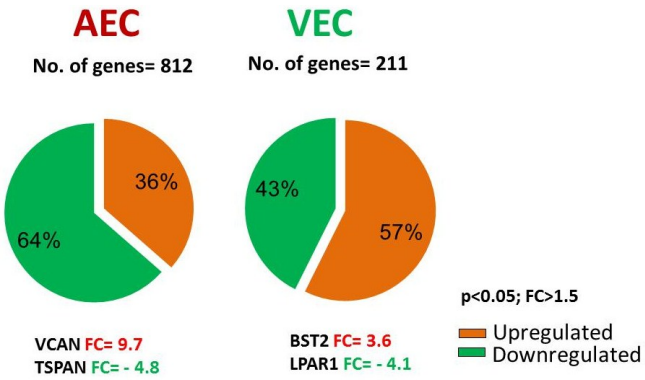

Figure 29. Differentially expressed genes in diabetic AEC and diabetic VEC. The number of differentially expressed genes in total is shown for both, diabetic AEC (dAEC) and diabetic VEC (dVEC) ($p<0.05$, $FC>1.5$) vs. control cells. Pie charts represent the percentage of up- and downregulated genes in relative to the total number of genes showing changes in expression. Genes showing greatest expression changes in diabetic AEC and diabetic VEC are shown under the pie charts. VCAN = versican, TSPAN1 = tetraspanin 1, BST2 = bone marrow stromal cell antigen 2, LPAR1 = lysophosphatidic acid receptor 1.

Table 5. Validation of microarray data with RT-qPCR for AEC.

Gene symbol	Gene name	Microarray		RT-qPCR	
		p-value	FC	p-value	FC
VCAN	Versican	<0.001	9.74	<0.001	41.06
FBN1	Fibrillin 1	<0.001	3.05	<0.001	5.58
TGFBI	Transforming growth factor, beta-induced	<0.001	2.84	<0.001	6.48
	Cyclin D2	0.025	2.39	0.028	3.39
IGF1R	Insulin-like growth factor 1 receptor	<0.001	1.67	0.002	5.53
GADD45B	Growth arrest and DNA-damage-inducible, beta	0.001	1.35	0.025	2.52
p300	E1A binding protein p300	0.001	1.28	0.002	2.95
GADD45A	Growth arrest and DNA-damage-inducible, alpha	0.04	1.18	0.057	1.75
FANCC	Fanconi anemia, complementation group C	<0.001	-1.31	0.003	-1.12

FC = fold-change is the ratio of mean expression for normal vs. diabetic cells.

GDM affected genes in diabetic AEC were mostly located in the nucleus, unlike the differentially methylated genes in the same cell type that reside in the cytoplasm (Table 6). In diabetic VEC the cytoplasm encompassed the highest number of differentially expressed genes (Table 6) that was in accordance with the differentially methylated genes (Table 1).

Table 6. Cellular localization of differentially expressed genes in diabetic AEC and diabetic VEC.

dAEC: Cellular localization	No of molecules	Proportion (%)
Nucleus	238	29
Cytoplasm	188	23
Plasma Membrane	97	12
Extracellular Space	59	7
Unknown	230	28
	812	100

dVEC: Cellular localization	No of molecules	Proportion (%)
Nucleus	56	27
Cytoplasm	59	28
Plasma Membrane	25	12
Extracellular Space	26	12
Unknown	45	21
	211	100

Cellular localization was investigated using Ingenuity Pathway Analysis (www.ingenuity.com) with differentially expressed genes in diabetic AEC and diabetic VEC vs. control cells ($p<0.05$, $FC>1.5$).

Molecular functions enriched with the genes showing differential expression in diabetic cells were cell cycle, cellular assembly and organization and DNA replication, recombination and repair in both, diabetic AEC and diabetic VEC (Table 7) indicating a common diabetic signature. Nevertheless, all functions regarding cell cycle phases were predicted to be decreased by GDM in diabetic AEC which was not the case for diabetic VEC, highlighting the fact that although GDM is affecting identical molecular functions in the two cell types, different sets of genes might be regulated which suggests also a cell type specific action (Table 8).

Table 7. Molecular functions of differentially expressed genes in diabetic AEC and VEC.

dAEC: Molecular functions	dVEC: Molecular functions
Cell Cycle	Cell Cycle
Cellular Assembly and Organization	Cell Death and Survival
DNA Replication, Recombination, and Repair	Cellular Assembly and Organization
Cellular Movement	Cellular Function and Maintenance
Cellular Growth and Proliferation	DNA Replication, Recombination, and Repair

Molecular functions were investigated using Ingenuity Pathway Analysis (www.ingenuity.com) with differentially expressed genes in diabetic AEC and diabetic VEC vs. control cells ($p<0.05$, $FC>1.5$).

Table 8. Molecular functions predicted to be most affected in diabetic AEC.

Molecular function	Functions annotation	p-Value	Predicted activation state	No: of molecules
Cell Cycle	M phase	3,15E-14	Decreased	41
	Cytokinesis	2,54E-08	Decreased	25
	M phase of tumor cell lines	7,28E-08	Decreased	17
	Interphase	2,51E-07	Decreased	65
	Cycling of centrosome	1,70E-06	Decreased	13
	Cytokinesis of tumor cell lines	3,25E-06	Decreased	12
	Entry into interphase of oocytes	3,85E-06	Decreased	4
	Cytokinesis of cervical cancer cell lines	7,54E-05	Decreased	9
	Separation of centrosome	1,04E-04	Decreased	6
	S phase	1,59E-04	Decreased	28
	Entry into interphase	7,01E-04	Decreased	17

Molecular functions were investigated using Ingenuity Pathway Analysis (www.ingenuity.com) with differentially expressed genes in diabetic AEC and diabetic VEC vs. control cells ($p<0.05$, $FC>1.5$).

Furthermore, regulation of cell cycle and DNA damage signaling and response by GDM was also identified in the pathway analysis of the differentially expressed genes ($p<0.05$, $FC>1.5$) (Table 9) in diabetic AEC and diabetic VEC. Interestingly, a pathway involving phospholipases was regulated specifically in diabetic VEC.

Similar results were obtained with the analysis of GDM affected networks (Table 10) where again cell cycle was regulated regardless of cell type while i.e. lipid metabolism network was linked specifically to the differentially expressed genes in diabetic VEC.

Table 9. Pathways of differentially expressed genes in diabetic AEC and diabetic VEC.

dAEC: Pathway	p-value	Ratio
Mitotic Roles of Polo-Like Kinase	5,75E-08	15/70
Cell Cycle: G2/M DNA Damage Checkpoint Regulation	2,27E-07	12/48
Cell Cycle Control of Chromosomal Replication	1,44E-06	9/31
Role of BRCA1 in DNA Damage Response	1,72E-06	13/65
Hereditary Breast Cancer Signaling	8,45E-06	17/128

dVEC: Pathway	p-value	Ratio
ATM Signaling	5,28E-06	7/61
Hereditary Breast Cancer Signaling	4,89E-05	8/128
Mitotic Roles of Polo-Like Kinase	8,22E-05	6/70
Phospholipases	4,05E-04	5/66
DNA damage-induced 14-3-3s Signaling	1,32E-03	3/21

Pathway analysis was investigated using Ingenuity Pathway Analysis (www.ingenuity.com) with differentially expressed genes in diabetic AEC and diabetic VEC vs. control cells ($p<0.05$, FC>1.5).

Table 10. Top networks influenced by differentially expressed genes in diabetic AEC and diabetic VEC.

dAEC: Top Networks	Score	Focus molecules
Cell Cycle, Cellular Assembly and Organization, DNA Replication, Recombination, and Repair	53	34
DNA Replication, Recombination, and Repair, Cell Cycle, Cellular Assembly and Organization	40	30
Cellular Assembly and Organization, DNA Replication, Recombination, and Repair, Cell Cycle	38	28
Infectious Disease, Cardiovascular Disease, Dermatological Diseases and Conditions	34	26
Cell Cycle, Nucleic Acid Metabolism, Small Molecule Biochemistry	32	25

dVEC: Top Networks	Score	Focus molecules
Cancer, Cellular Development, Cellular Growth and Proliferation	43	24
Lipid Metabolism, Small Molecule Biochemistry, Cell Cycle	37	21
Cell Cycle, Cellular Assembly and Organization, Carbohydrate Metabolism	36	22
Cardiac Damage, Cardiovascular Disease, Cellular Compromise	28	17
Cellular Assembly and Organization, Cell Cycle, Cellular Function and Maintenance	28	17

Network analysis was investigated using Ingenuity Pathway Analysis (www.ingenuity.com) with differentially expressed genes in diabetic AEC and diabetic VEC vs. control cells ($p<0.05$, FC>1.5).

Notably, the expression of six transcriptional regulators was identified to be influenced by GDM in arterial and only one in venous cells. *FOXM1*, *GATA3*, *TLR3* and *FBN1* were predicted to be inhibited while *INSIG1* and let-7 to be activated in diabetic AEC. *SELP* in diabetic VEC was predicted to be activated and involved in activation of its downstream targets *CYP1B1*, *CCL2* and *SERPINEB9* (Figure 30).

dAEC

Upstream regulator	Fold change	Molecule type	Predicted activation state
FOXM1	-2,28	transcription regulator	Inhibited
GATA3	-1,72	transcription regulator	Inhibited
TLR3	-1,61	transmembrane receptor	Inhibited
INSIG1	-1,60	other	Activated
let-7	1,65	microRNA	Activated
FBN1	3,05	other	Inhibited

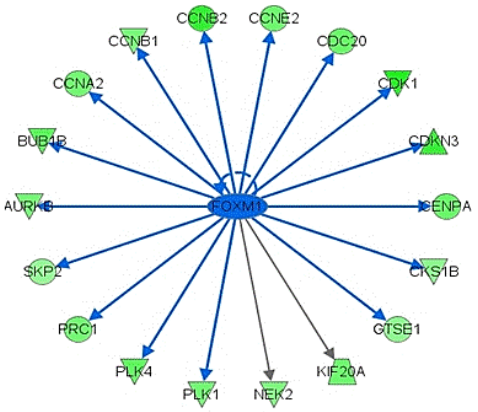

dVEC

Upstream regulator	Fold change	Molecule type	Predicted activation state
SELP	1,981	other	Activated

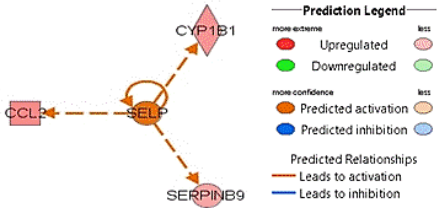

Figure 30. Upstream regulators in diabetic AEC and diabetic VEC whose expression is influenced by GDM. Differentially expressed upstream regulators and their predicted activation states are listed in the tables on the left. Schematic representation of affected regulators and their downstream targets is depicted on the right. Affected transcriptional regulators have been identified using Ingenuity Pathway Analysis (www.ingenuity.com) with differentially expressed genes in diabetic AEC and diabetic VEC vs. control cells ($p<0.05$, FC>1.5).

4.2.4. Concordant methylation and expression changes

In order to examine the relationship between DNA methylation and gene expression, the methylation and gene expression data sets were integrated. For each HM450 probe, differences in ß-values between normal and diabetic cells (Δβ) were calculated and these were compared with corresponding gene expression differences (Figure 31) for arterial and venous cells separately. Cutoff in the significant average methylation difference was set to ≥10% (Δβ≥0.1) and in the gene expression to fold change >1.3. Using these cutoffs concordant changes in the methylation and gene expression levels were detected (red dots in Figure 31). In diabetic AEC 287 genes in total were hypermethylated and downregulated while 116 were hypomethylated and upregulated. If only promoter related genes were assessed there were 24 genes with increased methylation levels and downregulated and 8 had lower methylation and were upregulated (Figure 32A). In diabetic VEC 42 genes in total were found to be hypermethylated and downregulated (3 promoter related genes) while 117 were hypomethylated and upregulated (5 promoter related genes) (Figure 32B).

Panther software clustered these genes to cell cycle, transcription, cell adhesion and angiogenesis related biological processes in diabetic AEC (Table 11). In diabetic VEC genes showing concordant changes in methylation and expression were involved in cell cycle, transport, protein modification, immune system and transcription related processes (Table 11). Table 12 lists all candidate genes implicated in cell cycle and angiogenesis that show methylation change in at least one CpG in the gene sequence and a concordant expression change.

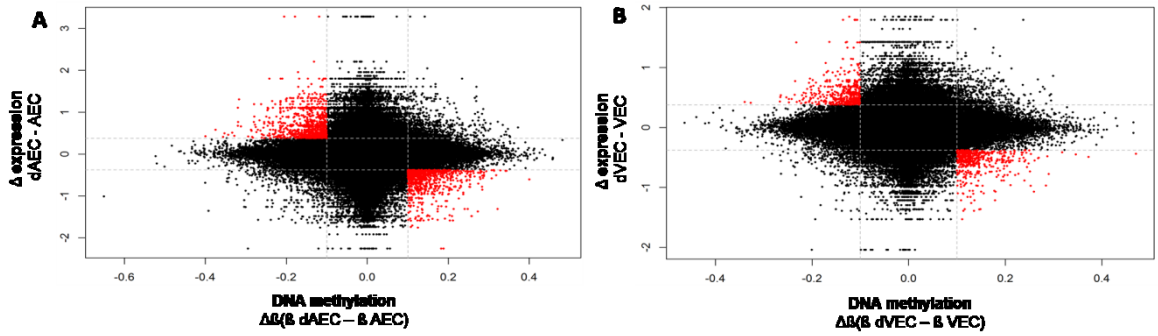

Figure 31. Relationship between DNA methylation and gene expression in normal and diabetic AEC and VEC. Scatterplot of DNA methylation (x-axis) and gene expression (y-axis) for HM450 probes with differences between normal and diabetic AEC (A) and VEC (B). Cutoffs are set to ≥10% (Δβ≥0.1) methylation difference and to fold change >1.3.in the gene expression. Points in red indicate genes likely to be under epigenetic regulation by DNA methylation with increased methylation associated with decreased gene expression and opposite.

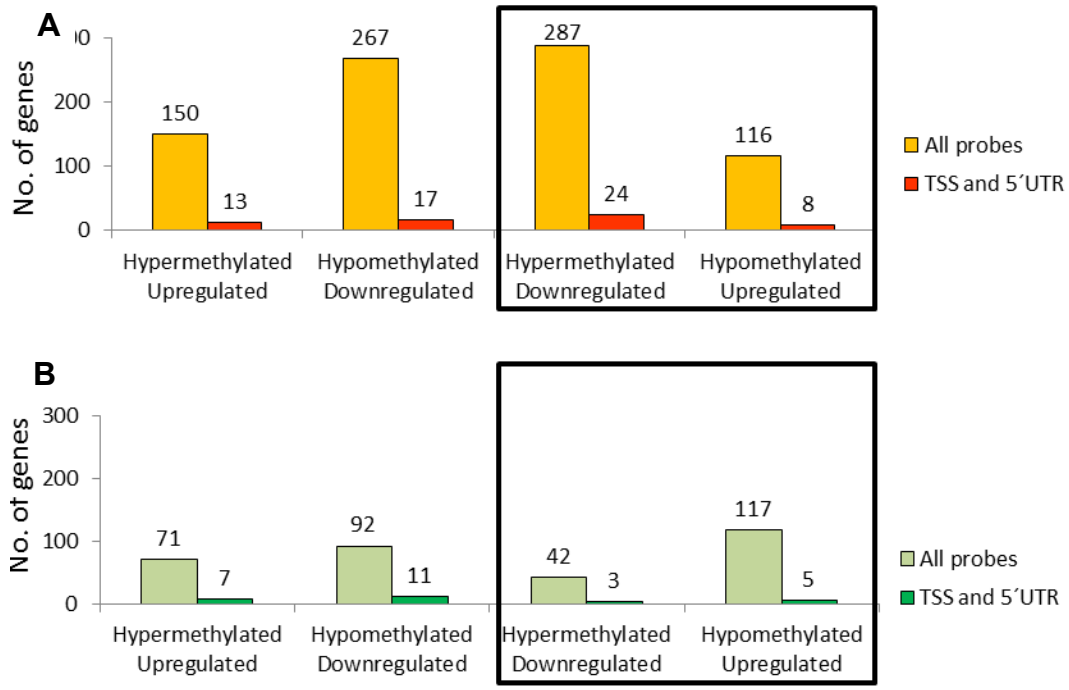

Figure 32. Number of genes associated with specific methylation and gene expression change in diabetic AEC and diabetic VEC. Number of all and promoter-related probes (TSS and 5`UTR) showing concurrent changes in DNA methylation ($p<0.05$, $\Delta\beta\geq0.1$) and expression ($p<0.05$, FC>1.3) for diabetic AEC (A) and diabetic VEC (B) vs. control cells.

Table 11. Processes regulated by genes with concurrent DNA methylation and expression changes in diabetic AEC and diabetic VEC.

dAEC			
HYPERMETHYLATED > DOWNREGULATED		**HYPOMETHYLATED > UPREGULATED**	
Process	**No. of genes**	**Process**	**No. of genes**
Cell cycle	12	Cell adhesion	38
Transcription	10	Cell cycle	21
Angiogenesis	3	Angiogenesis	8

dVEC			
HYPERMETHYLATED > DOWNREGULATED		**HYPOMETHYLATED > UPREGULATED**	
Process	**No. of genes**	**Process**	**No. of genes**
Cell cycle	11	Transport	5
Transport	10	Immune system process	6
Protein modification process	10	Transcription	3

Clustering of the genes that showed changes in DNA methylation ($p<0.05$, $\Delta\beta\geq0.1$) and concurrent changes in expression ($p<0.05$, $FC>1.3$) was investigated using Panther (www.pantherdborg.com).

Table 12. Cell cycle and angiogenesis related genes in diabetic AEC.

Cell cycle		Angiogenesis	
Hypomethylated and UPREGULATED in GDM		**Hypomethylated and UPREGULATED in GDM**	
CALD1	Caldesmon	**ADAMTSL1**	ADAMTS-like protein 1
CCND2	G1/S-specific cyclin-D2	**BMP1**	Bone morphogenetic protein 1
CCNL2	Cyclin-L2	**COL4A1**	Arresten
DDX60L	DEAD (Asp-Glu-Ala-Asp) box polypeptide 60-like	**COL4A2**	Canstatin
DYNC1H1	Cytoplasmic dynein 1 heavy chain 1	**COL5A1**	Collagen alpha-1(V) chain
EGFR	Epidermal growth factor receptor	**CTNNB1**	Catenin (cadherin-associated protein), beta 1
IGF1R	Insulin-like growth factor 1 receptor	**EDIL3**	EGF-like repeat and discoidin I-like domain-containing protein 3
KIF1B	Kinesin-like protein KIF1B	**EGFR**	Epidermal growth factor receptor
LPP	Lipoma-preferred partner	**IGF1R**	Insulin-like growth factor 1 receptor
MACF1	Microtubule-actin cross-linking factor 1, isoforms 1/2/3/5;	**IGFBP5**	Insulin-like growth factor-binding protein 5
MYO10	Myosin X	**LAMA3**	Laminin subunit alpha-3
NEDD9	Neural precursor cell expressed, developmentally down-regulated	**LAMA4**	Laminin subunit alpha-4
PLEC	Plectin	**MACF1**	Microtubule-actin cross-linking factor 1, isoforms 1/2/3/5
PTPRS	Receptor-type tyrosine-protein phosphatase S	**NRP2**	Neuropilin 2, VEGF165R2
PTPRU	Receptor-type tyrosine-protein phosphatase U	**PDGFC**	Platelet-derived growth factor C
SDK1	Protein sidekick-1	**PXN**	Paxillin
SMG1	Smg-1 homolog, phosphatidylinositol 3-kinase-related kinase (C. eleg	**SDK1**	Protein sidekick-1
SYNE1	Nesprin-1	**VCAN**	Versican core protein
TNS3	Tensin-3	**Hypermethylated and DOWNREGULATED in GDM**	
TRRAP	Transformation/transcription domain-associated protein	**ANGPT2**	Angiopoietin-2
UTRN	Utrophin	**HOXB2**	Homeobox protein Hox-B2
Hypermethylated and DOWNREGULATED in GDM		**HOXB8**	Homeobox protein Hox-B8
BLM	Bloom syndrome, RecQ helicase-like		
CDK4	Cyclin-dependent kinase 4		
FANCC	Fanconi anemia group C protein		
FKBP4	FK506 binding protein 4, 59kDa		
KIF22	Kinesin-like protein KIF22		
MAD2L1	Mitotic spindle assembly checkpoint protein MAD2A		
MAPRE3	Microtubule-associated protein, RP/EB family, member 3		
MCM7	Minichromosome maintenance complex component 7		
PAK1IP1	p21-activated protein kinase-interacting protein 1		
RFC5	Replication factor C (activator 1) 5, 36.5kDa		
SMC4	Structural maintenance of chromosomes protein 4		
TRIM24	Tripartite motif containing 24		

Clustering of the genes that showed changes in DNA methylation ($p<0.05$, $\Delta\beta\geq0.1$) and concordant changes in expression ($p<0.05$, $FC>1.3$) was investigated using Panther (www.pantherdborg.com). Genes marked in light orange have a methylation change within the promoter sequence.

4.2.5. GDM programming by DNA methylation might influence cellular function of AEC

By investigating the involvement of all genes that showed both a methylation ($p<0.05$, $\Delta\beta\geq0.1$) and an expression change ($p<0.05$, $FC>1.3$) in diabetic AEC vs. normal cells in signaling pathways G1/S checkpoint regulatory pathway was revealed, as well as many pathways involved in the DNA repair (Figure 33). Interestingly, it is known that the DNA repair mechanisms are activated upon cellular DNA damage and that this can lead to a G1/S cell cycle arrest. Notably, G1/S cell cycle block was also identified in the diabetic AEC by analyzing the cell cycle phases.

These results suggest that altered methylation and gene expression levels of particular genes in GDM might cause the observed functional differences in diabetic cells. Potential gene candidates are listed in Table 13.

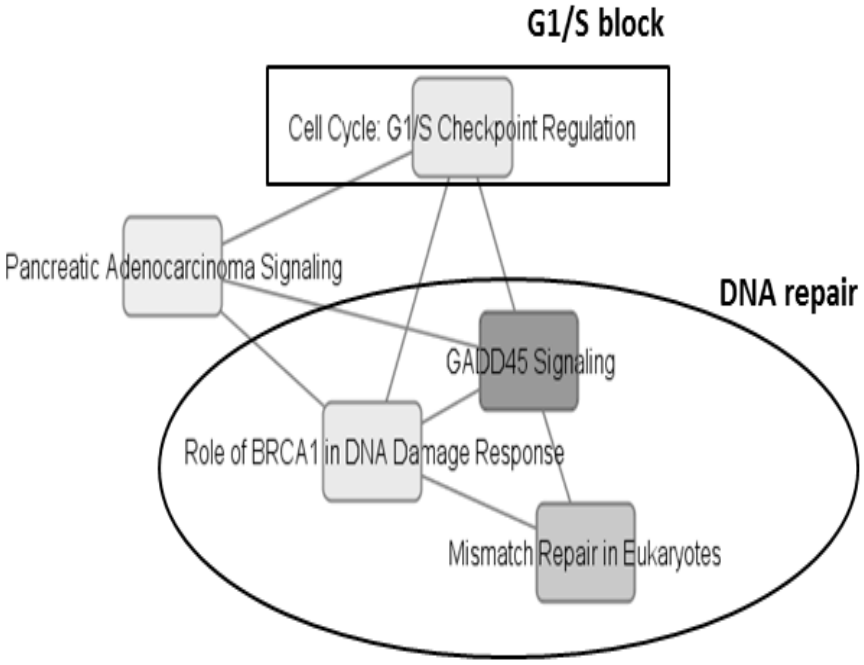

Figure 33. Important pathways associated with concordant DNA methylation and gene expression change in diabetic AEC. Clustering of genes that showed changes in DNA methylation ($p<0.05$, $\Delta\beta\geq0.1$) and changes in expression ($p<0.05$, $FC>1.3$) was investigated using Ingenuity Pathway Analysis (www.ingenuity.com).

Table 13. Significantly GDM regulated pathways in diabetic AEC.

	Methylation and expression change	
In the top 10 most significatnly regulated pathways	G1-S check point molecules	CCND2
		CDK4
		E2F5
		PAK1IP1
		TGFB2
	GADD45 signaling_molecules	BRCA1
		CCND2
		CDK4
		PCNA
	BRCA1 in dna damage response	BLM
		BRCA1
		E2F5
		FANCC
		RFC5
	Missmatch repair	EXO1
		PCNA
		RFC5
Other significantly regulated pathways	Cell cycle regulation of cromosomal replication	CDK4
		MCM5
		MCM7
	p53 Signalling	BIRC5
		BRCA1
		CCND2
		CDK4
		PCNA
		SNAI2

Clustering of genes that showed changes in DNA methylation ($p<0.05$, $\Delta\beta \geq 0.1$) and changes in expression ($p<0.05$, $FC>1.3$) was investigated using Ingenuity Pathway Analysis (www.ingenuity.com). Underlined genes have a concordant methylation and gene expression change.

4.3. *In utero* programming by fetal sex

Fetal sex influences *in utero* development in both uncomplicated pregnancies and pregnancies with sub-optimal outcomes. Furthermore, susceptibility to many adult disorders originates *in utero*, commonly secondary to the effects of placental dysfunction. To investigate the influence of fetal sex on gene expression and function of the feto-placental cells global gene expression pattern was analyzed in four distinct feto-placental cell-phenotypes: cytotrophoblasts (CT), syncytiotrophoblasts (SCT), arterial (AEC) and venous endothelial cells (VEC). To reveal potential functional differences proliferation and 2D-network formation was investigated in AEC.

4.3.1. Sex dependent gene expression in four distinct feto-placental cell types

Whole genome microarray analysis revealed that sex-biased gene expression varied among placental cell types (Figure 34).

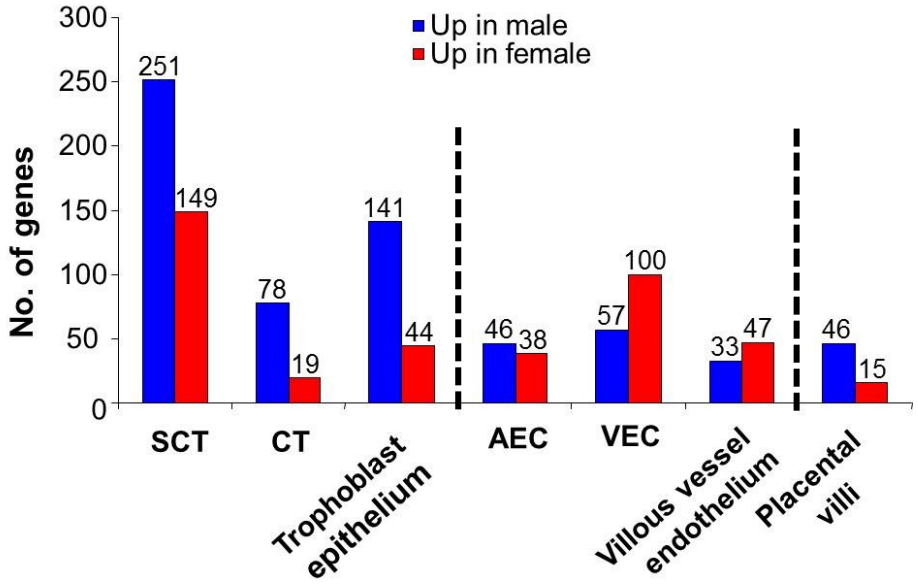

Figure 34. Number of genes showing sex-biased expression in four distinct placental cell types. Number of differentially expressed genes ($p < 0.05$, fold-change >1.3) between male and female syncytiotrophoblasts (SCT), cytotrophoblasts (CT), arterial (AEC) and venous endothelial cells (VEC), trophoblast epithelium, villous vessel endothelium, and for placental villi is shown as number of genes upregulated in males vs. the number of genes upregulated in females. Placental villi refers to combined analysis of all expressed transcripts in SCT, CT, AEC and VEC.

Genes that reached the significance level of p <0.05 and with a fold-change >1.3 were analyzed further. Only 1.3% of all annotated transcripts were differentially expressed between the two sexes in AEC, 2.4% in VEC, 6.3% in SCT, and 1.5% in CT, respectively. Table 14 shows top 10 genes with increased expression in male and 10 with increased expression in female placental cell types. In CT and SCT more genes were differentially expressed when derived from pregnancies with male fetuses than when derived from pregnancies with female fetuses, opposite to AEC and VEC that showed more differentially expressed genes if the fetus was a female (Figure 34). Eleven genes differentially expressed between males and females were in common for all cell types. Ten of these eleven genes were Y-linked and thus expressed at higher levels in male cells, while one was X-linked and expressed at higher levels in female cells (Figure 35A).

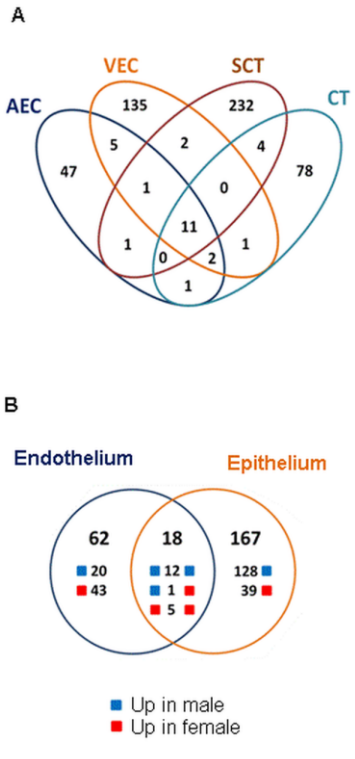

Gene symbol	Description	FC AEC|VEC|SCT|CT
DDX3Y	DEAD (Asp-Glu-Ala-Asp) box polypeptide 3, Y-linked	18.2|12.5|13.6|15.3
KDM5D	lysine (K)-specific demethylase 5D	3.5|3.7|3.4|3.7
EIF1AY	eukaryotic translation initiation factor 1A, Y-linked	16.2|18.6|12.2|14.5
UTY	ubiquitously transcribed tetratricopeptide repeat gene, Y-linked	4.6|4.8|11.5|14.2
CYorf15A	chromosome Y open reading frame 15A	4.8|5.8|2.5|2.7
RPS4Y1	ribosomal protein S4, Y-linked 1	26.9|18.8|9.5|15.5
ZFY	zinc finger protein, Y-linked	3.9|3.7|4.1|6.8
USP9Y	ubiquitin specific peptidase 9, Y-linked	3.8|4.8|3.4|5.3
RPS4Y2	ribosomal protein S4, Y-linked 1	1.9|1.9|2.0|1.7
CYorf15B	chromosome Y open reading frame 15B	2.3|3.1|1.8|1.8
ZFX	zinc finger protein, X-linked	-1.5|-1.6|-1.8|-1.4

Gene symbol	Description	FC endothelium|epithelium
EIF1AY	eukaryotic translation initiation factor 1A, Y-linked	17.3|13.5
DDX3Y	DEAD (Asp-Glu-Ala-Asp) box polypeptide 3, Y-linked	15.1|14.1
RPS4Y1	ribosomal protein S4, Y-linked 1	22.5|13.3
ZFY	zinc finger protein, Y-linked	3.8|5.8
CYorf15A	chromosome Y open reading frame 15A	5.3|2.5
UTY	ubiquitously transcribed tetratricopeptide repeat gene, Y-linked	4.7|13.6
USP9Y	ubiquitin specific peptidase 9, Y-linked	4.3|4.5
KDM5D	lysine (K)-specific demethylase 5D	3.6|4.2
CYorf15B	chromosome Y open reading frame 15B	2.6|1.8
RPS4Y2	ribosomal protein S4, Y-linked 2	1.9|1.7
CNTNAP3	contactin associated protein-like 3	2.2|1.3
PDGFD	platelet derived growth factor D	1.7|1.3
ICA1	islet cell autoantigen 1	1.4|-1.4
KDM6A	KDM6A // lysine (K)-specific demethylase 6A	-1.3|-1.5
KDM5C	lysine (K)-specific demethylase 5C	-1.4|-1.4
ZFX	zinc finger protein, X-linked	-1.5|-1.5
SMC1A	structural maintenance of chromosomes 1A	-1.5|-1.4
ERAP2	endoplasmic reticulum aminopeptidase 2	-2.7|-2.1

Figure 35. Differentially expressed genes in common to all cell phenotypes. Venn diagram depicting the number of gender regulated genes shared between (A) syncytiotrophoblast (SCT), cytotrophoblast (CT), arterial (AEC) and venous endothelial cells (VEC) (B) endothelial and epithelial compartment. Genes found to be in common are shown in boxes on the right (A and B).

Table 14. Top 10 genes showing higher expression in male and top 10 with higher expression in female placental cell types.

SCT			CT		
Gene symbol	**p-value**	**FC**	**Gene symbol**	**p-value**	**FC**
RBMY2EP	<0.001	23.83	RPS4Y1	<0.001	15.50
RBMY1A1	0.001	14.47	DDX3Y	<0.001	15.26
DDX3Y	<0.001	13.60	EIF1AY	<0.001	14.53
EIF1AY	<0.001	12.15	UTY	<0.001	14.16
UTY	<0.001	11.54	ZFY	<0.001	6.78
RBMY1B	0.001	9.96	USP9Y	<0.001	5.28
RBMY1A1	0.001	9.95	KDM5D	<0.001	4.70
RPS4Y1	<0.001	9.49	VNN2	0.040	2.81
RBMY1A1	<0.001	6.46	CYorf15A	0.004	2.69
ERAP2	<0.001	5.64	KRT6A	0.043	2.39
SPATA5L1	0.046	-1.75	SNORD80	0.013	-1.49
ZFX	0.010	-1.76	BLID	0.021	-1.50
SCARNA9L	0.008	-1.77	FLJ43390	0.037	-1.51
SGK269	0.040	-1.78	KDM6A	<0.001	-1.53
SNORD25	0.037	-1.80	RGS2	0.012	-1.55
SNORD116-24	0.037	-1.84	ABCC2	0.016	-1.55
PARVA	0.029	-1.94	SLC13A4	0.048	-1.64
ZNF674	0.004	-2.05	RNU5B-1	0.049	-1.92
UQCRH	0.012	-2.10	SNORD3A	0.010	-1.93
AQPEP	0.045	-2.24	SCARNA9L	0.004	-2.08

AEC			VEC		
Gene symbol	**p-value**	**FC**	**Gene symbol**	**p-value**	**FC**
RPS4Y1	<0.001	26.89	RPS4Y1	<0.001	18.81
DDX3Y	<0.001	18.21	EIF1AY	<0.001	18.62
EIF1AY	<0.001	16.16	DDX3Y	<0.001	12.50
NLGN4Y	<0.001	11.05	NLGN4Y	<0.001	7.36
CYorf15A	<0.001	4.82	CYorf15A	<0.001	5.79
UTY	<0.001	4.63	USP9Y	<0.001	4.80
ZFY	<0.001	3.86	UTY	<0.001	4.78
USP9Y	<0.001	3.82	MPZL2	0.047	3.92
GSTT1	0.033	3.76	KDM5D	<0.001	3.72
RGS5	0.023	3.75	ZFY	<0.001	3.69
PRKX	0.001	-1.62	LAMA2	0.017	-2.03
STEAP2	0.045	-1.66	NNAT	0.009	-2.18
MYOZ2	0.008	-1.68	JMY	0.006	-2.26
PARD6G	0.024	-1.91	SYT14	0.038	-2.30
C21orf94	0.006	-1.99	CHSY3	0.024	-2.30
TFPI2	0.042	-2.24	FAM26E	0.030	-2.43
GSTT2	0.032	-2.35	ITGA4	0.047	-2.55
MIR217	0.034	-2.55	LPHN2	0.017	-2.63
C21orf94	0.005	-3.98	FGF5	0.032	-2.72
F2RL2	0.009	-4.92	NRK	0.005	-4.73

FC = fold-change is the ratio of mean expression for male vs. female cells. SCT = syncytiotrophoblasts, CT = cytotrophoblasts, AEC = arterial endothelial cells and VEC = venous endothelial cells.

Genes with a different degree of sex bias, based on fold-change, were selected for validation by RT-qPCR (Table 15). All selected genes, except ANGPT1, were confirmed to be significantly changed in AEC and VEC. KRT6A in SCT, and KTR6A and PCD11X in CT did not reach statistical significance between the sexes, albeit average fold-changes were comparable between RT-qPCR and microarray analysis.

Table 15. Validation of microarray data with RT-qPCR.

Method	**Microarray**				**RT-PCR**			
Cell type	**SCT**		**CT**		**SCT**		**CT**	
Statistical parameters	p-value	FC	p-value	FC	p-value	FC	p-value	FC
DDX3Y	< 0.001	13.60	< 0.001	15.26	expressed only in male cells			
UTY	< 0.001	11.54	< 0.001	14.16	expressed only in male cells			
ZFY	< 0.001	4.06	< 0.001	6.78	expressed only in male cells			
KDM5D	0.001	3.39	< 0.001	4.70	expressed only in male cells			
PCDH11X	N.C.		0.001	1.78	N.T.		0.063	2.7
KRT6A	0.014	1.22	0.043	2.39	0.310	1.48	0.090	1.15
IDO1	N.C.		0.011	2.10	N.T.		0.008	2.98
ERAP2	< 0.001	5.64	N.C.		0.001	22.81	N.T.	
LAMA4*	< 0.001	1.45	N.C.		0.049	1.28	N.T.	
PLCB4*	0.002	1.35	N.C.		0.006	9.86	N.T.	
ERAP2*	< 0.001	5.64	N.C.		0.019	5.52	N.T.	
ADA*	N.C.		0.004	1.73	N.T.		0.022	4.91
KDM6A*	N.C.		< 0.001	-1.53	N.T.		0.046	-1.90
CCL4*	N.C.		0.030	1.81	N.T.		0.026	7.66

Method	**Microarray**				**RT-PCR**			
Cell type	**AEC**		**VEC**		**AEC**		**VEC**	
Statistical parameters	p-value	FC	p-value	FC	p-value	FC	p-value	FC
DDX3Y	< 0.001	18.21	< 0.001	12.50	expressed only in male cells			
UTY	< 0.001	4.63	< 0.001	4.78	expressed only in male cells			
ZFY	< 0.001	3.86	< 0.001	3.69	expressed only in male cells			
KDM5D	< 0.001	3.49	< 0.001	3.72	expressed only in male cells			
F2RL2	0.009	-4.92	N.C.		0.002	-7.69	N.T.	
PLSCR4*	0.008	1.75	N.C.		0.046	1.84	N.T.	
TFPI2*	0.045	-2.24	N.C.		0.028	-2.36	N.T.	
XAF1*	0.02	1.42	N.C.		0.060	2.39	N.T.	
PC*	N.C.		0.04	1.45	N.T.		0.01	1.38
FGF5*	N.C.		0.03	-2.72	N.T.		0.03	-4.72
ANGPT1*	N.C.		0.02	-1.33	N.T.		0.81	-3.33

FC = fold-change is the ratio of mean expression for male vs. female cells. N. C. = no change. N.T. = not tested. SCT = syncytiotrophoblasts, CT = cytotrophoblasts, AEC = arterial endothelial cells and VEC = venous endothelial cells. *= genes validated using samples distinct from those used in microarray analysis.

4.3.2. Sex dependent gene expression profile differences in trophoblast epithelium vs. villous vessel endothelium

In the trophoblast epithelium, 185 genes showed sex-biased expression vs. 80 genes in the villous vessel endothelium (Figure 36). Not only was the number of genes showing sexual dimorphic expression different between the two placental compartments, but also the direction of gene regulation was different. More female upregulated genes were found in the villous vessel endothelium, whereas trophoblast epithelium showed increased number of transcripts when derived from pregnancies with male fetuses. From the total of 265 sex-biased genes in trophoblast epithelium and villous vessel endothelium, 18 genes were in common for the two villous compartments. Among these, 12 were upregulated in males, five in females and one had a discordant expression in epithelium vs. endothelium (Figure 35B). Chromosomal distribution of male and female genes that were differentially expressed in trophoblast epithelium vs. villous vessel endothelium was analyzed to identify a preferential clustering of the sex-biased genes to a distinct chromosome. In endothelium the differentially regulated genes were distributed across all chromosomes, although, not surprisingly, chromosome X had the highest number of female-biased genes. Only three chromosomes (13, 16 and 21) did not harbor transcripts with sex bias. In the trophoblast epithelium, male upregulated genes were clearly overrepresented on all chromosomes, except for the X-chromosome and chromosome 14, where female upregulated genes prevailed, and for chromosome 22, which had an equal number of male- and female-biased genes. The chromosomal location of the genes whose expression is influenced by fetal sex on sex chromosomes is illustrated with an ideogram in Figure 36.

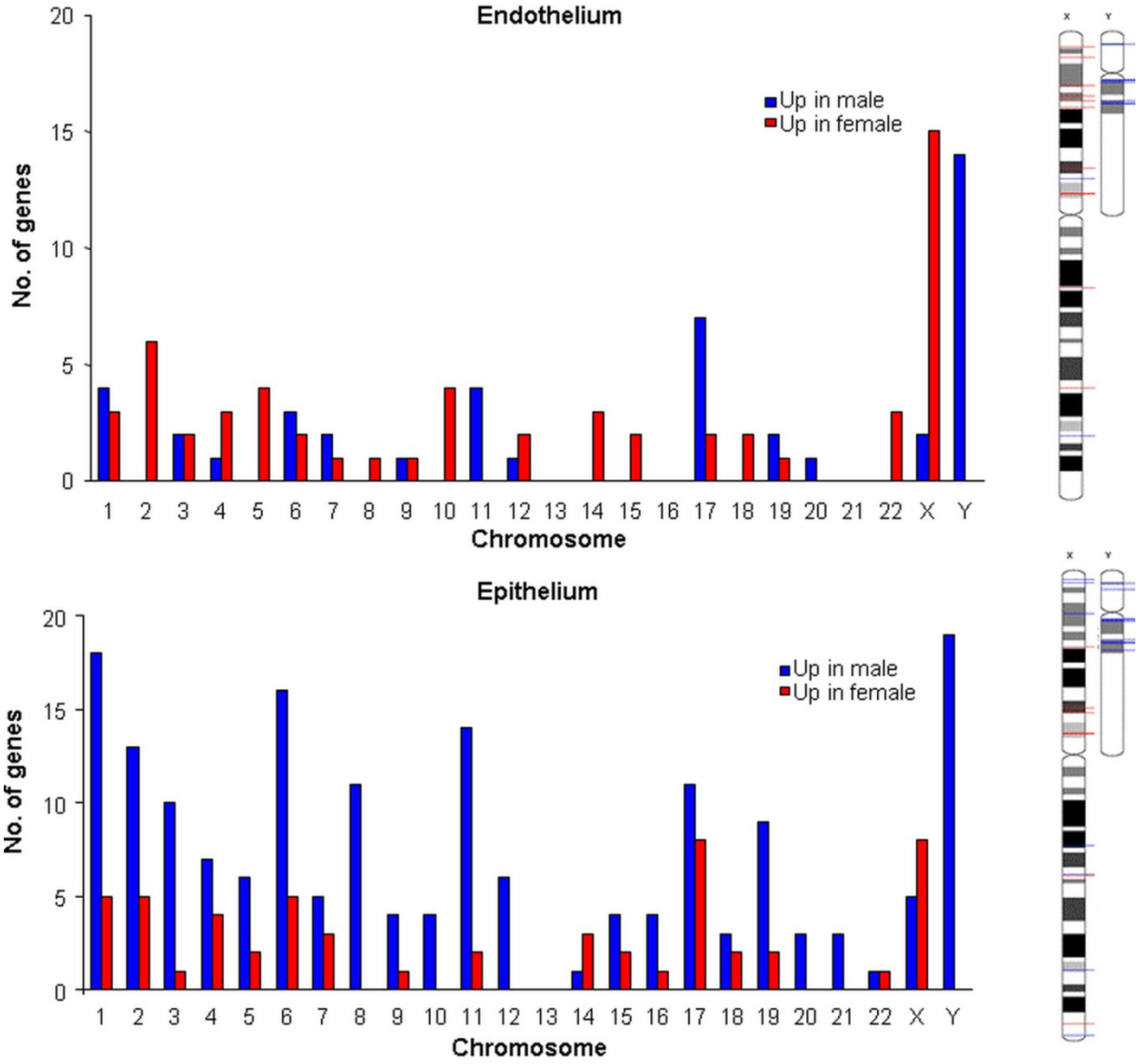

Figure 36. Chromosomal distribution of upregulated genes male vs. female for placental endothelium and epithelium. The number of male- and female-biased genes ($p < 0.05$, fold-change >1.3) is shown for each chromosome separately. An ideogram at the right depicts the specific location of upregulated genes in males (blue line) and females (red line) on two sex chromosomes.

4.3.3. Sex regulated genes in villous vessel endothelium and trophoblast epithelium and implications for biological relevance

Biological processes: Male-biased genes in the trophoblast epithelium were overrepresented in the clusters of genes involved in cell adhesion, and responses to stimuli, including inflammatory and immune responses. Remarkably, none of these processes were linked to female-biased genes in the trophoblast epithelium. Sex-biased genes related to cell adhesion and responses to stimuli were also noted in the villous vessel endothelium, where an additional pathway involving glutathione metabolism was also differentially influenced by fetal sex (Table 16).

Molecular functions: Male-biased genes in the trophoblast epithelium were associated with oxygen binding and oxygen transporter activity, as well as hydrolase, metallopeptidase, oxydoreductase and MHC class II receptor related activities. Female-biased genes were related only to ion binding. Genes upregulated in villous vessel endothelium from males were linked to glutathione transferase, estradiol 17-beta-dehydrogenase and RNA and rRNA binding activities, while actin binding, transferase and dioxygenase activities were enriched with female upregulated genes (Table 17).

Metabolic and signaling pathways: Fetal sex influenced gene enrichment for networks related to cellular movement, development, lipid metabolism, cell death, and antigen presentation in trophoblast epithelium (Table 18). Networks in the endothelial compartment amongst others also included genes important for cellular movement and cell trafficking (Table 18).

In the trophoblast epithelium, the highest enrichment score was for genes in i.e. atherosclerosis and graft-versus-host disease signaling pathways (Table 19) which parallel the identified sex regulated biological processes. The most significant canonical pathways that were different between the sexes of the villous vessel endothelium included genes involved in glutathione, androgen and estrogen metabolism (Table 19).

It was also important to identify upstream transcriptional regulators that could influence differential gene expression among cells from the two sexes. Surprisingly, none of the known upstream regulators reached the activation, or inhibition, threshold z-score in the endothelium. In contrast, fifteen regulators were identified as important for the sex-biased gene expression in the trophoblast epithelium (Table 20), with eleven regulators predicted to be activated.

Table 16. Biological processes displaying sex bias in villous vessel endothelium and trophoblast epithelium (DAVID).

Compartment	Expression	Biological process	Score	%	GENES
ENDOTHELIUM	Up in male	Cofactor metabolic process	195	9	GGT5, HMOX1, GSTT1
		Glutathione metabolic process	28	6	GGT5, GSTT1
	Up in female	Anatomical structure development	2527	26	GMFB, HSD17B10, MATN3, STS, CAP2, MET, CHM, TMOD2, SRR, KIAA1217, SPP1
EPITHELIUM	Up in male	Multicellular organismal process	4280	37	OR4F21, MMP9, PRRX1, ZEB2, MMP3, CDSN, TGFB1, MMP1, CXCL10, OR4C13, GPC3, TGFBI, CNTNAP3, ERAP2, HTR1F, KDM5D, OR4F16, MMP10, KRT14, RPS4Y1, STC1, ADAM19, PRDM1, EMP1, CYP1B1, TBC1D8, USP9Y, CDH2, BICC1, GREM1, RAC2, CAMK2D, SCARB1, HBB, SRGN, TXNIP, DAZ1, DAZ2, OR2A4, PLEK, OR2A7, IL8, NLGN1, CRYZ, FRZB, SNAI2, PCDH18, SFRP4, FABP4, HTR2B, IGFBP4, FABP5
		Response to stimulus	3502	31	HLA-DQB1, A2M, CYP1B1, OR4F21, MRE11A, CXCL11, MMP3, TGFB1, CXCL10, CD97, CD96, OR4C13, RAC2, TGFBI, CAMK2D, VNN1, SCARB1, ERAP2, TXNIP, CRISP3, OR2A4, GBP5, PLEK, OR2A7, IL8, IL1RN, LYZ, OR4F16, SNAI2, HLA-DQA2, HLA-DQA1, CD84, CD86, TNFSF10, VAMP7, LILRB4, KRT14, PLA2G7, FABP4, STC1, ALOX5, GBP4, IGFBP4
		Positive regulation of biological process	2033	19	TBC1D8, MMP9, KLRK1, PRRX1, ZEB2, TGFB1, CXCL10, GPC3, RAC2, CAMK2D, VNN1, SCARB1, PDGFD, HBB, TXNIP, LPL, DAZ1, DAZ2, IL8, PLEK, CD86, TNFSF10, FABP4, ALOX5, PRDM1, HTR2B
		Immune system process	998	16	HLA-DQB1, CRISP3, GBP5, IL8, PLEK, MMP9, IL1RN, KLRK1, CXCL11, HLA-DQA2, HLA-DQA1, TGFB1, CXCL10, CD97, CD96, TNFSF10, CD86, VAMP7, LILRB4, VNN1, ERAP2, GBP4
		Immune response	690	14	HLA-DQB1, CRISP3, GBP5, IL8, IL1RN, CXCL11, HLA-DQA2, HLA-DQA1, TGFB1, CXCL10, CD97, CD96, TNFSF10, CD86, VAMP7, LILRB4, VNN1, ERAP2, GBP4
		Response to chemical stimulus	1281	13	TXNIP, A2M, CYP1B1, IL8, IL1RN, MMP3, CXCL11, TGFB1, CXCL10, RAC2, KRT14, CAMK2D, FABP4, VNN1, SCARB1, STC1, ALOX5
		Cell adhesion	700	12	PLEK, PCDH11Y, PCDH11X, NLGN1, CD99, CDH2, NEO1, CDSN, PCDH18, CD97, CD84, CD96, TGFBI, CNTNAP3, VNN1, SCARB1
		Defense response	615	10	CRISP3, A2M, IL8, IL1RN, LYZ, CXCL11, TGFB1, CXCL10, CD97, CD84, PLA2G7, VNN1, ALOX5, IGFBP4
		Response to wounding	530	10	A2M, IL8, PLEK, IL1RN, LYZ, CXCL11, TGFB1, CXCL10, CD97, PLA2G7, VNN1, SCARB1, ALOX5, IGFBP4

Compartment	Expression	Biological process	Score	%	GENES
		Regulation of signal transduction	878	10	TBC1D3F, TBC1D8, TBC1D3G, PLEK, TBC1D3H, PRRX1, FSTL3, ZEB2, CDH2, GREM1, FRZB, TGFB1, TBC1D3B, TNFSF10, GPC3, HTR2B, TBC1D3
		Tissue development	665	9	TXNIP, GPC3, KRT14, PRRX1, ZEB2, GREM1, SNAI2, CDSN, EMP1, FABP5, TGFB1, SRGN
		Inflammatory response	325	9	CD97, A2M, IL8, IL1RN, LYZ, PLA2G7, VNN1, ALOX5, CXCL11, TGFB1, IGFBP4, CXCL10
		Cell motion	475	7	CD97, IL8, PSG2, VNN1, ZEB2, SCARB1, CDH2, VNN2, TGFB1
		Regulation of response to stimulus	465	7	A2M, CD86, PLEK, IL8, KLRK1, FABP4, ZEB2, GREM1, TGFB1
		Cell proliferation	436	7	CD86, TGFBI, ZEB2, MAPRE2, SCARB1, PSPH, EMP1, TGFB1, IGFBP4
	Up in female	-	-	-	-

Only genes with FC >1.3 were used. Significance level was set to $p < 0.05$ for both genes and processes. FC = fold-change is the ratio of mean expression for male vs. female cells; score = number of genes after enrichment involved in the respective biological process and related to genes that show sex-biased expression. The proportion (%) refers to the amount of sex-biased genes found to play a role in the respective biological process. FDR = false discovery rate.

Table 17. Molecular functions displaying sex bias in endothelium and epithelium (DAVID).

Compartment	Expression	Molecular function	Score	%	FDR [%]	GENES
Villous vessel endothelium	Up in male	RNA binding	718	15	25	RPS4Y2, DDX3Y, EIF1AY, RPS4Y1, OAS1
		rRNA binding	29	6	41	RPS4Y2, RPS4Y1
	Up in female	transferase activity	49	7	8	CHM, GSTT2, SMS
		actin binding	326	12	10	GMFB, CAP2, XIRP2, TMOD2, JMY
		dioxygenase activity	66	7	13	KDM6A, ASPHD2, KDM5C
Trophoblast epithelium	Up in male	metallopeptidase activity	183	5	3	MMP10, PAPPA, MMP9, ERAP2, ADAM19, MMP3, MMP1
		oxygen binding	43	3	5	CYP1B1, HBG1, HBA2, HBA1, HBB
		oxygen transporter activity	13	2	5	HBG1, HBA2, HBA1, HBB
		metalloendopeptidase activity	104	4	10	MMP10, MMP9, ADAM19, MMP3, MMP1
		peptidase activity, acting on L-amino acid peptides	549	8	10	NRIP3, MMP10, CTSL2, USP9Y, PAPPA, MMP9, DPP10, ERAP2, ADAM19, MMP3, MMP1
		MHC class II receptor activity	19	2	11	HLA-DQB1, HLA-DQA2, HLA-DQA1
		peptidase activity	574	8	13	NRIP3, MMP10, CTSL2, USP9Y, PAPPA, MMP9, DPP10, ERAP2, ADAM19, MMP3, MMP1
		cytokine activity	195	4	18	TNFSF10, IL8, IL1RN, CXCL11, GREM1, CXCL10
		pantetheine hydrolase activity	3	1	26	VNN1, VNN2

Compartment	Expression	Molecular function	Score	%	FDR [%]	GENES
		hydrolase activity	2283	19	30	CTSL2, USP9Y, MRE11A, MMP9, DPP10, MMP3, PSPH, MMP1, PLCB4, RAC2, PAPPA, DDX3Y, VNN1, ERAP2, VNN2, PTPRB, NRIP3, LPL, GBP5, PTPRG, LYZ, ACPP, MMP10, PLA2G7, ADAM19, GBP4
		oxidoreductase activity	6	1	45	PAM, MOXD1
		chemokine activity	46	2	46	IL8, CXCL11, CXCL10
		lipid binding	450	6	49	LPL, PLEK, APOD, PLA2G7, VNN1, FABP4, SCARB1, FABP5
	Up in female	ion binding	4241	39	34	NOX4, ZMAT1, KDM6A, IMPA2, PDP2, NUDT12, ZFX, ZNF354B, CACNG4, COLEC12, ZNF674, ZNF717, ZSCAN16, PHOSPHO1, SLC13A4, CASQ1, KDM5C

Significance level was set to $p < 0.05$ for both genes and processes. FC = fold-change is the ratio of mean expression for male vs. female cells; score = number of genes after enrichment involved in the respective molecular function and related to genes that show sex-biased expression. The proportion (%) refers to the amount of sex-biased genes found to play a role in the respective molecular function. FDR = false discovery rate.

Table 18. Metabolic and signaling pathways identified by Pathway studio for villous vessel endothelium and trophoblast epithelium.

Compartment	Pathways	p-value	Genes
Villous vessel endothelium	Translation control	0.002	RPS4Y2,SPP1,IL1A,MET, HTR1B,TNFRSF10A, SF2RB,PDGFD,TNFSF18, EIF1AX, EIF1AY,RPS4Y1
	Glutathione metabolism	0.013	GSTT1,GSTT2,GGT5
	Ser/Gly/Thr/Cys metabolism	0.031	SRR,GGT5,HSD17B14
Trophoblast epithelium	B Cell Activation	0.008	RPS4Y2,ALOX5,RAC2,GPX 7,CD84,PLCB4,CD99,CBR1, VAMP7,EIF1AY,EMR2, CD96,CAMK2D,PCDH11X, RPS4Y1,PCDH11Y, CDH18
	Gonadotrope cell activation	0.022	ALOX5,MMP9,MMP1,MMP3, RAC2,STC1,PLA2G7,GPX7, PDGFD,PLCB4,CBR1, VAMP7,CACNG4,CAMK2D
	Arachidonic acid metabolism	0.019	ALOX5,CYP1B1,PLA2G7, GPX7,CBR1
	Omega-6-fatty acid metabolism	0.039	CYP1B1,PLA2G7,CBR1, SLC27A2
	Omega-3-fatty acid metabolism	0.048	ALOX5,CYP1B1,PLA2G7, SLC27A2
	Heme oxidation and biosynthesis	0.007	HBB,HBA1,HBA2
	Double Strand DNA Homologous Repair	0.039	MRE11A,SMC1A,RFC1
	TGFBR/BMPR -> SMAD2/3 signaling	0.010	TGFB1,SMAD3
	CCR5 -> TP53 signaling	0.015	IL8,CXCL11
	CCR2/5 -> STAT signaling	0.020	IL8,CXCL11
	TGFBR -> MEF/MYOD/MYOG signaling	0.035	TGFB1,SMAD3
	Vitamin B5 (pantothenate) metabolism	0.014	VNN1,VNN2

Genes significantly differentially expressed between males and females ($p < 0.05$; FC >1.3) in villous vessel endothelium and trophoblast epithelium were enriched using Pathway studio. FC = fold-change is the ratio of mean expression for male vs. female cells.

Table 19. Top 5 significantly enriched canonical pathways in Ingenuity Pathway Analysis.

	Top canonical pathways	Molecules	%
Villous vessel endothelium	Glutathione Metabolism	GSTT2/GSTT2B, GSTT1, GGT5	6.0
	Androgen and Estrogen Metabolism	HSD17B10, STS, HSD17B14	4.3
	Estrogen-Dependent Breast Cancer Signaling	HSD17B10, HSD17B14	3.1
	IL-10 Signaling	HMOX1, IL1A	2.8
	Regulation of eIF4 and p70S6K Signaling	EIF1AY, EIF1AX, RPS4Y2, RPS4Y1	2.5
Trophoblast epithelium	Airway Pathology in Chronic Obstructive Pulmonary Disease	IL8, MMP9, MMP1	37.5
	Atherosclerosis Signaling	ALOX5, IPOD, IL8	9.4
	Graft-versus-Host Disease Signaling	CD86, HLA-DQA1, IL1RA	8.7
	Arginine and Proline Metabolism	ABP1, VNN2, VNN1	5.0
	Role of Macrophages, Fibroblasts and Endothelial Cells in Rheumatoid Arthritis	CAMK2D, FRZB, FZD5, IL8, MMP1, MMP3, PDGFD, PLCB4, SFRP, TGFB1	3.5

The proportion (%) refers to the amount of sex-biased genes found to play a role in the respective pathway.

Table 20. List of regulators whose downstream target genes are differentially expressed between male and female trophoblast epithelium identified using Ingenuity Pathway Analysis.

Molecule	Molecule type	Predicted activation state	Regulation z-score	Overlap p-value	Target molecules
IL1RN	cytokine	inhibited	-2.2	3.9E-04	CXCL11, ERAP2, HLA-DQB1, MMP1, TNFSF10
IL1B	cytokine	activated	2.8	9.7E-08	ACPP, CXCL10, CXCL11, FABP5, IL1RN, IL8, MMP1, MMP3, MMP9, SRGN
RELA	transcription regulator	activated	2.2	1.2E-07	CXCL10, CXCL11, ERAP2, HAS2, IL1RN, IL8, MMP1, MMP9, TGFB1
NFkB (complex)	complex	activated	2.8	6.6E-07	CD86, CXCL10, ERAP2, HAS2, IL8, MMP1, MMP3, MMP9, TNFSF10
P38 MAPK	group	activated	2.8	2.4E-06	CD86, CXCL10, IL8, MMP1, MMP3, MMP9, TGFB1, TNFSF10
Jnk	group	activated	2.4	4.8E-06	CD86, CDH2, GJA1, IL8, MMP1, MMP3
IFNG	cytokine	activated	2.1	7.1E-06	CD86, CXCL10, CXCL11, ERAP2, HLA-DQB1, IGFBP4, IL1RN, IL8, MMP1, MMP9
CCL5	cytokine	activated	2.2	3.7E-05	CD97, CYP1B1, EMP1, IL8, MMP9
IL18	cytokine	activated	2.2	3.7E-05	IL8, MMP1, MMP3, MMP9, SMAD3
TNF	cytokine	activated	3.0	9.1E-05	CD86, CXCL10, CXCL11, IL1RN, IL8, L SS, MMP1, MMP3, MMP9, PRDM1
IL1A	cytokine	activated	2.2	2.8E-04	CXCL10, IL8, MMP1, MMP10, TGFB1
TREM1	other	activated	2.4	1.2E-03	ARRDC4, GREM1, IL8, LPL, MMP1, MMP10, NRIP3

IL1RN was the only upstream regulator that shows sex-bias. No upstream regulator has been identified for sex-biased genes in the villous vessel endothelium.

Altogether, these results show that fetal sex differentially affects gene expression in a cell-phenotype dependent manner among all four cell-phenotypes studied. Furthermore, distinct biological processes and molecular functions were identified for sex-biased genes in two main placental compartments villous vessel endothelium and trophoblast epithelium. Hence; the cellular and placental function might also be dependent on fetal sex.

4.3.4. Fetal sex influences proliferation and 2D-network formation of AEC

To address sex influence on cellular function proliferation and 2D-network formation potential of male and female AEC were investigated.

Male AEC had a significantly lower number of viable cells than female AEC after 96 h (2-way ANOVA p=0.01, at 96 h p<0.05) in culture at 21% O_2 (Figure 37A). Reduced proliferation potential of male AEC was confirmed with ELISA by adding BrdU after 48 h culture of male and female cells and measuring its integration into the newly synthesized DNA during DNA replication. Male AEC had significantly less incorporated BrdU (p<0.05) than normal cells indicating lower amount of cells in the S-phase of the cell cycle (Figure 37B). Furthermore, when investigating 2D-network formation in the presence of 5% FCS male AEC had increased total tube length as compared to female AEC at 3, 6 and 12 h (all hours p<0.05) (Figure 38).

These results demonstrate that feto-placental cellular function is dependent on fetal sex in normal endothelial cells isolated from healthy pregnancies.

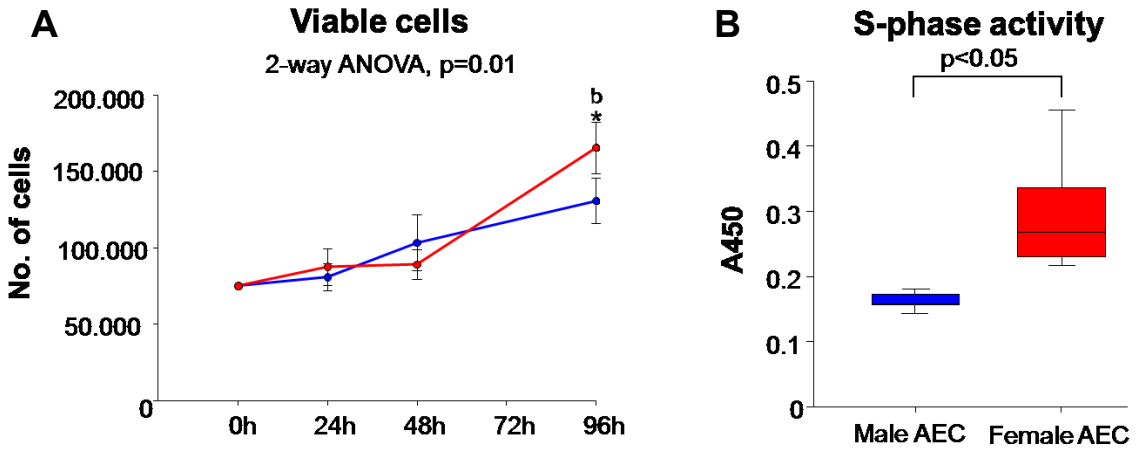

Figure 37. Proliferation of male and female normal AEC at 21% O_2 determined by direct .cell counting and ELISA measuring BrdU incorporation into the DNA. Number of viable cells after 24, 48 and 96 h in culture (A). Data are indicated as mean ± SD of 3 male vs. 4 female endothelial cell isolations each in triplicates. The amount of the incorporated BrdU was determined in cells cultured for 48 h (B). Data are indicated as mean ± SD of 3 male vs. 5 female endothelial cell isolations each in duplicates.

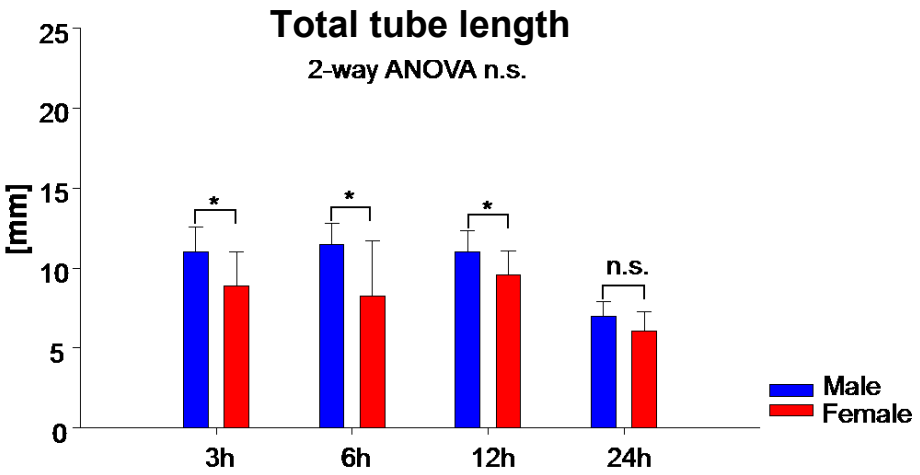

Figure 38. 2D-network formation of male and female normal AEC. The total tube length (mm) was evaluated after 3, 6, 12 and 24 h on a growth reduced matrigel in the presence of 5% FCS at 21% O_2. Data are indicated as mean ± SD of 4 male vs. 4 female endothelial cell isolations each in quadruplicates.

Whether fetal sex also influences function of endothelial cells exposed to the diabetic *in utero* environment was investigated by measuring proliferation and 2D-network formation in diabetic AEC.

Interestingly, there was no difference neither in proliferation nor in 2D-network formation between male and female diabetic AEC (Figure 39A and B). This suggests that the maternal diabetic intrauterine environment differently (or to a different extent) programs male and female endothelial cells so the functional sex differences observed *in vitro* between normal AEC disappear between diabetic cells.

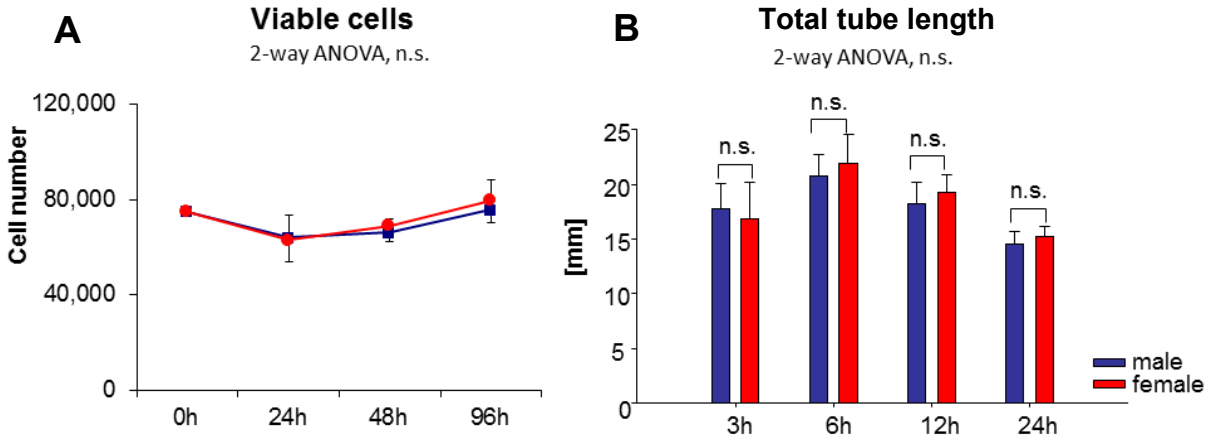

Figure 39. Proliferation and 2D-network formation of male and female diabetic AEC. Number of viable cells after 24, 48 and 96 h in culture (A). Data are indicated as mean ± SD of 3 male vs. 4 female endothelial cell isolations each in triplicates. The total tube length (mm) was evaluated after 3, 6, 12 and 24 h on a growth reduced matrigel in the presence of 5% FCS at 21% O_2. Data are indicated as mean ± SD of 4 male vs. 4 female endothelial cell isolations each in quadruplicates.

5. Discussion

Fetal metabolic programming hypothesis was firstly proposed by Barker and colleagues already two decades ago (64). Based on myriad of epidemiological studies, he postulated that fetal and perinatal events, i.e. maternal nutrition, were crucial to determine individual risk of developing chronic metabolic diseases in adulthood. Such conditions, including diabetes, obesity and cardiovascular diseases, have become a very important population health concern. In the 20 years of research, the concept of fetal programming has been corroborated by many animal and human studies (106-108), but the molecular mechanisms involved are still poorly understood. Hence, more research is needed in human models of fetal metabolic programming. One impressive model is gestational diabetes mellitus (GDM).

Because of its location at the interface between the mother and the fetus, placenta is subject to a plethora of environmental factors, some of which have been shown to influence placental gene expression, epigenetic marks and function (109). These include diet (24), smoking (25), and diabetes (26-29). As the there are limitations in studying environmental influences on other fetal tissues, the human placenta with its complex vascular system, represents an easily available source of primary feto-placental cells with established protocols for their isolation, characterization and culture (90).

The current thesis investigated the intrauterine programming of the feto-placental cells by maternal diabetes, whereby endothelial cells from two distinct vascular beds were used, arterial (AEC) and venous endothelial cells (VEC). The cellular batch was further extended by adding cytotrophoblasts (CT) and syncytiotrophoblast (SCT) when investigating fetal sex influence on placental gene expression.

Key findings of this study are: (i) primary cells isolated from human term placentas after GDM pregnancies (diabetic AEC) when cultured under the identical conditions differ in their functional characteristics, i.e. proliferation and network formation, from the cells isolated after healthy pregnancies (normal AEC), (ii) DNA methylation and transcription profile of diabetic AEC and diabetic VEC clearly show diabetic signature accentuating and potentially explaining the observed functional differences i.e. cell cycle when compared to normal cells (iii) all four cell types

analyzed *in vitro*, SCT, CT, AEC and VEC varied in the extent of sex-biased gene expression, despite the fact that these cells originate from the same organ. Moreover, transcripts of male fetuses prevailed in the epithelial compartment, represented by SCT and CT, whereas the endothelial compartment, represented by AEC and VEC, showed more female-biased genes.

Overall, the data reveal that GDM derived feto-placental endothelial cells persistently differ from cells isolated from uncomplicated pregnancies. This demonstrates that the placental endothelial cells *in vitro* remember their diabetic *in vivo* phenotype. Furthermore, the observed differences in gene expression and functional differences between male and female feto-placental cells argue for an intrinsic program that enables cells to remember fetal sex. Hence, this thesis introduces new evidence of cellular memory and intrinsic cellular changes depending on the *in utero* exposure to the adverse maternal environment i.e. GDM, affected placental vascular bed i.e arterial vs. venous and fetal sex. It is plausible to assume that these intrinsic changes *in utero* contribute to altered disease susceptibility in adulthood.

5.1. Feto-placental endothelial cells remember their *in utero* diabetic environment

Distinct derangements of endothelial function are well recognized in diabetic patients and there is new evidence that endothelial dysfunction arises already in three-year-old children born to GDM pregnancies (110). To reveal whether diabetes associated endothelial dysfunction originates *in utero* and whether maternal diabetic environment evokes persistent changes in the feto-placental endothelial cells two key processes were investigated - proliferation and network formation.

Grown under identical culture conditions, diabetic AEC had significantly fewer viable (36±10%) and fewer dead cells (33±8%) as compared to normal AEC. Furthermore, diabetic AEC showed a significant decrease in S-phase and a significant increase in G1-phase vs. normal AEC whereas the G2/M-phase was unchanged. As the proportion of apoptotic cells was similar in both groups, it is evident that the noted difference in the number of viable cells arises from reduced proliferation of diabetic cells due to a G1/S-cell cycle arrest. The results were corroborated by increased levels of proteins in diabetic AEC that through different signaling pathways may lead to a cell cycle arrest, i.e. observed upregulation of

p27Kip1 may prevent activation of CyclinE-Cdk-2 and CyclinD-Cdk-4 complexes and hence, control G1-S transition. Interestingly, reduced proliferation of endothelial cells exposed to the diabetic environment was also noted by Lehle K. and colleagues who investigated *in vitro* function of adult human saphenous vein endothelial cells (111). The data presented in this thesis ad up to the findings of Lehle K. and colleagues and demonstrate that not only long term influence of Type 2 diabetes, but also short term exposure such as GDM can program endothelial cell phenotype that persists also in culture. Furthermore, the data demonstrate that programming of endothelial function may begin already *in utero*.

Fetal levels of insulin and other growth factors i.e. fibroblast growth factor 2 are elevated in diabetic pregnancies (112) and have the potential to stimulate placental angiogenesis. Increased vascular growth and enhanced branching angiogenesis have been reported for GDM pregnancies (Leach L and Mayhew TM, 2005). Hence, endothelial function of diabetic AEC was further investigated by their ability to form tube-like structures in a growth factor reduced Matrigel. This assay is commonly used as a proxy measure of endothelial cell angiogenic activity (113,114). When compared to their healthy counterparts, diabetic AEC had increased network formation presented by longer tubes in total, increased number of branching points and number of meshes (45±10%, 311±28% and 163±50%, respectively). This increased ability of diabetic cells to form tube-like structures was not influenced by the presence of diabetic cord blood serum indicating that observed differences in endothelial function are not due to the environmental factors *in vitro* and rather reflect an intrinsic cellular program.

High glucose levels occurring in diabetes are now widely recognized as detrimental factors in long term diabetic complications as is the need for a good glucose control in affected individuals most efficient if introduced early at the onset of a disease (115). In this thesis, high glucose treatment of normal AEC was used to investigate its potential to induce a diabetic-like phenotype of endothelial cells. Indeed, 25 mM glucose increased network formation of normal AEC up to 40±26%. These data suggest the ability of elevated glucose levels to program the function of feto-placental endothelial cells. Glucose memory effect of endothelial cells has been demonstrated also by other research groups (116,117). El-Osta and colleagues demonstrate significant change in histone posttranslational modifications in the healthy human aortic endothelial cells following exposure to high glucose that

persist even when returning the exposed cells to normal glucose levels. The novelty of data presented here is the important functional consequence of high glucose exposure of placenta-derived cells, which paralleled the finding of increased network formation observed in diabetic endothelial cells. It would be of great interest to investigate whether such induced changes in normal AEC are persistent also after switching the culture conditions to normal glucose levels.

Depending on the type, diabetes is known to alter concentration of many cytokines, chemokines and cell adhesion molecules synthesized and released by the placenta (104,118) resulting in an adverse metabolic milieu not only in maternal but also fetal circulation. Interestingly, ICAM1 was altered in the culture medium of diabetic AEC, showing 41% reduction in the expression when compared to normal cells. The expression of other low-grade inflammation markers IL6, IL8, MCP1, Serpin E1 and VCAM1 was not affected in diabetic cells.

Increasing number of studies is linking epigenetic changes and fetal programming with DNA methylation being mostly investigated (119-122). Hence, the global DNA methylation and gene expression profile was analyzed in normal and diabetic AEC to delineate molecular mechanisms underlying the observed functional differences in proliferation and network formation. Besides a global hypomethylation of diabetic AEC (5%, $p \leq 0.001$), the analysis revealed a proportion of differentially methylated and differentially expressed genes that clustered to angiogenesis and cell cycle related processes. Among the top significantly regulated pathways in diabetic vs. normal AEC was the G1/S-check point regulation and pathways involving DNA damage and DNA repair response. It is tempting to speculate that *in utero* hyperglycemia, occurring in GDM pregnancies, might induce hypomethylation of the-fetoplacental endothelial cells making them vulnerable to environmental conditions. Such conditions might include increased intracellular formation of reactive oxygen species (ROS) and of advanced glycation end-products (AGEs) that may lead to DNA damage in diabetic cells and finally to a cell cycle arrest. Increased glucose levels are already reported to have the potential of inducing persistent, global epigenetic changes in endothelial cells (117) as well was DNA damage (123).

Only a small portion of revealed genes showed reciprocal change in methylation and expression indicating that although DNA methylation might

influence differential gene expression in diabetic AEC it is not the leading mechanism.

Collectively, the altered endothelial function of diabetic AEC even when cultured under identical conditions as normal AEC argues for changes in the cells that seem to reflect an intrinsic program to which epigenetic modifications contribute.

5.2. Feto-placental endothelial cells display cell type specific metabolic memory

Two vascular beds, arterial and venous, exist in the placenta where feto-placental endothelial cells come in direct contact with fetal blood. Veins serve to supply the fetus with oxygen and nutrients from the mother, while arteries carry deoxygenated blood and waste products from fetal circulation. Hence, it is not surprising that arterial (AEC) and venous (VEC) endothelial cells display physiologic and functional differences *in vivo* (119). In contrast, the fact that they maintain their phenotype during *in vitro* culture and after continuous passaging (12) reveals stunning cellular memory underlined by distinct epigenetic signatures (119). Recent evidence demonstrate distinct DNA methylation patterns of key regulatory genes between AEC and VEC i.e *NOS3*, *VWF*, *CDH5*, *ICAM2*, *VEGFR1* and -*R2*, *TEK* and *NOTCH4* (119). The authors suggest that these genes represent potential targets for environmentally mediated epigenetic disruption *in utero* in association with cardiovascular risk later in life. Hence, one of the main aims in this thesis was to investigate how the *in utero* exposure to GDM metabolic environment influences global DNA methylation and gene expression profile in primary AEC and VEC and whether they display individual and/or shared diabetic signatures.

Global-wide analyses are nowadays widely used as profiling tools to get insight into molecular mechanism of distinct pathologies (124-126). Only a few studies report genome-wide gene expression (127-129) and DNA methylation studies (122,130) from placentas of GDM pregnancies. However, they used whole placental tissue with myriad of distinct cell types. There are around 200 distinct cell types in the human body that undergo specific differentiation processes whereby specific epigenetic as well as gene expression patterns are established. Thus, studying individual cell types could provide a better insight into molecular mechanisms of a disease.

In this study, genome-wide DNA methylation profile significantly differed between normal and diabetic feto-placental endothelial cells with a distinct degree of global hypomethylation noted in diabetic AEC (5%, p≤0.001) and diabetic VEC (3%, p≤0.001) as compared to their normal counterparts. Hence, although the GDM-induced changes manifest in the same direction the effect of maternal diabetes on feto-placental AEC and VEC varies in its extent. This is supported by gene ontology analysis where differentially methylated genes in both, diabetic AEC and diabetic VEC were linked with the highest significance to diabetes mellitus and glucose metabolism related disorders, but sequent in depth analysis of specific molecular functions and signaling pathways revealed dissimilarities between the two cell types in response to maternal diabetes, i.e. cellular growth, proliferation and inflammatory response pathways were significantly enriched in diabetic AEC, while cell and tissue morphology and cellular assembly and organization were linked to the differentially methylated genes in diabetic VEC. Interestingly, metabolic disease and diabetes mellitus related pathways are reported to be epigenetically affected by GDM in whole placental tissue and cord blood (131). Also Nomura and colleagues report changes in the global DNA methylation profile in the same tissues with significant hypomethylation paralleled by *in utero* exposure to maternal diabetic environment (130). Notably, these studies do not report consequences of GDM-altered DNA methylation in terms of complementary phenotypes i.e. mRNA and protein levels. Thus, to understand the relationship between DNA methylation and regulation of gene expression this study analyzed global gene expression patterns in normal and diabetic feto-placental endothelial cells. Only a small portion of genes in both diabetic AEC and diabetic VEC showed concordance in DNA methylation and gene expression, suggesting that DNA methylation is contributing to the observed gene expression changes but other epigenetic mechanisms i.e. posttranslational modifications of histones and RNA based mechanisms, not studied here, may also play an important role.

Only six genes that were responsive to *in utero* exposure to GDM, by displaying changes in DNA methylation and expression, were shared between AEC and VEC. These, among others, include epidermal growth factor receptor (*EGFR*) and sulfatase 2 (*SULF2*) whose altered levels are linked to diabetic complications. *EGFR* is reported to mediate crucial pathways related to diabetic cardiac myopathy including ROS, ER-stress and members of RAAS system (132) while *SULF2* is

implicated in postprandial maintenance of lipid levels in Type 2 diabetes (133). The low number of genes regulated by GDM in common to AEC and VEC represents strong argument for cell type specific responses of feto-placental cells to the intrauterine environment.

One limitation of the study reported here is the low sample size, hence, making association studies with fetal developmental indices i.e. birth weight challenging. Nevertheless, the sample size was increased when validating methylation status of four distinct genes with a locus-specific SEQUENOM MassARRAY EpiTYPER platform. Strong correlations were observed between the results, thus validating HM450 platform, as was the case in other recent studies (134,135).

The remaining question that needs urgent attention is whether DNA methylation and gene expression changes between normal and diabetic cells are a consequence of differential responses of these cells to isolation and *in vitro* culture or are they already present *in utero*. Thus, one suggestion for future studies would be to investigate methylation and gene expression patterns in freshly isolated, uncultured cells.

5.3. Feto-placental cells remember fetal sex

Earlier studies on sexual dimorphism in mammals used RNA isolated from whole tissues, which included placental villi (88,136). The study conducted here extends these findings to identify sex effects on gene expression in four distinct placental cell types. Moreover, this is the first study to compare global gene expression by microarray analysis in isolated, characterized somatic cells from the same tissue, human placental villi. The results show that fetal sex differentially affects gene expression in a cell-phenotype dependent manner in human placental villi, and fetal sex influences gene expression among all four cell phenotypes studied: cytotrophoblasts (CT) and syncytiotrophoblast (SCT) epithelial cells and arterial (AEC) and venous (VEC) endothelial cells.

Stark and colleagues (87,137) showed that the enzymatic activity of placental 11-beta hydroxysteroid dehydrogenase 2 differs between male and female fetuses, framing potential differences in steroid levels and stress responses in the two sexes. This study build on these reports to show there is a disparity in sex biased gene expression in two of the main functional components of placental

villi, villous trophoblast epithelium and the villous core endothelium. Data presented here demonstrate: (i) all four cell types analyzed *in vitro* varied in the extent of sex-biased gene expression, despite the fact that these cells originate from the same organ; (ii) transcripts of male fetuses prevailed in the epithelial compartment, represented by CT and SCT, whereas the endothelial compartment, represented by AEC and VEC, showed more female-biased genes; (iii) sex-biased genes in both the epithelial and endothelial compartments clustered with groups of genes linked to distinct biological functions and molecular pathways.

The overlapping results obtained from use of different gene ontology analysis tools show the robust nature of reported findings. The overlapping biological processes especially influenced by sex were inflammatory and immune response, cell adhesion and responses to stimuli in the epithelium, while glutathione metabolic processes and responses to stimuli were overrepresented in the endothelium. Hence, sex biases gene expression in human placental cells based on cell type and tissue compartment studied. It is tempting to speculate that such sex-biased gene expression contributes to the differential responses of male and female offspring to developmental and environmental modulators to yield part of the different outcomes known to occur in male and female newborns based on sex.

Although sexual dimorphism in mammals correlates with hormonal differences, hormones are not the only determinants of such dimorphism. Before gonad differentiation occurs, male and female bovine preimplantation embryos display phenotypic differences that can only be due to the differences in sex chromosome dosage (138). Male and female cells from mice isolated prior to sexual differentiation respond differently to exogenous stressors *in vitro* (139). As these responses cannot be attributed to sex hormone differences inherent *in vivo*, they raise the question about the mechanism of the disparate response.

Compared to the female, the male sex is a risk factor for adverse pregnancy outcome, with pregnancies with male fetuses exhibiting a higher incidence of gestational diabetes, preterm birth, premature preterm rupture of membranes, and macrosomia (reviewed in (78,140)). The reason remains to be elucidated as to why male fetuses are more vulnerable (or why the females are less susceptible) for such complications while *in utero*.

Like Sood and coauthors (88), this study notes that the sex-biased gene expression is distributed across all chromosomes, although X and Y chromosomes

harbored the highest number of genes whose expression is influenced by fetal sex. Male-specific, Y-linked genes in the fetus may pose a special challenge to mothers during pregnancy. Several genes on the Y-chromosome encode epitopes that contribute to HY antigen, a group of male-specific peptides acting as minor histocompatibility antigens (reviewed in (141)). Some of these genes *(DDX3Y*, *UTY*, *KDM5D*, *USP9Y*, *EIF1AY* and *RPS4Y1*) are predominantly expressed in males in both villous trophoblast and endothelium. These epitopes associate with sub-optimal pregnancy outcome, because miscarriages are more frequent after a firstborn male (142). The presence or absence of HY antigens is also associated with transplantation success, as kidneys from male donors have an increased rate of rejection in female hosts compared to kidneys received from female donors (143). Notably, Ingenuity Pathway Analysis identified that one of the markedly enriched pathways in the data reported here was graft-versus-host disease signaling.

Male-biased genes in the trophoblast compartment are also markedly enriched in genes related to the immune and inflammatory system, which further supports the hypothesis of reduced maternal-fetal compatibility for male fetuses. These genes included *HLA-DQB*1 (SCT), *HLA-DQA1* (SCT and CT), *HCP5* (CT), *NOS1* (CT), *FSTL3*, *PAPPA*, *SPARCL* and *FCGR2C* (trophoblast epithelium), *CD34* (CT), *HLA-F* (CT), *BCL2* (SCT). These and other immune-related genes were also found in a heterogeneous cell isolate prepared from placental villous mesenchyme (88). It is plausible that differences between this study and the results presented by Sood and colleagues (88) relate to expression profiles from stromal cells and macrophages present in the Sood study but absent from more purified isolates used here. These findings parallel the hypothesis of increased vulnerability *in utero* of male fetuses related to sex differences of the feto-placental immune system in relation to preterm delivery (144). Placentas from male fetuses showed more prominent evidence of chronic inflammation and more advanced histopathological lesions associated with this inflammatory response, especially at the basal plate interface.

The study of fetal sex influences has limitations, despite careful planning. Firstly, the CT and SCT studied *in vitro* and used for the microarray analysis necessarily originated from different placentas than the specimens from which the AEC and VEC phenotypes were derived. Different procedures were needed to

isolate the epithelial and endothelial cell types and the bulk of the placenta was required for a given tissue isolate. Importantly, we controlled for this approach as a potential source of variance by including the patient as one random variable in the statistical analysis. Trophoblasts required *in vitro* culture (though not cell division) while both endothelial phenotypes required *in vitro* propagation to obtain enough cells for the microarray analysis. Thus, we acknowledge our study uses models, not *in vivo* exposed specimens, where results may be different.

The data reported by this thesis, combined with emerging evidence on the influence of fetal sex on placental development and function (83-85) offer a partial explanation for the increased risk for preterm birth and premature preterm rupture of membranes in pregnancies carrying male fetuses. The maternal immune responses are critical to the success of the allograft of pregnancy. Hence, these data predict that the sex differences in placental gene expression, specifically related increased male expression of immune and inflammatory genes and genes involved in graft-versus-host disease, contribute a sex-biased profile of placental gene expression that adds up to differential outcomes for male and female newborns after exposure to clinical entities such as preterm birth or premature rupture of membranes. Furthermore, data here identify a sex bias in genes important for cellular metabolism and cellular responses to injury in the placental villous cell phenotypes studied. Therefore, our results highlight the need to consider fetal sex as an independent variable in studies of placental villi and cell culture experiments of villous components.

6. References

(1) Gude NM, Roberts CT, Kalionis B, King RG. Growth and function of the normal human placenta. Thromb Res 2004;114(5-6):397-407.

(2) Kay H, Nelson DM, Wang Y. The Placenta: From Development to Disease. : Wiley; 2011.

(3) Loregger T, Pollheimer J, Knofler M. Regulatory transcription factors controlling function and differentiation of human trophoblast--a review. Placenta 2003 Apr;24 Suppl A:S104-10.

(4) Aplin JD, Kimber SJ. Trophoblast-uterine interactions at implantation. Reprod Biol Endocrinol 2004 Jul 5;2:48.

(5) Yetter JF,3rd. Examination of the placenta. Am Fam Physician 1998 Mar 1;57(5):1045-1054.

(6) Wang Y, Zhao S. Vascular Biology of the Placenta. : Morgan & Claypool Life Sciences; 2010.

(7) Benirschke K, Kaufmann P. Pathology of the human placenta. : Springer-Verlag; 1995.

(8) Castellucci M, Scheper M, Scheffen I, Celona A, Kaufmann P. The development of the human placental villous tree. Anat Embryol (Berl) 1990;181(2):117-128.

(9) Daiter E, Omigbodun A, Wang S, Walinsky D, Strauss JF,3rd, Hoyer JR, et al. Cell differentiation and endogenous cyclic adenosine 3',5'-monophosphate regulate osteopontin expression in human trophoblasts. Endocrinology 1996 May;137(5):1785-1790.

(10) Kliman HJ, Nestler JE, Sermasi E, Sanger JM, Strauss JF,3rd. Purification, characterization, and in vitro differentiation of cytotrophoblasts from human term placentae. Endocrinology 1986 Apr;118(4):1567-1582.

(11) dela Paz NG, D'Amore PA. Arterial versus venous endothelial cells. Cell Tissue Res 2009 Jan;335(1):5-16.

(12) Lang I, Schweizer A, Hiden U, Ghaffari-Tabrizi N, Hagendorfer G, Bilban M, et al. Human fetal placental endothelial cells have a mature arterial and a juvenile venous phenotype with adipogenic and osteogenic differentiation potential. Differentiation 2008 Dec;76(10):1031-1043.

(13) Mehta D, Malik AB. Signaling mechanisms regulating endothelial permeability. Physiol Rev 2006 Jan;86(1):279-367.

(14) Simionescu M. Structural, biochemical and functional differentiation of the vascular endothelium. Morphogenesis of Endothelium :1-21.

(15) Abumaree MH, Al Jumah MA, Kalionis B, Jawdat D, Al Khaldi A, AlTalabani AA, et al. Phenotypic and functional characterization of mesenchymal stem cells from chorionic villi of human term placenta. Stem Cell Rev 2013 Feb;9(1):16-31.

(16) Hughes CC. Endothelial-stromal interactions in angiogenesis. Curr Opin Hematol 2008 May;15(3):204-209.

(17) Carpenter MW. Gestational diabetes, pregnancy hypertension, and late vascular disease. Diabetes Care 2007 Jul;30 Suppl 2:S246-50.

(18) Buckley BS, Harreiter J, Damm P, Corcoy R, Chico A, Simmons D, et al. Gestational diabetes mellitus in Europe: prevalence, current screening practice and barriers to screening. A review. Diabet Med 2012 Jul;29(7):844-854.

(19) Ben-Haroush A, Yogev Y, Hod M. Epidemiology of gestational diabetes mellitus and its association with Type 2 diabetes. Diabet Med 2004 Feb;21(2):103-113.

(20) Haubner F, Lehle K, Munzel D, Schmid C, Birnbaum DE, Preuner JG. Hyperglycemia increases the levels of vascular cellular adhesion molecule-1 and monocyte-chemoattractant-protein-1 in the diabetic endothelial cell. Biochem Biophys Res Commun 2007 Aug 31;360(3):560-565.

(21) Kim C. Gestational diabetes: risks, management, and treatment options. Int J Womens Health 2010 Oct 7;2:339-351.

(22) Anfossi G, Russo I, Doronzo G, Trovati M. Contribution of insulin resistance to vascular dysfunction. Arch Physiol Biochem 2009 Oct;115(4):199-217.

(23) Knudson JD, Payne GA, Borbouse L, Tune JD. Leptin and mechanisms of endothelial dysfunction and cardiovascular disease. Curr Hypertens Rep 2008 Dec;10(6):434-439.

(24) Waterland RA, Jirtle RL. Transposable elements: targets for early nutritional effects on epigenetic gene regulation. Mol Cell Biol 2003 Aug;23(15):5293-5300.

(25) Bruchova H, Vasikova A, Merkerova M, Milcova A, Topinka J, Balascak I, et al. Effect of maternal tobacco smoke exposure on the placental transcriptome. Placenta 2010 Mar;31(3):186-191.

(26) Deierlein AL, Siega-Riz AM, Chantala K, Herring AH. The association between maternal glucose concentration and child BMI at age 3 years. Diabetes Care 2011 Feb;34(2):480-484.

(27) Kanaka-Gantenbein C. Fetal origins of adult diabetes. Ann N Y Acad Sci 2010 Sep;1205:99-105.

(28) Burguet A. Long-term outcome in children of mothers with gestational diabetes. Diabetes Metab 2010 Dec;36(6 Pt 2):682-694.

(29) Luo ZC, Delvin E, Fraser WD, Audibert F, Deal CI, Julien P, et al. Maternal glucose tolerance in pregnancy affects fetal insulin sensitivity. Diabetes Care 2010 Sep;33(9):2055-2061.

(30) Bjarnegard N, Morsing E, Cinthio M, Lanne T, Brodszki J. Cardiovascular function in adulthood following intrauterine growth restriction with abnormal fetal blood flow. Ultrasound Obstet Gynecol 2013 Feb;41(2):177-184.

(31) Sookoian S, Pirola CJ. DNA methylation and hepatic insulin resistance and steatosis. Curr Opin Clin Nutr Metab Care 2012 Jul;15(4):350-356.

(32) Matouk CC, Marsden PA. Epigenetic regulation of vascular endothelial gene expression. Circ Res 2008 Apr 25;102(8):873-887.

(33) Sawan C, Vaissiere T, Murr R, Herceg Z. Epigenetic drivers and genetic passengers on the road to cancer. Mutat Res 2008 Jul 3;642(1-2):1-13.

(34) Miranda TB, Jones PA. DNA methylation: the nuts and bolts of repression. J Cell Physiol 2007 Nov;213(2):384-390.

(35) Ching TT, Maunakea AK, Jun P, Hong C, Zardo G, Pinkel D, et al. Epigenome analyses using BAC microarrays identify evolutionary conservation of tissue-specific methylation of SHANK3. Nat Genet 2005 Jun;37(6):645-651.

(36) Futscher BW, Oshiro MM, Wozniak RJ, Holtan N, Hanigan CL, Duan H, et al. Role for DNA methylation in the control of cell type specific maspin expression. Nat Genet 2002 Jun;31(2):175-179.

(37) Walsh CP, Bestor TH. Cytosine methylation and mammalian development. Genes Dev 1999 Jan 1;13(1):26-34.

(38) Bird A. DNA methylation patterns and epigenetic memory. Genes Dev 2002 Jan 1;16(1):6-21.

(39) Eckhardt F, Lewin J, Cortese R, Rakyan VK, Attwood J, Burger M, et al. DNA methylation profiling of human chromosomes 6, 20 and 22. Nat Genet 2006 Dec;38(12):1378-1385.

(40) Song F, Smith JF, Kimura MT, Morrow AD, Matsuyama T, Nagase H, et al. Association of tissue-specific differentially methylated regions (TDMs) with differential gene expression. Proc Natl Acad Sci U S A 2005 Mar 1;102(9):3336-3341.

(41) Weber M, Hellmann I, Stadler MB, Ramos L, Paabo S, Rebhan M, et al. Distribution, silencing potential and evolutionary impact of promoter DNA methylation in the human genome. Nat Genet 2007 Apr;39(4):457-466.

(42) Oda M, Yamagiwa A, Yamamoto S, Nakayama T, Tsumura A, Sasaki H, et al. DNA methylation regulates long-range gene silencing of an X-linked homeobox gene cluster in a lineage-specific manner. Genes Dev 2006 Dec 15;20(24):3382-3394.

(43) Yan MS, Matouk CC, Marsden PA. Epigenetics of the vascular endothelium. J Appl Physiol 2010 Sep;109(3):916-926.

(44) Khalil AM, Guttman M, Huarte M, Garber M, Raj A, Rivea Morales D, et al. Many human large intergenic noncoding RNAs associate with chromatin-modifying complexes and affect gene expression. Proc Natl Acad Sci U S A 2009 Jul 14;106(28):11667-11672.

(45) Silverman BL, Rizzo T, Green OC, Cho NH, Winter RJ, Ogata ES, et al. Long-term prospective evaluation of offspring of diabetic mothers. Diabetes 1991 Dec;40 Suppl 2:121-125.

(46) Bunt JC, Tataranni PA, Salbe AD. Intrauterine exposure to diabetes is a determinant of hemoglobin A(1)c and systolic blood pressure in pima Indian children. J Clin Endocrinol Metab 2005 Jun;90(6):3225-3229.

(47) West NA, Crume TL, Maligie MA, Dabelea D. Cardiovascular risk factors in children exposed to maternal diabetes in utero. Diabetologia 2011 Mar;54(3):504-507.

(48) Paradisi G, Biaggi A, Ferrazzani S, De Carolis S, Caruso A. Abnormal carbohydrate metabolism during pregnancy : association with endothelial dysfunction. Diabetes Care 2002 Mar;25(3):560-564.

(49) Leach L. Placental vascular dysfunction in diabetic pregnancies: intimations of fetal cardiovascular disease? Microcirculation 2011 May;18(4):263-269.

(50) Sobrevia L, Abarzua F, Nien JK, Salomon C, Westermeier F, Puebla C, et al. Review: Differential placental macrovascular and microvascular endothelial dysfunction in gestational diabetes. Placenta 2011 Mar;32 Suppl 2:S159-64.

(51) Dollberg S, Brockman DE, Myatt L. Nitric oxide synthase activity in umbilical and placental vascular tissue of gestational diabetic pregnancies. Gynecol Obstet Invest 1997;44(3):177-181.

(52) Figueroa R, Martinez E, Fayngersh RP, Tejani N, Mohazzab-H KM, Wolin MS. Alterations in relaxation to lactate and H(2)O(2) in human placental vessels from gestational diabetic pregnancies. Am J Physiol Heart Circ Physiol 2000 Mar;278(3):H706-13.

(53) Babawale MO, Lovat S, Mayhew TM, Lammiman MJ, James DK, Leach L. Effects of gestational diabetes on junctional adhesion molecules in human term placental vasculature. Diabetologia 2000 Sep;43(9):1185-1196.

(54) Jirkovska M, Kubinova L, Janacek J, Moravcova M, Krejci V, Karen P. Topological properties and spatial organization of villous capillaries in normal and diabetic placentas. J Vasc Res 2002 May-Jun;39(3):268-278.

(55) Winick M, Noble A. Cellular growth in human placenta. II. Diabetes mellitus. J Pediatr 1967 Aug;71(2):216-219.

(56) Desoye G, Hauguel-de Mouzon S. The human placenta in gestational diabetes mellitus. The insulin and cytokine network. Diabetes Care 2007 Jul;30 Suppl 2:S120-6.

(57) Leach L, Gray C, Staton S, Babawale MO, Gruchy A, Foster C, et al. Vascular endothelial cadherin and beta-catenin in human fetoplacental vessels of pregnancies complicated by Type 1 diabetes: associations with angiogenesis and perturbed barrier function. Diabetologia 2004 Apr;47(4):695-709.

(58) Gaither K, Quraishi AN, Illsley NP. Diabetes alters the expression and activity of the human placental GLUT1 glucose transporter. J Clin Endocrinol Metab 1999 Feb;84(2):695-701.

(59) Taricco E, Radaelli T, Rossi G, Nobile de Santis MS, Bulfamante GP, Avagliano L, et al. Effects of gestational diabetes on fetal oxygen and glucose levels in vivo. BJOG 2009 Dec;116(13):1729-1735.

(60) Myatt L, Cui X. Oxidative stress in the placenta. Histochem Cell Biol 2004 Oct;122(4):369-382.

(61) Qi W, Chen X, Gilbert RE, Zhang Y, Waltham M, Schache M, et al. High glucose-induced thioredoxin-interacting protein in renal proximal tubule cells is independent of transforming growth factor-beta1. Am J Pathol 2007 Sep;171(3):744-754.

(62) Peuchant E, Brun JL, Rigalleau V, Dubourg L, Thomas MJ, Daniel JY, et al. Oxidative and antioxidative status in pregnant women with either gestational or type 1 diabetes. Clin Biochem 2004 Apr;37(4):293-298.

(63) Makino A, Scott BT, Dillmann WH. Mitochondrial fragmentation and superoxide anion production in coronary endothelial cells from a mouse model of type 1 diabetes. Diabetologia 2010 Aug;53(8):1783-1794.

(64) Barker DJ, Gluckman PD, Godfrey KM, Harding JE, Owens JA, Robinson JS. Fetal nutrition and cardiovascular disease in adult life. Lancet 1993 Apr 10;341(8850):938-941.

(65) Hanson M, Gluckman P. Endothelial dysfunction and cardiovascular disease: the role of predictive adaptive responses. Heart 2005 Jul;91(7):864-866.

(66) Aitsebaomo J, Portbury AL, Schisler JC, Patterson C. Brothers and sisters: molecular insights into arterial-venous heterogeneity. Circ Res 2008 Oct 24;103(9):929-939.

(67) Swift MR, Weinstein BM. Arterial-venous specification during development. Circ Res 2009 Mar 13;104(5):576-588.

(68) Kume T. Specification of arterial, venous, and lymphatic endothelial cells during embryonic development. Histol Histopathol 2010 May;25(5):637-646.

(69) Fish JE, Marsden PA. Endothelial nitric oxide synthase: insight into cell-specific gene regulation in the vascular endothelium. Cell Mol Life Sci 2006 Jan;63(2):144-162.

(70) Napoli C, Hayashi T, Cacciatore F, Casamassimi A, Casini C, Al-Omran M, et al. Endothelial progenitor cells as therapeutic agents in the microcirculation: an update. Atherosclerosis 2011 Mar;215(1):9-22.

(71) Harding JE. The nutritional basis of the fetal origins of adult disease. Int J Epidemiol 2001 Feb;30(1):15-23.

(72) Bennett-Baker PE, Wilkowski J, Burke DT. Age-associated activation of epigenetically repressed genes in the mouse. Genetics 2003 Dec;165(4):2055-2062.

(73) Chan Y, Fish JE, D'Abreo C, Lin S, Robb GB, Teichert AM, et al. The cell-specific expression of endothelial nitric-oxide synthase: a role for DNA methylation. J Biol Chem 2004 Aug 13;279(33):35087-35100.

(74) Bracero LA, Cassidy S, Byrne DW. Effect of gender on perinatal outcome in pregnancies complicated by diabetes. Gynecol Obstet Invest 1996;41(1):10-14.

(75) Bekedam DJ, Engelsbel S, Mol BW, Buitendijk SE, van der Pal-de Bruin KM. Male predominance in fetal distress during labor. Am J Obstet Gynecol 2002 Dec;187(6):1605-1607.

(76) Zeitlin J, Ancel PY, Larroque B, Kaminski M, EPIPAGE Study. Fetal sex and indicated very preterm birth: results of the EPIPAGE study. Am J Obstet Gynecol 2004 May;190(5):1322-1325.

(77) Cui W, Ma CX, Tang Y, Chang V, Rao PV, Ariet M, et al. Sex differences in birth defects: a study of opposite-sex twins. Birth Defects Res A Clin Mol Teratol 2005 Nov;73(11):876-880.

(78) Di Renzo GC, Rosati A, Sarti RD, Cruciani L, Cutuli AM. Does fetal sex affect pregnancy outcome? Gend Med 2007 Mar;4(1):19-30.

(79) Engel PJ, Smith R, Brinsmead MW, Bowe SJ, Clifton VL. Male sex and pre-existing diabetes are independent risk factors for stillbirth. Aust N Z J Obstet Gynaecol 2008 Aug;48(4):375-383.

(80) van Abeelen AF, de Rooij SR, Osmond C, Painter RC, Veenendaal MV, Bossuyt PM, et al. The sex-specific effects of famine on the association between placental size and later hypertension. Placenta 2011 Sep;32(9):694-698.

(81) Mingrone G, Manco M, Mora ME, Guidone C, Iaconelli A, Gniuli D, et al. Influence of maternal obesity on insulin sensitivity and secretion in offspring. Diabetes Care 2008 Sep;31(9):1872-1876.

(82) Gabory A, Attig L, Junien C. Sexual dimorphism in environmental epigenetic programming. Mol Cell Endocrinol 2009 May 25;304(1-2):8-18.

(83) Gabory A, Ferry L, Fajardy I, Jouneau L, Gothie JD, Vige A, et al. Maternal diets trigger sex-specific divergent trajectories of gene expression and epigenetic systems in mouse placenta. PLoS One 2012;7(11):e47986.

(84) Gallou-Kabani C, Gabory A, Tost J, Karimi M, Mayeur S, Lesage J, et al. Sex- and diet-specific changes of imprinted gene expression and DNA methylation in mouse placenta under a high-fat diet. PLoS One 2010 Dec 21;5(12):e14398.

(85) Scott NM, Hodyl NA, Murphy VE, Osei-Kumah A, Wyper H, Hodgson DM, et al. Placental cytokine expression covaries with maternal asthma severity and fetal sex. J Immunol 2009 Feb 1;182(3):1411-1420.

(86) Murphy VE, Gibson PG, Giles WB, Zakar T, Smith R, Bisits AM, et al. Maternal asthma is associated with reduced female fetal growth. Am J Respir Crit Care Med 2003 Dec 1;168(11):1317-1323.

(87) Stark MJ, Clifton VL, Wright IM. Sex-specific differences in peripheral microvascular blood flow in preterm infants. Pediatr Res 2008 Apr;63(4):415-419.

(88) Sood R, Zehnder JL, Druzin ML, Brown PO. Gene expression patterns in human placenta. Proc Natl Acad Sci U S A 2006 Apr 4;103(14):5478-5483.

(89) Arnold AP, Lusis AJ. Understanding the sexome: measuring and reporting sex differences in gene systems. Endocrinology 2012 Jun;153(6):2551-2555.

(90) Lang I, Pabst MA, Hiden U, Blaschitz A, Dohr G, Hahn T, et al. Heterogeneity of microvascular endothelial cells isolated from human term placenta and macrovascular umbilical vein endothelial cells. Eur J Cell Biol 2003 Apr;82(4):163-173.

(91) Chen B, Longtine MS, Sadovsky Y, Nelson DM. Hypoxia downregulates p53 but induces apoptosis and enhances expression of BAD in cultures of human syncytiotrophoblasts. Am J Physiol Cell Physiol 2010 Nov;299(5):C968-76.

(92) Hawker JR,Jr. Chemiluminescence-based BrdU ELISA to measure DNA synthesis. J Immunol Methods 2003 Mar 1;274(1-2):77-82.

(93) Wang J, Bingaman S, Huxley VH. Intrinsic sex-specific differences in microvascular endothelial cell phosphodiesterases. Am J Physiol Heart Circ Physiol 2010 Apr;298(4):H1146-54.

(94) Lahn BT, Page DC. Functional coherence of the human Y chromosome. Science 1997 Oct 24;278(5338):675-680.

(95) Downey T. Analysis of a multifactor microarray study using Partek genomics solution. Methods Enzymol 2006;411:256-270.

(96) Sturn A, Quackenbush J, Trajanoski Z. Genesis: cluster analysis of microarray data. Bioinformatics 2002 Jan;18(1):207-208.

(97) Nikitin A, Egorov S, Daraselia N, Mazo I. Pathway studio--the analysis and navigation of molecular networks. Bioinformatics 2003 Nov 1;19(16):2155-2157.

(98) Dennis G,Jr, Sherman BT, Hosack DA, Yang J, Gao W, Lane HC, et al. DAVID: Database for Annotation, Visualization, and Integrated Discovery. Genome Biol 2003;4(5):P3.

(99) Thomas PD, Campbell MJ, Kejariwal A, Mi H, Karlak B, Daverman R, et al. PANTHER: a library of protein families and subfamilies indexed by function. Genome Res 2003 Sep;13(9):2129-2141.

(100) Kosaki A, Pillay TS, Xu L, Webster NJ. The B isoform of the insulin receptor signals more efficiently than the A isoform in HepG2 cells. J Biol Chem 1995 Sep 1;270(35):20816-20823.

(101) Maksimovic J, Gordon L, Oshlack A. SWAN: Subset-quantile within array normalization for illumina infinium HumanMethylation450 BeadChips. Genome Biol 2012 Jun 15;13(6):R44-2012-13-6-r44.

(102) Ehrich M, Nelson MR, Stanssens P, Zabeau M, Liloglou T, Xinarianos G, et al. Quantitative high-throughput analysis of DNA methylation patterns by base-specific cleavage and mass spectrometry. Proc Natl Acad Sci U S A 2005 Nov 1;102(44):15785-15790.

(103) Leach L, Mayhew TM. The intra-uterine environment and placentation. J Anat 2009 Jul;215(1):1-2.

(104) Xie L, Galettis A, Morris J, Jackson C, Twigg SM, Gallery ED. Intercellular adhesion molecule-1 (ICAM-1) expression is necessary for monocyte adhesion to the placental bed endothelium and is increased in type 1 diabetic human pregnancy. Diabetes Metab Res Rev 2008 May-Jun;24(4):294-300.

(105) Lehnen H, Zechner U, Haaf T. Epigenetics of gestational diabetes mellitus and offspring health: the time for action is in early stages of life. Mol Hum Reprod 2013 Jul;19(7):415-422.

(106) Clausen TD, Mathiesen ER, Hansen T, Pedersen O, Jensen DM, Lauenborg J, et al. Overweight and the metabolic syndrome in adult offspring of women with diet-treated gestational diabetes mellitus or type 1 diabetes. J Clin Endocrinol Metab 2009 Jul;94(7):2464-2470.

(107) Desai M, Beall M, Ross MG. Developmental origins of obesity: programmed adipogenesis. Curr Diab Rep 2013 Feb;13(1):27-33.

(108) Wu S, Divall S, Wondisford F, Wolfe A. Reproductive tissues maintain insulin sensitivity in diet-induced obesity. Diabetes 2012 Jan;61(1):114-123.

(109) Roberts CT. IFPA Award in Placentology Lecture: Complicated interactions between genes and the environment in placentation, pregnancy outcome and long term health. Placenta 2010 Mar;31 Suppl:S47-53.

(110) Wright CS, Rifas-Shiman SL, Rich-Edwards JW, Taveras EM, Gillman MW, Oken E. Intrauterine exposure to gestational diabetes, child adiposity, and blood pressure. Am J Hypertens 2009 Feb;22(2):215-220.

(111) Lehle K, Haubner F, Munzel D, Birnbaum DE, Preuner JG. Development of a disease-specific model to evaluate endothelial dysfunction in patients with diabetes mellitus. Biochem Biophys Res Commun 2007 May 25;357(1):308-313.

(112) Arany E, Hill DJ. Fibroblast growth factor-2 and fibroblast growth factor receptor-1 mRNA expression and peptide localization in placentae from normal and diabetic pregnancies. Placenta 1998 Mar-Apr;19(2-3):133-142.

(113) Arnaoutova I, George J, Kleinman HK, Benton G. The endothelial cell tube formation assay on basement membrane turns 20: state of the science and the art. Angiogenesis 2009;12(3):267-274.

(114) Francescone RA,3rd, Faibish M, Shao R. A Matrigel-based tube formation assay to assess the vasculogenic activity of tumor cells. J Vis Exp 2011 Sep 7;(55). pii: 3040. doi(55):10.3791/3040.

(115) Bianchi C, Miccoli R, Del Prato S. Hyperglycemia and vascular metabolic memory: truth or fiction? Curr Diab Rep 2013 Jun;13(3):403-410.

(116) Roy S, Sala R, Cagliero E, Lorenzi M. Overexpression of fibronectin induced by diabetes or high glucose: phenomenon with a memory. Proc Natl Acad Sci U S A 1990 Jan;87(1):404-408.

(117) El-Osta A, Brasacchio D, Yao D, Pocai A, Jones PL, Roeder RG, et al. Transient high glucose causes persistent epigenetic changes and altered gene expression during subsequent normoglycemia. J Exp Med 2008 Sep 29;205(10):2409-2417.

(118) Hauguel-de Mouzon S, Guerre-Millo M. The placenta cytokine network and inflammatory signals. Placenta 2006 Aug;27(8):794-798.

(119) Joo JE, Hiden U, Lassance L, Gordon L, Martino DJ, Desoye G, et al. Variable promoter methylation contributes to differential expression of key genes in human placenta-derived venous and arterial endothelial cells. BMC Genomics 2013 Jul 15;14:475-2164-14-475.

(120) Novakovic B, Gordon L, Robinson WP, Desoye G, Saffery R. Glucose as a fetal nutrient: dynamic regulation of several glucose transporter genes by DNA methylation in the human placenta across gestation. J Nutr Biochem 2013 Jan;24(1):282-288.

(121) Novakovic B, Saffery R. DNA methylation profiling highlights the unique nature of the human placental epigenome. Epigenomics 2010 Oct;2(5):627-638.

(122) Ruchat SM, Houde AA, Voisin G, St-Pierre J, Perron P, Baillargeon JP, et al. Gestational diabetes mellitus epigenetically affects genes predominantly involved in metabolic diseases. Epigenetics 2013 Jul 18;8(9).

(123) Chen S, Feng B, George B, Chakrabarti R, Chen M, Chakrabarti S. Transcriptional coactivator p300 regulates glucose-induced gene expression in endothelial cells. Am J Physiol Endocrinol Metab 2010 Jan;298(1):E127-37.

(124) Mufson EJ, Counts SE, Che S, Ginsberg SD. Neuronal gene expression profiling: uncovering the molecular biology of neurodegenerative disease. Prog Brain Res 2006;158:197-222.

(125) Bauer JW, Bilgic H, Baechler EC. Gene-expression profiling in rheumatic disease: tools and therapeutic potential. Nat Rev Rheumatol 2009 May;5(5):257-265.

(126) Espinosa E, Gamez-Pozo A, Sanchez-Navarro I, Pinto A, Castaneda CA, Ciruelos E, et al. The present and future of gene profiling in breast cancer. Cancer Metastasis Rev 2012 Jun;31(1-2):41-46.

(127) Radaelli T, Varastehpour A, Catalano P, Hauguel-de Mouzon S. Gestational diabetes induces placental genes for chronic stress and inflammatory pathways. Diabetes 2003 Dec;52(12):2951-2958.

(128) Radaelli T, Lepercq J, Varastehpour A, Basu S, Catalano PM, Hauguel-De Mouzon S. Differential regulation of genes for fetoplacental lipid pathways in pregnancy with gestational and type 1 diabetes mellitus. Am J Obstet Gynecol 2009 Aug;201(2):209.e1-209.e10.

(129) Enquobahrie DA, Williams MA, Qiu C, Meller M, Sorensen TK. Global placental gene expression in gestational diabetes mellitus. Am J Obstet Gynecol 2009 Feb;200(2):206.e1-206.13.

(130) Nomura Y, Lambertini L, Rialdi A, Lee M, Mystal EY, Grabie M, et al. Global Methylation in the Placenta and Umbilical Cord Blood From Pregnancies With Maternal Gestational Diabetes, Preeclampsia, and Obesity. Reprod Sci 2013 Jun 13.

(131) El Hajj N, Pliushch G, Schneider E, Dittrich M, Muller T, Korenkov M, et al. Metabolic programming of MEST DNA methylation by intrauterine exposure to gestational diabetes mellitus. Diabetes 2013 Apr;62(4):1320-1328.

(132) Akhtar S, Benter IF. The role of epidermal growth factor receptor in diabetes-induced cardiac dysfunction. Bioimpacts 2013;3(1):5-9.

(133) Hassing HC, Mooij H, Guo S, Monia BP, Chen K, Kulik W, et al. Inhibition of hepatic sulfatase-2 in vivo: a novel strategy to correct diabetic dyslipidemia. Hepatology 2012 Jun;55(6):1746-1753.

(134) Bibikova M, Barnes B, Tsan C, Ho V, Klotzle B, Le JM, et al. High density DNA methylation array with single CpG site resolution. Genomics 2011 Oct;98(4):288-295.

(135) Roessler J, Ammerpohl O, Gutwein J, Hasemeier B, Anwar SL, Kreipe H, et al. Quantitative cross-validation and content analysis of the 450k DNA methylation array from Illumina, Inc. BMC Res Notes 2012 Apr 30;5:210-0500-5-210.

(136) Yang X, Schadt EE, Wang S, Wang H, Arnold AP, Ingram-Drake L, et al. Tissue-specific expression and regulation of sexually dimorphic genes in mice. Genome Res 2006 Aug;16(8):995-1004.

(137) Stark MJ, Wright IM, Clifton VL. Sex-specific alterations in placental 11beta-hydroxysteroid dehydrogenase 2 activity and early postnatal clinical course following antenatal betamethasone. Am J Physiol Regul Integr Comp Physiol 2009 Aug;297(2):R510-4.

(138) Bermejo-Alvarez P, Rizos D, Rath D, Lonergan P, Gutierrez-Adan A. Sex determines the expression level of one third of the actively expressed genes in bovine blastocysts. Proc Natl Acad Sci U S A 2010 Feb 23;107(8):3394-3399.

(139) Penaloza C, Estevez B, Orlanski S, Sikorska M, Walker R, Smith C, et al. Sex of the cell dictates its response: differential gene expression and sensitivity to cell death inducing stress in male and female cells. FASEB J 2009 Jun;23(6):1869-1879.

(140) Clifton VL. Review: Sex and the human placenta: mediating differential strategies of fetal growth and survival. Placenta 2010 Mar;31 Suppl:S33-9.

(141) Graves JA. Review: Sex chromosome evolution and the expression of sex-specific genes in the placenta. Placenta 2010 Mar;31 Suppl:S27-32.

(142) Nielsen HS, Steffensen R, Varming K, Van Halteren AG, Spierings E, Ryder LP, et al. Association of HY-restricting HLA class II alleles with pregnancy outcome in patients with recurrent miscarriage subsequent to a firstborn boy. Hum Mol Genet 2009 May 1;18(9):1684-1691.

(143) Kim SJ, Gill JS. H-Y incompatibility predicts short-term outcomes for kidney transplant recipients. J Am Soc Nephrol 2009 Sep;20(9):2025-2033.

(144) Ghidini A, Salafia CM. Histologic placental lesions in women with recurrent preterm delivery. Acta Obstet Gynecol Scand 2005 Jun;84(6):547-550.